The Pricing of Options with Jump Diffusion and Stochastic Volatility

Linghao Yi

Faculty of Industrial Engineering, Mechanical Engineering and Computer Science
University of Iceland
2010

THE PRICING OF OPTIONS WITH JUMP DIFFUSION AND STOCHASTIC VOLATILITY

Linghao Yi

60 ECTS thesis submitted in partial fulfillment of a
Magister Scientiarum degree in Financial Engineering

Advisors
Olafur Petur Palsson
Birgir Hrafnkelsson

Faculty Representative
Eggert Throstur Thorarinsson

Faculty of Industrial Engineering, Mechanical Engineering and
Computer Science
School of Engineering and Natural Sciences
University of Iceland
Reykjavik, July 2010

The Pricing of Options with Jump Diffusion and Stochastic Volatility

60 ECTS thesis submitted in partial fulfillment of a M.Sc. degree in Financial Engineering

Copyright © 2010 Linghao Yi
All rights reserved

Faculty of Industrial Engineering, Mechanical Engineering and
Computer Science
School of Engineering and Natural Sciences
University of Iceland
Hjardarhagi 2-6
107, Reykjavik, Reykjavik
Iceland

Telephone: 525 4000

Bibliographic information:
Linghao Yi, 2010, The Pricing of Options with Jump Diffusion and Stochastic Volatility, M.Sc. thesis, Faculty of Industrial Engineering, Mechanical Engineering and Computer Science, University of Iceland.

ISBN XX

Printing: Háskólaprent, Fálkagata 2, 107 Reykjavik
Reykjavik, Iceland, July 2010

Abstract

The Black-Scholes model has been widely used in option pricing for roughly four decades. However, there are two puzzles that have turned out to be difficult to explain with the Black-Scholes model: the leptokurtic feature and the volatility smile. In this study, the two puzzles will be investigated. An improved model – a double exponential jump diffusion model (referred to as the Kou model) will be introduced. The Monte Carlo method will be used to simulate the Black-Scholes model and the double exponential jump diffusion model to price the IBM call option. The call option prices estimated by both models will be compared to the market call prices. The results show that the call option prices estimated by the double exponential jump diffusion model fit the IBM market call option prices better than the call option prices estimated by the Black-Scholes model do.

The volatility in both the Black-Scholes model and the double exponential jump diffusion model is assumed to be a constant. However, it is stochastic in reality. Two new models based on the Black-Scholes model and the double exponential jump diffusion model with a stochastic volatility will be developed. The stochastic volatility is determined by a GARCH(1,1) model. The advantage of GARCH model is that GARCH model captures some features associated with financial time series, such as, fat tails, volatility clustering, and leverage effects. First, the structure of

both the new models will be presented. Then the Monte Carlo simulation will be applied to the two new models to price the IBM call option. Finally, the call option prices estimated by the four models will be compared to the market call option prices. The performance of the four models will be evaluated by statistical methods such as mean absolute error (MAE), mean square error (MSE), root mean square error (RMSE), normalized root mean square error (NRMSE), and information ratio (IR). The results show that the double exponential jump diffusion model performs the best for the lower strike prices and the Kou & GARCH model has the best performance for the higher strike prices. Theoretically, the Kou & GARCH model is expected to be the best model among the four models. Some possible reasons and suggestions will be given in the discussion.

Preface

It was good to study Financial Engineering in Faculty of Industrial Engineering, Mechanical Engineering and Computer Science at the University of Iceland.

First, I am thankful to my advisor, professor Olafur Petur Palsson, for his advice, comments and corrections on my thesis. He introduced to me two good tools, time series analysis and technical analysis. In the summer of 2008, I worked on the "Currency Exchange Trading Strategy Analysis" under his supervision.

I also give my thanks to my second advisor, research professor Birgir Hrafnkelsson, for his advice, in particular, for his comments and corrections on statistics.

I spent one year at the University of California at Berkeley in the school year of 2008 – 2009 as a visiting research student where I took several financial engineering and economics courses. I got expertise guidance and help from professor Xin Guo, professor Ilan Adler, professor J. G. Shanthikumar, as well as help from professor Philip M. Kaminsky and staff Mike Campbell. I am grateful to these great people.

Finally, I would like to give my thanks to my husband, professor Jon Tomas Gudmundsson, for his encouragement, support and help.

Linghao Yi

Faculty of Industrial Engineering, Mechanical Engineering

and Computer Science

University of Iceland

Reykjavik, Iceland

July 2010

Contents

Nomenclature

α	the GARCH error coefficient
β	the GARCH lag coefficient
B	a Bernoulli random variable
c	call option price
d	dividend rate
dq	a Poisson counter
Δt	time period
δ	standard deviation of the logarithm of the jump size distribution
$\mathbb{E}$	the expectation value
η_{u}	means of positive jump
η_{d}	means of negative jump
J	jump size
K	strike price
κ	a mean-reverting rate
λ	jump intensity
μ	drift, mean of daily log return, mean of normal distribution
ν	mean of the logarithm of the jump size distribution
$N(t)$	a Poisson process

$\mathbb{P}$	physical probability
$\mathbb{Q}$	risk-neutral probability
ω	a constant for GARCH(1,1)
ϕ	normal distribution process
p	put option price
p	probability of upward jump
q	probability of downward jump
ρ	correlation coefficient
r	daily log return
R_{t}	daily simple return
r_{t}	daily log return
r_{f}	riskfree interest rate
S	asset price, underlying price, stock price
S_0	an initial stock price
$S(t)$	asset price, underlying price, stock price in continuous time
S_t	asset price, underlying price, stock price in discrete time
σ	volatility, standard deviation of daily log return
T	time to maturity
t	time
τ	time period
θ	a log-term variance
ε	a volatility of volatility
$\mathbb{V}$	the variance
$V(t)$	the diffusion component of return variance
$W(t)$	a standard Wiener process in continuous time
W_t	a standard Wiener process in discrete time

$W^s(t)$ a standard Wiener process, used to describe $S(t)$

$W^v(t)$ a standard Wiener process, used to describe $V(t)$

$W^\lambda(t)$ a standard Wiener process, used to describe $\lambda(t)$

$\xi+$ an exponential random variable with probability p upward

$\xi-$ an exponential random variable with probability q downward

Z a standard normal variable

1 Introduction

1.1 Background

The Black-Scholes model (Black and Scholes, 1973), which is based on Brownian motion and normal distribution, has been widely used to model the return of assets and to price financial option for almost four decades. However, many empirical evidences have recently shown two puzzles, namely the leptokurtic feature that the return distribution of assets may have a higher peak and two asymmetric heavy tails than those of normal distribution, as well as an abnormality, often referred to as 'volatility smile', that is observed in option pricing (Kou, 2002; Kou and Wang, 2003, 2004).

Before these empirical puzzles are explored, a few fundamental concepts and models that this study is based on will be introduced.

1.1.1 Asset returns

Asset is an investment instrument that can be bought and sold. Let S_t be the price of an asset at time t. Assume that the asset pays no dividends, then the one-period

simple gross return when holding an asset for one period from date $t-1$ to date t is given as (Tsay, 2005)

$$1 + R_t = \frac{S_t}{S_{t-1}}$$

The corresponding one-period simple net return (often referred to as simple return) is

$$R_t = \frac{S_t}{S_{t-1}} - 1 = \frac{S_t - S_{t-1}}{S_{t-1}}$$

and the multiperiod simple gross return when holding the asset for k periods between date $t-k$ to date t is given as

$$\begin{aligned} 1 + R_t[k] &= \frac{S_t}{S_{t-k}} = \frac{S_t}{S_{t-1}} \times \frac{S_{t-1}}{S_{t-2}} \times \cdots \times \frac{S_{t-k+1}}{S_{t-k}} \\ &= (1 + R_t)(1 + R_{t-1}) \cdots (1 + R_{t-k+1}) \\ &= \prod_{j=0}^{k-1} (1 + R_{t-j}) \end{aligned}$$

The log return is the natural logarithm of the simple gross return of an asset. Thus the one-period log return is

$$r_t = \log(1 + R_t) = \log\left(\frac{S_t}{S_{t-1}}\right) = \log(S_t) - \log(S_{t-1})$$

and the multiperiod log return is

$$\begin{aligned} r_t[k] &= \log(1 + R_t[k]) = \log\left[(1 + R_t)(1 + R_{t-1}) \cdots (R_{t-k+1})\right] \\ &= \log(1 + R_t) + \log(1 + R_{t-1}) + \cdots + \log(1 + R_{t-k+1}) \\ &= r_t + r_{t-1} + \cdots + r_{t-k+1} \end{aligned}$$

Most of the time, log return will be used in this study. The advantages of the log return over the simple return are that the multiperiod log return is simply the sum

of the one-period returns involved and the statistical properties of log returns are more tractable.

1.1.2 Geometric Brownian motion

Geometric Browian motion (GBM) is the simplest and probably the most popular specification in financial models. The Black-Scholes option pricing model assumes that the underlying state variable follows GBM. GBM specifies that the instantaneous percentage change of the underlying asset has a constant drift μ and volatility σ (Baz and Chacko, 2004; Craine et al., 2000; Merton, 1971). It can be described by a stochastic differential equation

$$\frac{dS}{S} = \mu dt + \sigma dW_t \tag{1.1}$$

where dW_t is a Wiener process with a mean of zero and a variance equal to dt. Equation (1.1) is known as the Black-Scholes equation (Derman and Kani, 1994a).

1.1.3 Black-Scholes option pricing model and return

Recall the Black-Scholes equation,

$$dS = \mu S dt + \sigma S dW_t \tag{1.2}$$

then applying Ito's Lemma, the following equation is obtained (Baz and Chacko, 2004).

$$d[\log S] = \left[\mu - \frac{\sigma^2}{2}\right] dt + \sigma dW_t \tag{1.3}$$

Now, suppose that asset prices are observed at discrete times t_i, i.e. $S(t_i) = S_i$, with $\Delta t = t_{i+1} - t_i$, then the following equation can be derived from equation (1.3).

$$\begin{aligned} \log S_{i+1} - \log S_i &= \log\left(\frac{S_{i+1}}{S_i}\right) \\ &\approxeq \left[\mu - \frac{\sigma^2}{2}\right]\Delta t + \sigma\phi\sqrt{\Delta t} \end{aligned} \tag{1.4}$$

where ϕ follows a standard normal distribution. Now, if Δt is sufficient small, then Δt is much smaller than $\sqrt{\Delta t}$, so that equation (1.4) can be approximated by

$$\begin{aligned} \log\left(\frac{S_{i+1}}{S_i}\right) &= \log\left(\frac{S_{i+1} - S_i + S_i}{S_i}\right) \\ &= \log\left(1 + \frac{S_{i+1} - S_i}{S_i}\right) \\ &\approxeq \sigma\phi\sqrt{\Delta t} \end{aligned} \tag{1.5}$$

Lets define the return R_i in the period $t_{i+1} - t_i$ as

$$R_i = \frac{S_{i+1} - S_i}{S_i} \tag{1.6}$$

then equation (1.5) becomes

$$\log(1 + R_i) \approxeq R_i = \sigma\phi\sqrt{\Delta t} \tag{1.7}$$

Equation (1.7) shows that the return of asset S should be normally distributed (Forsyth, 2008). This study is based on this conclusion.

1.2 Learning from the data

S&P 500 index historical data from January 1950 to June 2010 and IBM historical stock prices from January 1962 to June 2010, as well as IBM option price on June 10, 2010 are used in this study. The data is downloaded from Yahoo finance (`http://finance.yahoo.com`).

The S&P 500 index daily log return from January 1950 to June 2010 is shown in Figure 1.1. From this figure, it can be noted that the largest spikes occurred around October 1987 due to the 1987 stock market crash. The biggest negative return appeared on October 19, 1987. The range of the daily log return during this period was from -21.155 to 7.997. The second largest spikes occurred in October 2008 at the beginning of the global financial crisis. It can also be observed that significant fluctuations occurred during the period 2000–2002, which are due to the internet bubble burst and the September 11 attacks. From the data shown in Figure 1.1, it is obvious that the stock market became significantly more volatile after 1985 than it was the preceding 35 years. Therefore, the focus in further study will be on the S&P 500 index value from 1985 to 2010.

The S&P 500 index from January 1985 to June 2010 on a linear scale and a log scale are shown in Figures 1.2 (a) and (b), respectively. From both figures, it can be noted that the tendency of the index value is upward before the year 2000, but the index value has become more volatile during the past decade. The stock crash in 1987 can also be observed, it appears to be a relatively small downward jump. Why is it different from what are observed in Figure 1.1? The reason is that the S&P index value is not so high in 1987 and it caused a huge negative return even though the price did not fall as much as today.

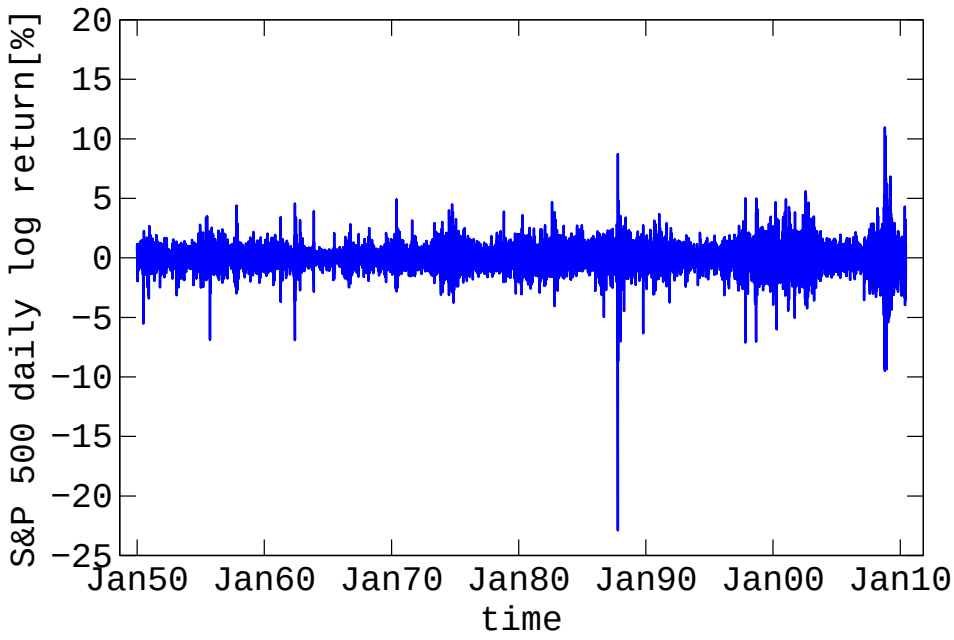

Figure 1.1: The S&P 500 index daily log return from January 1950 to June 2010. The biggest negative spikes occurred on October 19, 1987 when the stock market crashed. The second biggest spikes occurred due to the "Panic of 2008". The spikes around 2000–2002 are due to the internet bubble burst and the September 11 attacks.

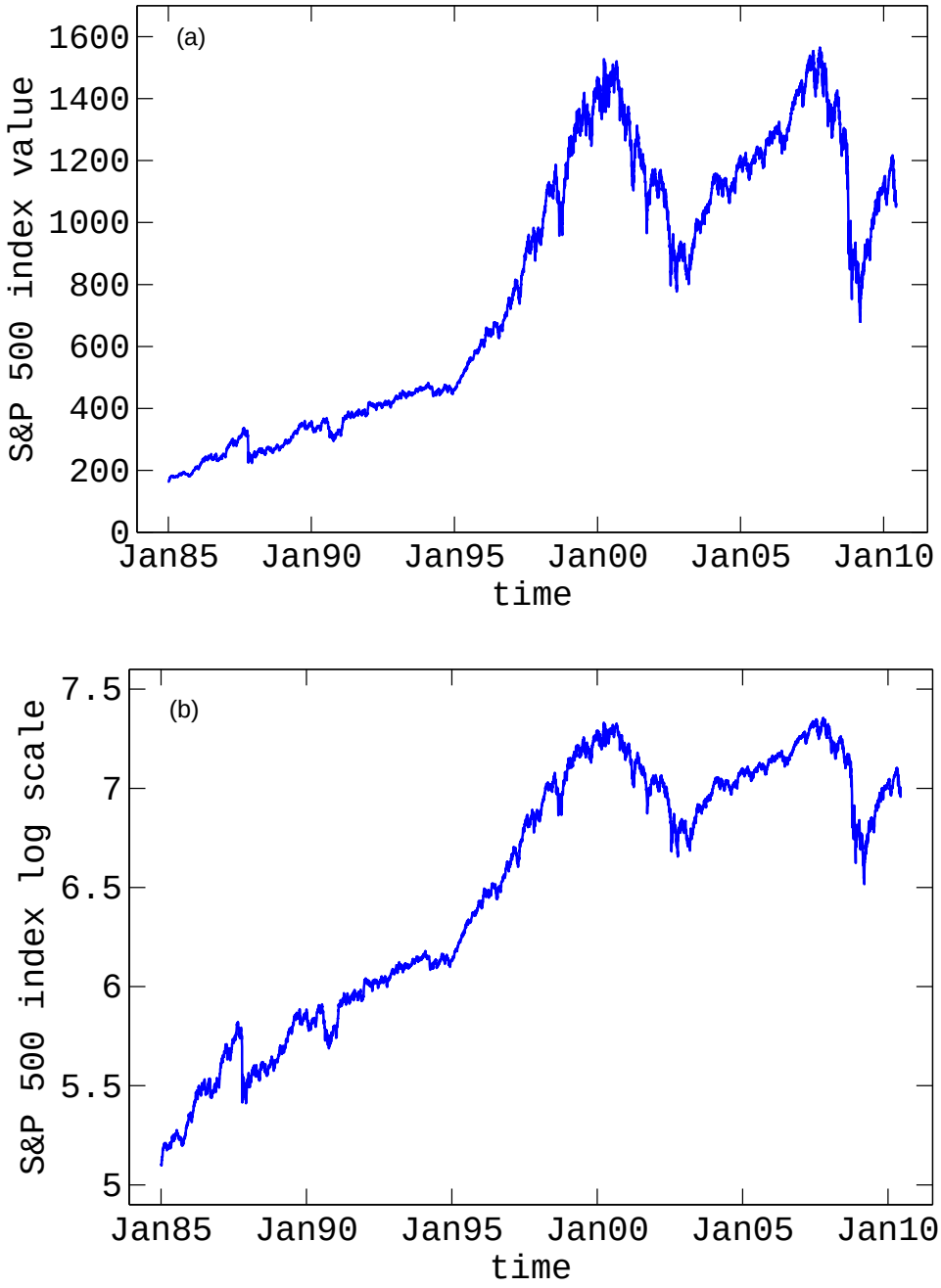

Figure 1.2: The S&P 500 index value from January 1985 to June 2010. (a) on a linear scale and (b) on a log scale. The tendency of index value is upward before the year 2000, However, it has become very volatile in the past decade. The 1987 stock market crash can be clearly observed.

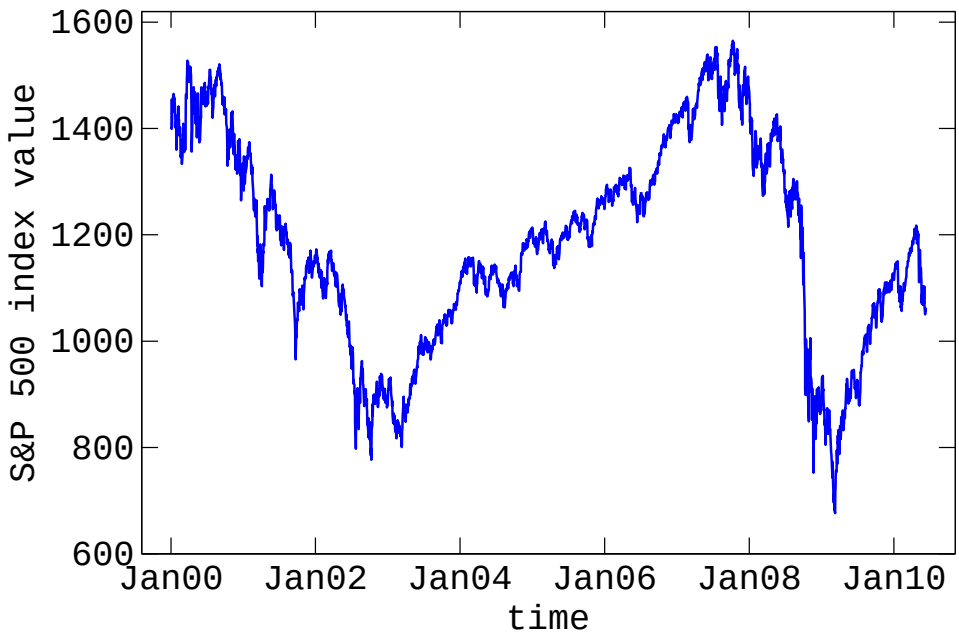

Figure 1.3: The S&P 500 index value from January 2000 to June 2010 on a linear scale. The stock market has been very volatile during this decade.

In order to explore further the increasingly volatile period of the past decade, the S&P 500 index from January 2000 to June 2010 is shown in Figure 1.3. The value has fluctuated around the index value of about 1200 in the recent ten years and the upward tendency has disappeared. A big drop in the index value occurred after September 11, 2001 and the index value plummeted again around the global financial crisis in October 2008.

The distribution of the S&P 500 index daily log return is plotted in Figure 1.4. It is not normally distributed. The peak is significantly higher and the tails are fatter than a normal distribution would predict. This is the leptokurtic feature, which will be discussed in section 2.1.1. In the next chapter, the S&P data from 1950 to 2010 will be divided into two data sets in order to investigate whether there exists a difference in the distribution for different periods.

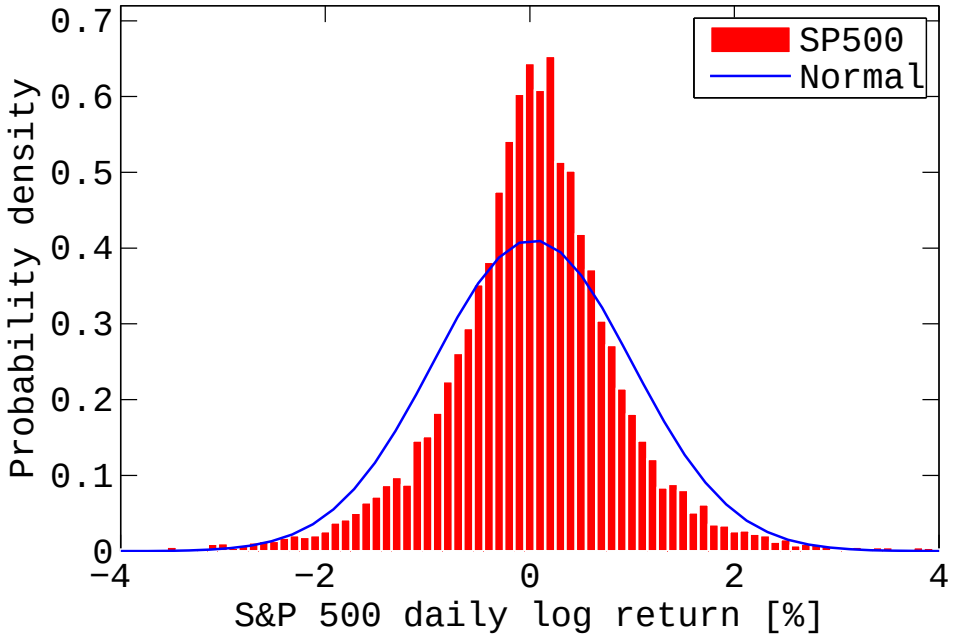

Figure 1.4: Distribution of S&P 500 index daily log return from January 1950 to June 2010. It is clear that the daily log return is not normally distributed. The peak is higher and the tails are fatter than a normal distribution would predict.

1.3 Structure of the thesis

This thesis is organized as follows: In this chapter, some basic concepts and models and assumptions are introduced. In Chapter 2, the two puzzles of the Black-Scholes model, which are not supported by the empirical phenomena, will be substantiated by real data. In Chapter 3, some modifications to the Black-Scholes model will be summarized; their advantages and disadvantages will be discussed, evaluated and compared. In Chapter 4, the double exponential jump-diffusion model (also referred to as the Kou model), will be discussed in more detail. In Chapter 5, the implementation and the algorithms simulating the Black-Scholes model and the Kou model will be given. Do they fit the real data? What are their errors? Which one is the better model? In Chapter 6, a stochastic volatility model based on GARCH will be developed. In Chapter 7, two new models based on the Black-Scholes model and the Kou model, respectively, but with stochastic volatility, will be introduced. These two new models are compared with the Black-Sholes model and the Kou model visually and statistically. Finally, the conclusion, limitation and future work is discussed in Chapter 8.

2 Problem Description

In this chapter, the two puzzles (often referred to as the two phenomena) not supported by the Black-Scholes model in empirical studies will be demonstrated using real market data. Furthermore, the reasons for the two puzzles will be analyzed.

2.1 The two puzzles

Many empirical studies show two phenomena, the asymmetric leptokurtic features and the volatility smile, which are not accounted for by the Black-Sholes model (Kou, 2002; Maekawa et al., 2008). The leptokurtic feature emerged in Section 1.2. In the coming sections, the real market data and individual stock price data will be applied to explore the existence of the two phenomena.

2.1.1 Leptokurtic distributions

The asymmetric leptokurtic features – the return distribution is skewed to the one side (left side or right side) and has a higher peak and two heavier tails than those of normal distribution – are commonly observed empirically.

The purpose of this section is to check whether the leptokurtic phenomena exists on different data sets. First, the market data (S&P 500 index) is divided into two parts, one data set is for the period from January 1950 to December 1984, and the other data set is for the period from January 1985 to June 2010. The distribution of S&P 500 daily log return from 1950 to 1985 is shown in Figure 2.1(a). This daily log return does not follow a normal distribution because the peak is higher than a normal distribution would predict. Figure 2.1(b) shows the distribution of the S&P 500 index daily log return from January 1985 to June 2010. The leptokurtic feature can be noted in Figure 2.1(b). The peak is significantly higher than that of normal distribution. The skewness can be estimated by (Kou, 2008; Thomas, 2005).

$$\hat{S} = \frac{1}{(n-1)\hat{\sigma}^3} \sum_{i=1}^{n} (X_i - \bar{X})^3 \tag{2.1}$$

and the kurtosis is given as

$$\hat{K} = \frac{1}{(n-1)\hat{\sigma}^4} \sum_{i=1}^{n} (X_i - \bar{X})^4 \tag{2.2}$$

For the time period from 1950 to 1984, the kurtosis of S&P 500 is about 7.27, and the skewness is about -0.08. For the time period from 1985 to 2010, the kurtosis of S&P 500 is about 32.71, and the skewness is about -1.36. The negative skewness means that the return has a heavier left tail than the right tail. Or, the distribution is skewed to left side. So, the kurtosis is indeed significantly higher and the left tail is heavier than right tail for the period from 1985 to 2010.

An individual stock is also taken as an example, the data set is IBM historical stock price data from January 1962 to June 2010. The data set is split into two parts, one is for the period from January 1962 to December 1984, the other is for the period from January 1985 to June 2010. Their distributions of the daily log

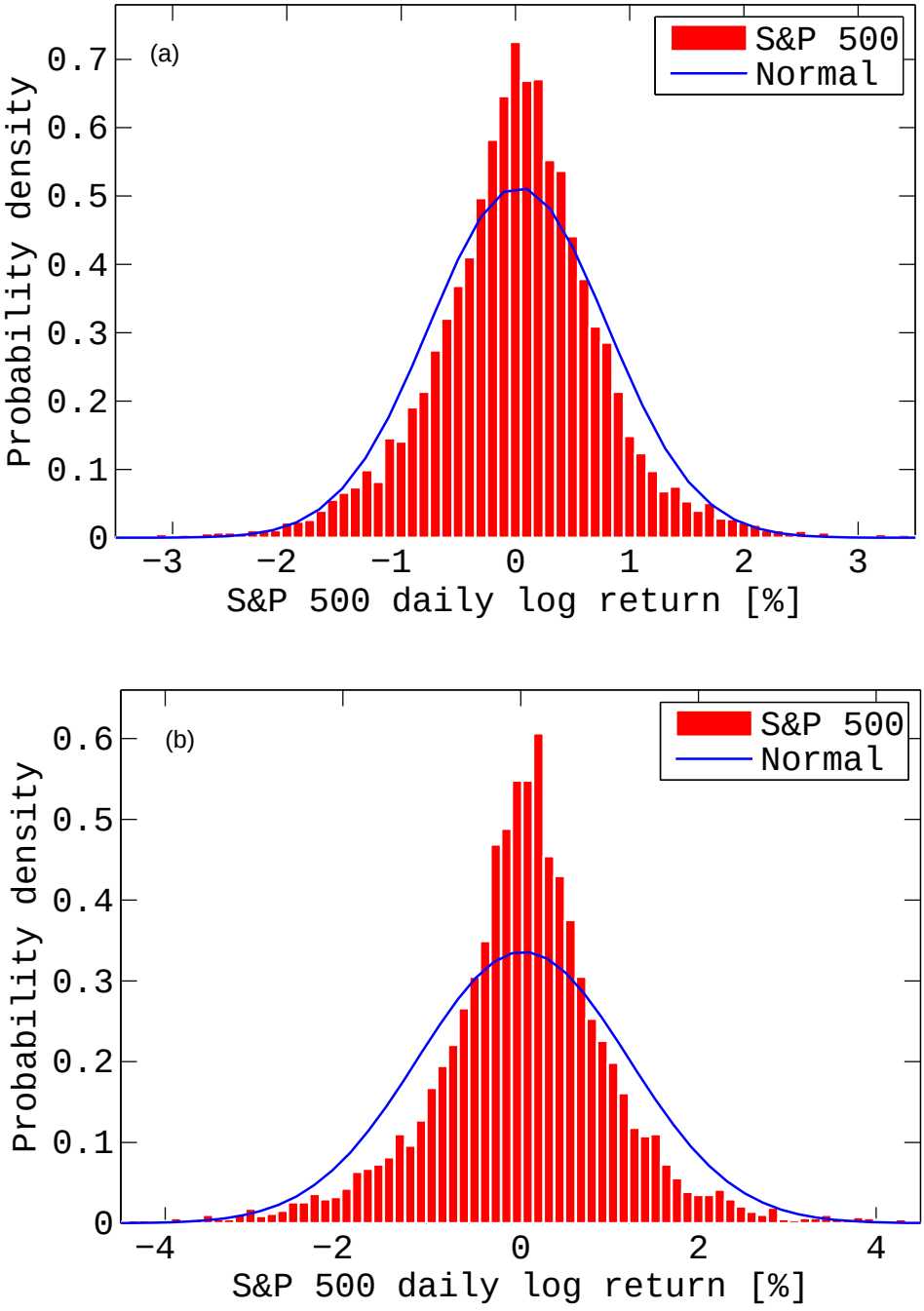

Figure 2.1: (a) Distribution of the S&P 500 index daily log return from January 2, 1950 to December 31, 1984. (b) Distribution of the S&P 500 index daily log return from January 2, 1985 to June 10, 2010. Neither distributions is normally distributed; rather they are skewed to left side and have a higher peak and fatter tails compared to a normal distribution.

return are shown on Figures 2.2 (a) and (b). It is noted that neither is normally distributed but the IBM daily log return for the period from 1962 to 1984 fits a normal distribution somewhat better than the IBM daily log return for the period from 1985 to 2010. Both distributions have a high peak and two fatter tails than those of normal distribution. But the distribution from 1985 to 2010 has a heavier high peak. In other words, it is much more distributed around zero return. For the time period from 1962 to 1984, the kurtosis of IBM is about 6.32, and the skewness is about 0.24. For the time period from 1985 to 2010, the kurtosis of IBM is about 16.5, and the skewness is about -0.46. The kurtosis is significantly higher for the latter period. Also the distribution is slightly skewed to right side for the earlier period but to the left side for the later period.

As discussed in Section 1.1, the daily return distribution, according to the Black-Scholes model, is expected to be a normal distribution (Hull, 2005). However, the distribution of S&P 500 daily log return as seen in Figures 2.1 (a) and (b), and the distribution of IBM stock daily log return as seen in Figures 2.2 (a) and (b) do not follow a normal distribution. A normal distribution is also shown for comparison in all these figures with μ and σ equal to the ML estimates. Note that the distribution for real data has a higher peak and fatter tails than those of the normal distribution. This means that there is a higher probability of zero return, and a large gain or loss compared to a normal distribution. Furthermore, as $\Delta t \to 0$, Geometric Brownian motion (Equation (1.1)) assumes that the probability of a large return also tends to zero. The amplitude of the return is proportional to $\sqrt{\Delta t}$, so that the tails of the distribution become unimportant. But, some large returns in small time increments can be seen in Figures 2.2 (a) and (b). It therefore appears that the Block-Scholes model is missing some important features.

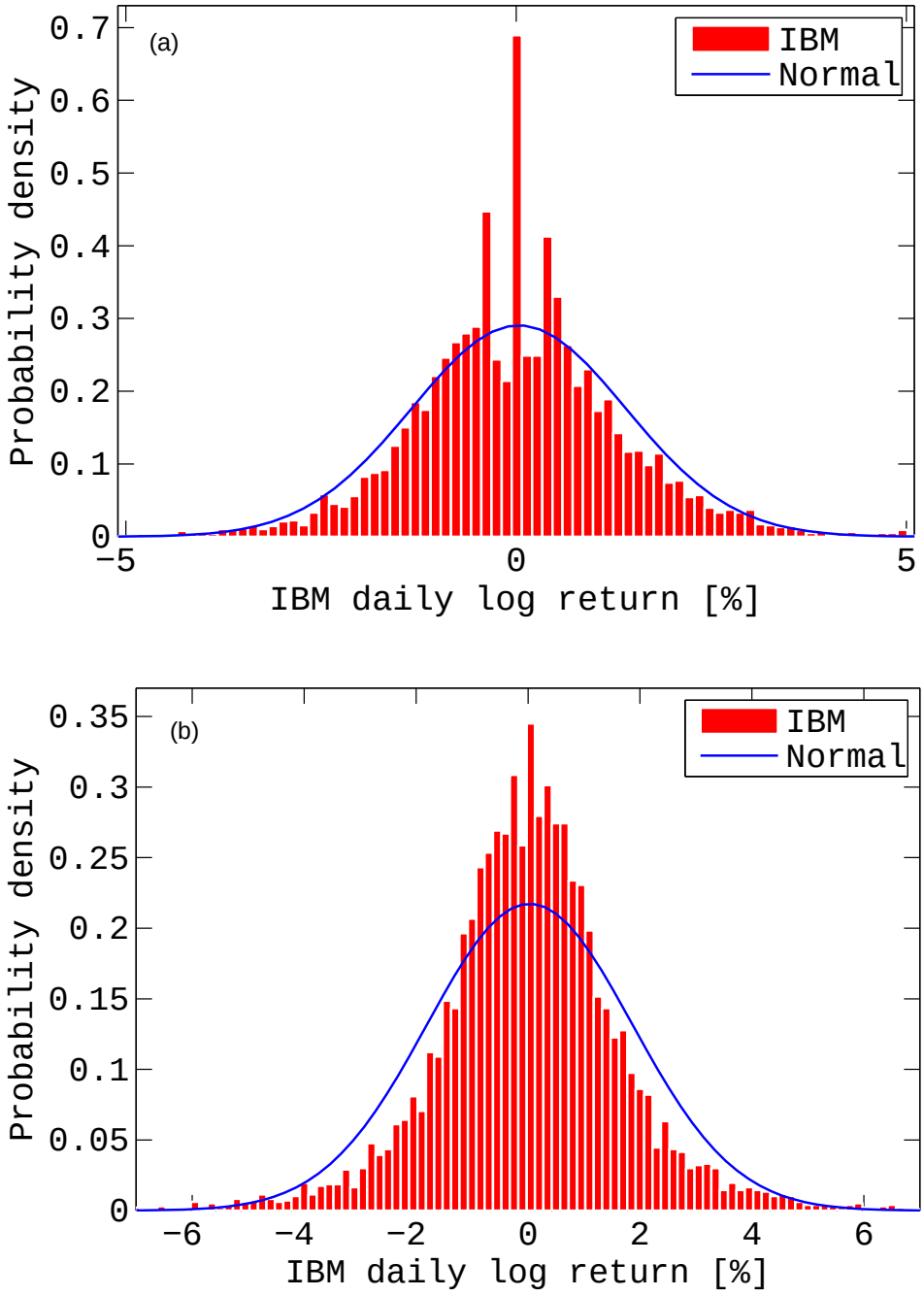

Figure 2.2: (a) Distribution of IBM daily log return from January 2, 1962 to December 31, 1984. (b) Distribution of IBM daily log return from January 2, 1985 to June 10, 2010. Neither distributions is normally distributed; they have a high peak and two fatter tails than those of normal distribution; but the high peak in (b) is heavier.

The leptokurtic features can also be proved by a quantile-quantile plot (Q-Q plot). The same data sets are used. A Q-Q plot of the S&P 500 index for the period from January 1985 to June 2010 is shown in Figure 2.3 (a), and a Q-Q plot of the IBM stock price for the period January 1985 to June 2010 is shown in Figure 2.3 (b). For a normal distribution, the plot should show a linear variation. However, as seen in Figures 2.3 (a) and (b), there is clearly a deviation from linear behavior.

The third proof of the feature is achieved by applying the Kolmogorov-Smirnov test (often referred to as KS-test) (Allen, 1978). By the Kolmogorov-Smirnov test, the values in the data vector x are compared to a standard normal distribution.

The null hypothesis is H_0 and the alternative hypothesis is H_1, where

$$\begin{cases} H_0: & x \text{ has a standard normal distribution,} \\ H_1: & x \text{ does not have a standard normal distribution.} \end{cases} \tag{2.3}$$

if the test statistic of the KS-test is greater than the corresponding critical value, the null hypothesis, H_0, is rejected at the 5% significance level; otherwise, the null hypothesis, H_0, is not rejected (Massey, 1951; Miller, 1956).

Lets define

$$x = \frac{r - \mu}{\sigma} \tag{2.4}$$

where r is daily log return, μ is the mean of daily log return, σ is a standard deviation of daily log return.

Based on a KS-test on the S&P 500 daily log return and the IBM stock daily log return, respectively, the null hypothesis is rejected in both cases. Therefore, it can be concluded that neither the daily log return of S&P 500 nor the daily log return

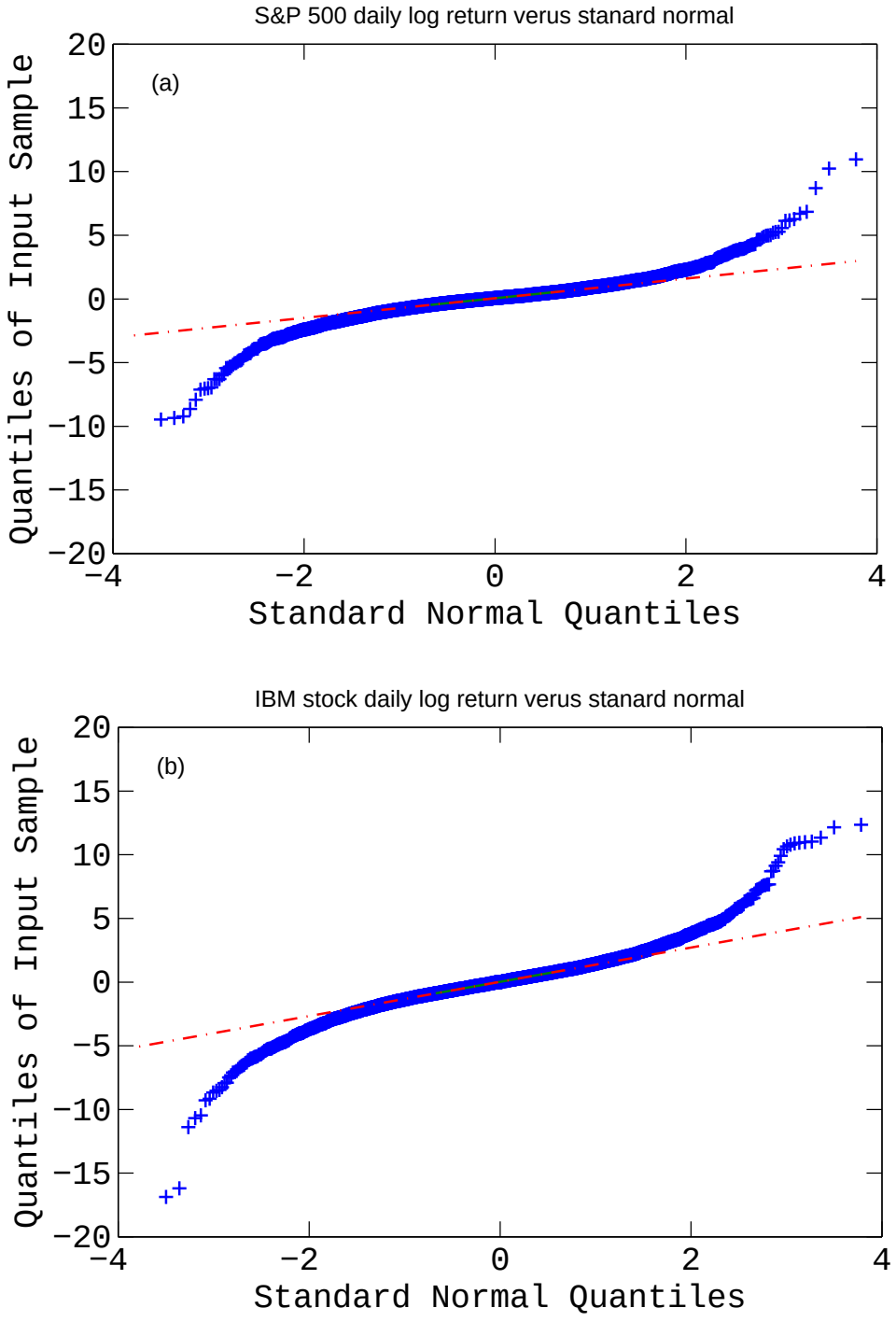

Figure 2.3: (a) A Q-Q plot of the S&P 500 daily log return from January 2, 1985 to June 10, 2010. (b) A Q-Q plot of the IBM stock daily log return from January 2, 1985 to June 10, 2010. If the distribution of daily return is normal, the plot should be close to linear. It is clear that neither plots is linear, therefore, they are not normally distributed.

of IBM stock are normally distributed.

2.1.2 The volatility smile

If the Black-Scholes model is correct, then the implied volatility should be constant. That is, the observed implied volatility curve should look flat (Kou and Wang, 2004). But, in reality, the implied volatility curve often looks like a smile or a smirk. A plot of the implied volatility of an option versus its strike price is known as a volatility smile when the plotted curve looks like a human smile (Derman, 2003; Hull, 2005).

Take the IBM call option as an example. For a 7-days maturity time, the IBM call option price versus the strike price is shown in Figure 2.4(a); the IBM implied volatility versus the strike price is shown in Figure 2.4(b), in which the "IBM volatility smile" is observed. For a 92-days maturity time, Figure 2.5(a) shows the IBM call option price versus the strike price and Figure 2.5(b) shows the IBM implied volatility versus the strike price, including the "IBM volatility smile". When the IBM implied volatility versus the strike price is plotted for 162-days and 422-days, the curve of the implied volatility looks more like a "volatility skew" than a "volatility smile", which are demonstrated in Appendix A.2 and A.3. That is, when the maturity time increase, the implied volatility monotonically decreases as the strike price increases (Hull, 2005).

The evolution of a "volatility smile" to a "volatility skew" with increasing maturity time is explored further in Figure 2.6. The x-axis is the time to maturity, the y-axis is the strike price, the z-axis is the implied volatility. A "volatility smile" for a short time to maturity can clearly be observed; as the time to maturity is increased the curve becomes more flat. For multiple maturities T and multiple strike

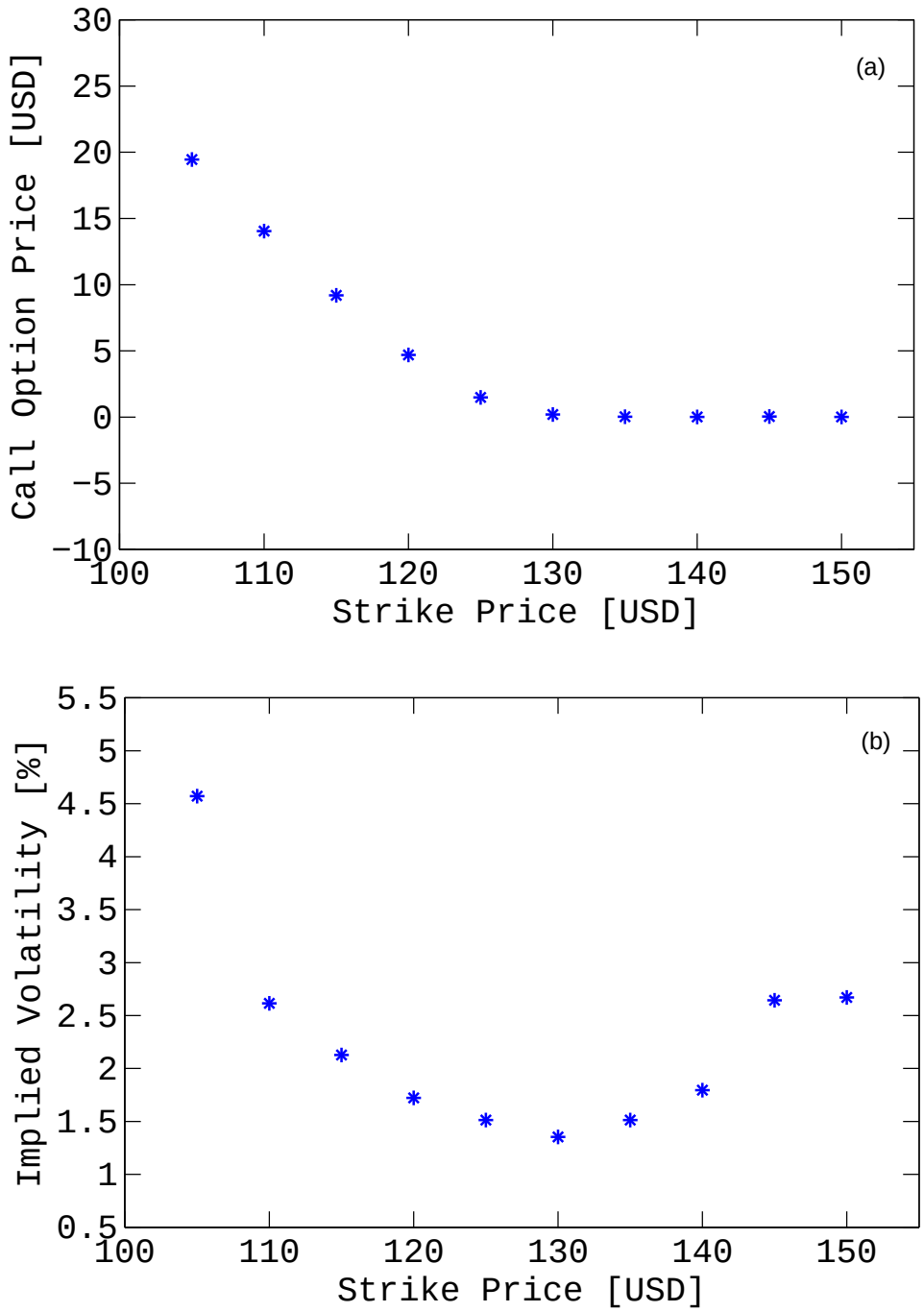

Figure 2.4: (a) The call option price versus the strike price for IBM stock. (b) The observed implied volatility curve. The implied volatility versus the strike price of IBM just looks like a human smile; it is called the "IBM Volatility smile". The date of the analysis is June 10, 2010; the expiration date is June 18, 2010; the time to maturity T is 7 days; the initial IBM stock price, S_0 is USD 123.9.

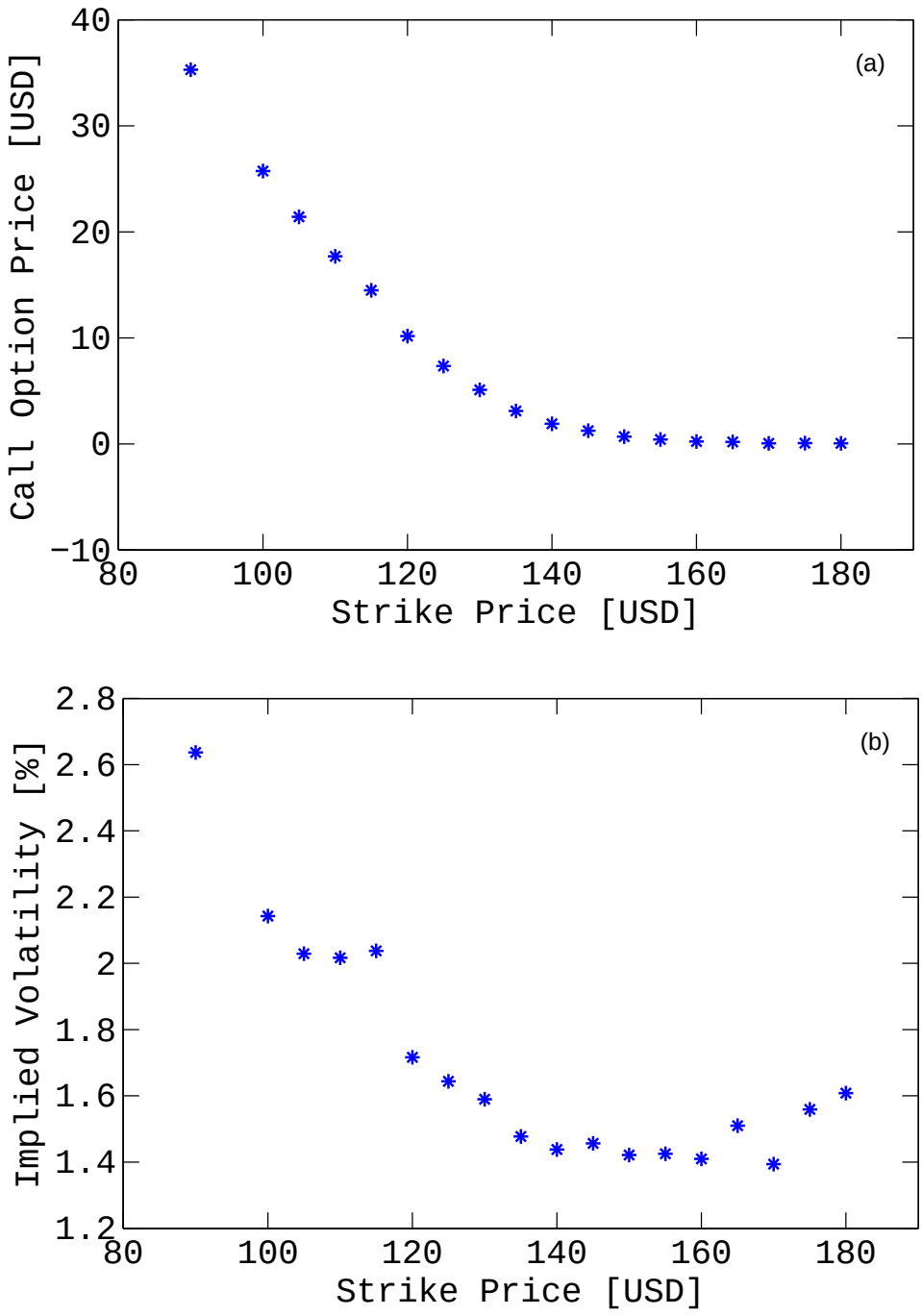

Figure 2.5: (a) The call option price versus the strike price for IBM stock. The observed implied volatility curve. The implied volatility versus the strike price of IBM just looks like a human smile; it is called the "IBM Volatility smile". The date of the analysis is June 10, 2010; the expiration date is October 15, 2010; the time to maturity T is 92 days; the initial IBM stock price, S_0 is USD 123.9.

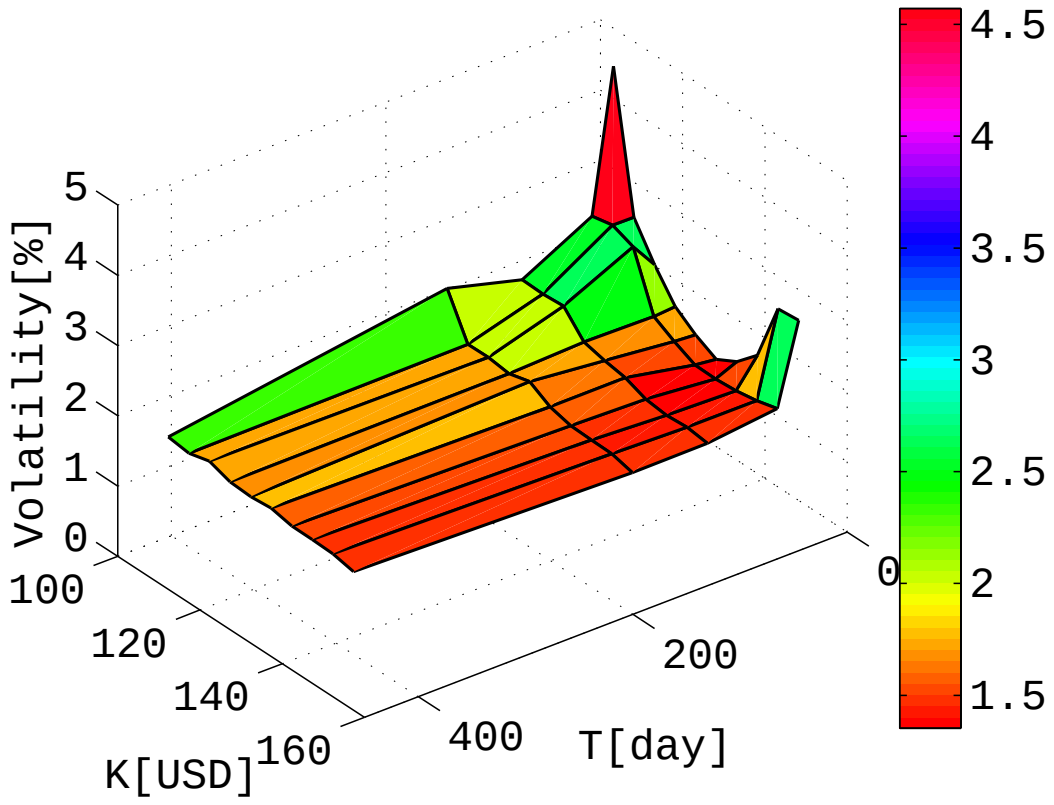

Figure 2.6: The observed 3-D IBM implied volatility with multiple maturities T and multiple strike prices K. It can be noted that the implied volatility plane is not flat and the implied volatility looks like a smile for shorter time to maturity T, but it becomes monotonously decreasing with increasing strike prices for longer time to maturity T.

prices K, when facing to the y-z plane (that is, the strike price - implied volatility plane), one notices that the curve looks more like a 'smile' as the maturity time is shorter, but the curve is more like a 'smirk' as the maturity time becomes longer. This phenomena is also discussed by Hull (2005) and by Andersen and Andersen (2000). One explanation for the smile in equity option concerns leverage. As a company's equity declines in value, the company's leverage increases. This means that the equity becomes more risky and its volatility increases. As a company's equity increase in value, leverage decreases. Then the equity becomes less risky and its volatility decreases (Hull, 2005).

2.2 What is the reason ?

From the observation of the two phenomena, it can be concluded that the Black-Scholes model is not completely correct in describing neither the market behavior such as S&P 500 nor the behavior of individual stock price such as IBM. What is missing in the Black-Scholes model ?

The first problem is that the Black-Scholes model ignores the jump part in the process of asset pricing caused by overreaction or underreaction due to good and/or bad news coming from the market and/or from an individual company. In other words, the Black-Scholes model is completely correct in an ideal situation without outside world information. Thus, an extra jump part must be added to the Black-Scholes model in order to give a response to the underreaction (attributed to the high peak) and the overreaction (attributed to the heavy tails) to outside news (Kou, 2002, 2008).

The time series plots of market data (S&P 500 index) and individual stock data (IBM) capture those jumps from good news or bad news, as seen in Figures 2.7 and 2.8. Figure 2.7 shows the temporal variation of the S&P 500 index from January 2005 to June 2010. There are indeed upward and downward jumps observed in the stock market such as the S&P 500 index; a big downward jump occurred around the global financial crisis in October 2008. Figure 2.8 shows the evolution of the IBM stock price from January 2005 to June 2010. The similar upward and downward jumps in the IBM stock price can be noticed, and the similar downward jump occurred around the global financial crisis time in October 2008.

These upward or downward jumps are also reflected in the daily log return time series plot, Figures 2.9 (a) and (b). Figure 2.9 (a) shows some upwards jumps (positive

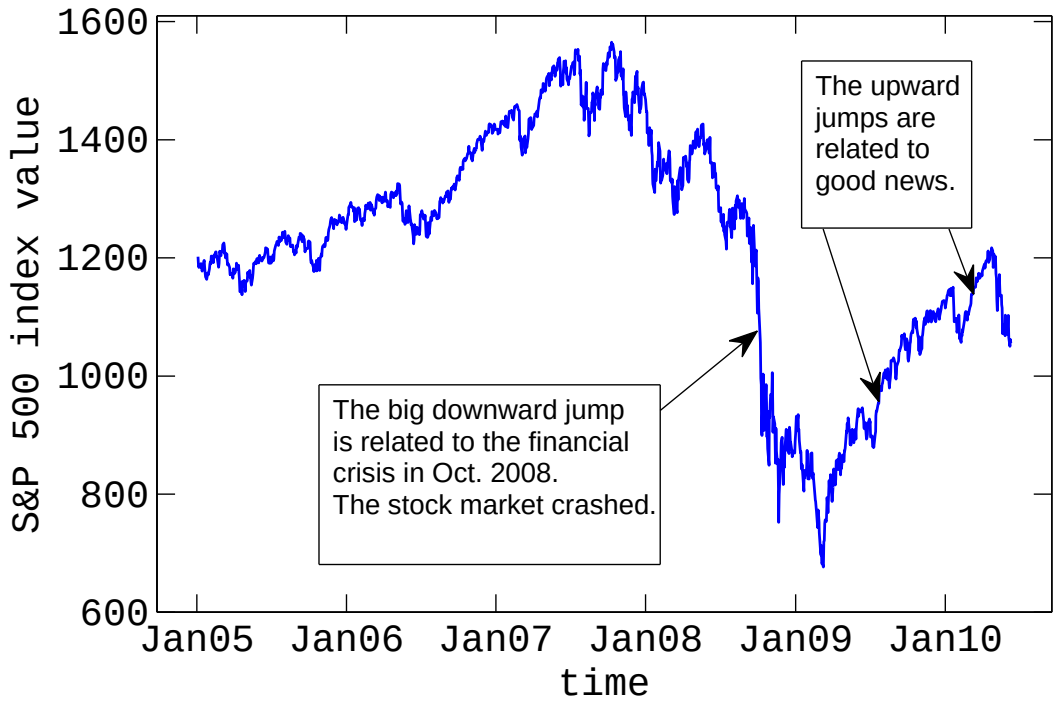

Figure 2.7: The time series of S&P 500 index value in January 2005 - June 2010. It can be observed that there are some upward and downward jumps in the market price during these years. In October 2008, there is a large downward jump indicating the stock market crash due to the global financial crisis.

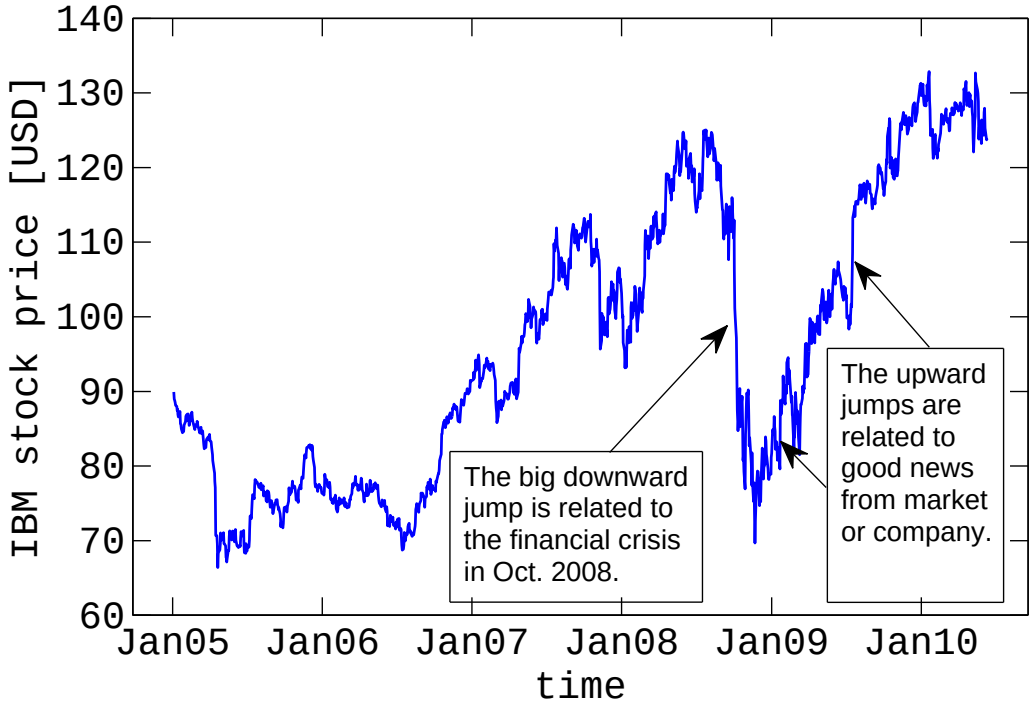

Figure 2.8: The time series of IBM stock price in January 2005 - June 2010. It can be observed that there are some upward and downward jumps in the IBM stock price during these years. In October 2008, there is a large jump downwards indicating that IBM stock was effected by the "Panic of 2008" due to the global financial crisis.

return) and some downwards jumps (negative return) in S&P 500 index value from 1985 to 2010. The biggest negative return is reflected in a large downward jump in the index value that is due to the stock market crash in October 1987. The spikes around October 2008 are related to the global financial crisis. Those upward and downward jumps were caused by the overreaction of investors. Figure 2.9 (b) shows some upwards jumps (positive return) and some downwards jumps (negative return) in IBM stock price from 1985 to 2010. The biggest spike is a huge downward jump in IBM stock price caused by the stock market crash in October 1987. There are a lot of spikes around 2000–2002; these spikes are upward and downward jumps in stock price related to the internet bubble bursts and the September 11 attacks. The same jumps are apparent in the IBM stock price as in the S&P 500 index value around the global financial crisis in October 2008. Throughout the period there are countless smaller spikes both upwards and downwards that are due to news from market and/or from individual companies. These jumps are ignored by the Black-Scholes model.

The second issue is that the volatility is assumed to be a constant in the Black-Scholes model, but it is stochastic in real life (Andersen and Andersen, 2000; Andersen and Brotherton-Ratcliffe, 1998; Andersen et al., 2002; Derman and Kani, 1994a,b; Dupire, 1994; Heston, 1993; Stein and Stein, 1991). Figures 2.4 (b), 2.5 (b) and 2.6 demonstrate how the implied volatility changes as the time to maturity and the strike prices increases. Therefore, it is necessary to improve the Black-Scholes model in order to capture the two empirical phenomena mentioned above (Kou, 2002; Maekawa et al., 2008, 2005).

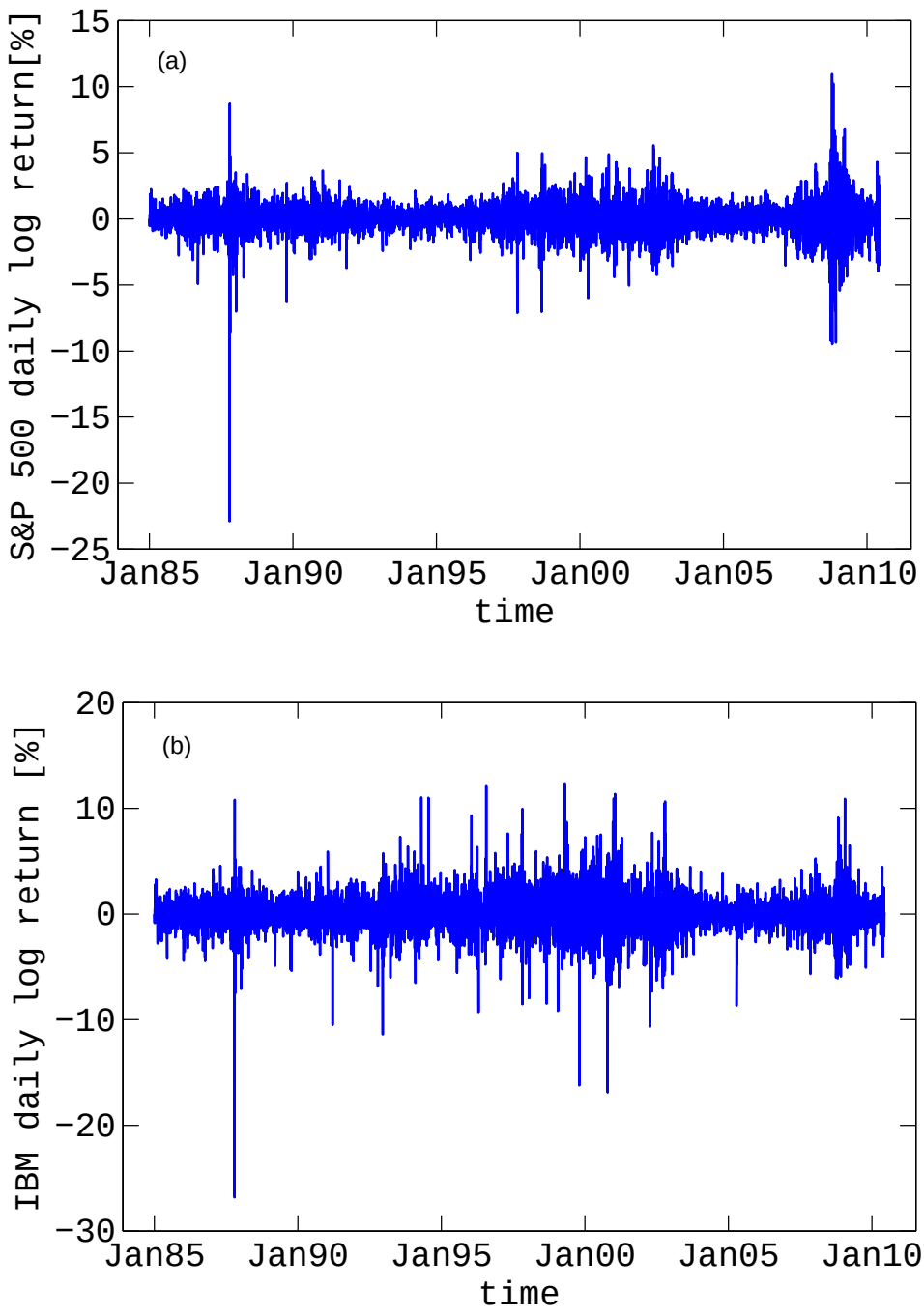

Figure 2.9: (a) The time series of the S&P 500 index daily log return. (b) The time series of the IBM stock daily log return. The spike around October 1987 indicates a large negative return. This is the biggest stock market crash in history. IBM stock is also affected by the crash. The spikes around 2001 are related to the internet bubble burst and the September 11 attacks. There are many downwards and upwards jumps around 2000 to 2002 according to bad news or good news. The spikes around October 2008 are caused by the global financial crisis.

3 Overview of the Models

Many studies have been conducted to modify the Black-Scholes model in order to explain the two empirical phenomena discussed in Chapter 2. In this chapter, some modifications to the Black-Scholes model will be summarized and their advantages and disadvantages will be discussed.

3.1 Jump diffusion Processes

To obtain more realistic models, researchers have added jumps to the Black-Scholes model. Merton (1976) suggested that asset price dynamics may be modeled as jump-diffusion process and proposed that an asset's returns process may be decomposed into three components; a linear drift, a Brownian motion representing "normal" price variations, and a compound Poisson process generating an "abnormal" change (jump) in asset prices due to the "news". The jump magnitudes are determined by sampling from an independent and identically distributed ($i.i.d.$) random variable. For the purpose of pricing options, Merton assumed that the jumps are log-normally distributed. This special case renders estimation and hypothesis testing tractable and has become the most important representation of the jump-diffusion process

(Rameszani and Zeng, 1998, 2006, 2007). Moreover, by adding discontinuous jumps to the Black-Scholes model and choosing the appropriate parameters of the jump process, the log normal jump models generate volatility smile or skew as described in Section 2.1.2. In particular, by setting the mean of the jump process to be negative, steep short-term skews are easily captured in this framework (Andersen and Andersen, 2000).

However, it is difficult to study the first passage times for log normal jump diffusion model when a jump diffusion crosses boundary level (that is, an overshoot). The overshoot makes it impossible to simulate the jump unless the exact distribution of the overshoot is obtained. Fortunately, the exponential distribution does not have the overshoot problem because of its memoryless property (Kou, 2008; Kou and Wang, 2004). This is one of the reasons why the double exponential jump diffusion model is popular. In this section, various jump diffusion models will be discussed.

3.1.1 Log-normal jump diffusions

Merton (1976) added Poisson jumps to a standard GBM process to approximate the movement of stock prices subject to occasional discontinuous breaks (Craine et al., 2000; Feng and Linetsky, 2008; Sepp, 2003; Tankov and Voltchkova, 2009).

$$\frac{dS}{S} = \mu dt + \sigma dW_t + J dq \tag{3.1}$$

where dq is a Poisson counter with intensity λ, i.e. $\mathbb{P}(dq = 1) = \lambda\, dt$, and J is a draw from a normal distribution, lets $y = \log(J)$, the logarithm of jump size is normally distributed:

$$g(y) = \frac{1}{\sqrt{2\pi\delta^2}} \exp\left(-\frac{(y-\nu)^2}{2\delta^2}\right) \tag{3.2}$$

where y is the logarithm of the jump size, ν is the mean of the logarithm of the jump size distribution, δ is the standard deviation of the logarithm of the jump size distribution.

Merton (1976) showed that it is possible for the jump diffusion to represent the price of a vanilla call or put as a weighted average of the standard Black-Scholes prices:

$$F(S,\sigma,\lambda,\tau)=\sum_{n=0}^{\infty}\frac{e^{-\lambda'\tau}(\lambda'\tau)^n}{n!}F_{\mathrm{BS}}(S,\sigma_n,r_n,\tau) \tag{3.3}$$

where $\lambda'=\lambda(1+m)$, $\sigma_n^2=\sigma^2+\frac{n\delta^2}{\tau}$, $r_n=r-\lambda m+\frac{n\log(1+m)}{\tau}$, $m=\exp\{\nu+\frac{1}{2\delta^2}\}-1$, $\tau=T-t$, F is call or put price in log-normal jump diffusion model, and F_{BS} is call or put price in Black-Scholes model.

3.1.2 Double exponential jump diffusion

In the double exponential jump diffusion model (Kou, 2002; Kou and Wang, 2004), the jump size has an asymmetric double exponential distribution.

The double exponential jump diffusion model has one more parameter than the log-normal jump diffusion, so it is able to produce more flexible smile shapes.

More details about the double exponential jump diffusion model will be given in Chapter 4.

3.1.3 Jump diffusion with a mixture of independent jumps

A jump diffusion with a mixture of independent price jumps with jump size J. Lets $y = \log(J)$, the probability density function is defined by Sepp (2003).

$$g(y) = \sum_{i=1}^{n} w_i g_i(y) \tag{3.4}$$

where w_i is a weight function, $\sum_{i=1}^{n} w_i = 1$, and $g_i(y)$ is a probability density function corresponding to the logarithm of an individual jump size.

3.2 Other models

The following models were introduced to reflect the empirical evidence that the volatility of asset returns is not constant. A complete survey of these models is provided by Ait-Sahalia (2002), Chernov et al. (2003), Eraker et al. (2003), Bakshi et al. (1997), Sepp (2003), and Garcia et al. (2004).

3.2.1 Stochastic volatility models

Stochastic volatility models assume that volatility itself is volatile and fluctuates towards a long-term mean. A number of models were proposed for the volatility dynamics, see Bakshi et al. (1997); Doran and Ronn (2005); Heston (1993); Hull and White (1987); Stein and Stein (1991). The most popular model among them

was developed by Heston (1993) as follows.

$$\begin{cases} dS(t) = (r_{\mathrm{f}} - d)S(t)dt + \sqrt{V(t)}S(t)dW^{s}(t), S(0) = S; \\ dV(t) = \kappa(\theta - V(t))dt + \varepsilon\sqrt{V(t)}dW^{v}(t), V(0) = V. \end{cases} \tag{3.5}$$

where r_{f} is the riskfree interest rate, d is a dividend rate, $S(t)$ is the asset (underlying) price, $V(t)$ is the diffusion component of return variance (conditional on no jump occurring), κ is a mean-reverting rate, θ is a long-term variance, ε is a volatility of volatility, $W^{s}(t)$ and $W^{v}(t)$ are correlated wiener processes with constant correlation ρ. That is, $\mathrm{Cov}[dW^{s}(t), dW^{v}(t)] = \rho$.

The advantage is that stochastic volatility models agreed with implied volatility surfaces with long-term smiles well. The implied smiles of these models are quite stable and unchanging over time (Broadie and Kaya, 2006). The disadvantage is that stochastic volatility models can not handle short-term smiles properly and that it is necessary to hedge stochastic volatility to replicate and price the option.

3.2.2 Jump diffusions with stochastic volatility

Bates (1996) added a jump part to these stochastic volatility models to make them more realistic:

$$\begin{cases} dS(t) = (r_{\mathrm{f}} - d)S(t)dt + \sqrt{V(t)}S(t)dW^{s}(t) + (e^{J} - 1)S(t)dN(t), S(0) = S; \\ dV(t) = \kappa(\theta - V(t))dt + \varepsilon\sqrt{V(t)}dW^{v}(t), V(0) = V. \end{cases} \tag{3.6}$$

where $N(t)$ is a Poisson process with constant intensity λ, λ is the frequency of jumps per year, J is jump amplitude (often referred to as jump size), m is the

average jump amplitude. Jumps can be drawn from either normal distribution or double exponential distribution.

These models combine the advantage and the disadvantage of both jumps and stochastic volatility. Therefore, they propose the most realistic dynamics for the smile. It has been also supported by numerous empirical studies, see e.g. Bates (1996), Fang (2000), and Duffie et al. (2000).

3.2.3 Jump diffusions with stochastic volatility and jump intensity

Based on the Bates model, Fang (2000) proposed a model with a stochastic jump intensity rate:

$$\begin{cases} dS(t) = (r_{\mathrm{f}} - d)S(t)dt + \sqrt{V(t)}S(t)dW^s(t) + (e^J - 1)S(t)dN(t), S(0) = S; \\ dV(t) = \kappa(\theta - V(t))dt + \varepsilon\sqrt{V(t)}dW^v(t), V(0) = V; \\ d\lambda(t) = \kappa_\lambda(\theta_\lambda - \lambda(t))dt + \varepsilon_\lambda\sqrt{V(t)}dW^\lambda(t), \lambda(0) = \lambda. \end{cases} \tag{3.7}$$

where κ_λ is a mean-reverting rate, θ_λ is a long-term intensity, ε_λ is volatility of jump intensity, a Wiener process $W^\lambda(t)$ is independent of $W^s(t)$ and $W^v(t)$. This is a very ambitious and complicated model, but it should be avoided in practice.

3.2.4 Jump diffusions with deterministic volatility and jump intensity

Jump diffusions with stochastic volatility result in two-dimensional pricing problem and quite complicated hedging strategy. This can be avoided by introducing time-dependent volatility and jump intensity:

$$\begin{cases} dS(t) = (r_{\mathrm{f}} - d)S(t)dt + \sqrt{V(t)}S(t)dW^s(t) + (e^J - 1)S(t)dN(t), S(0) = S; \\ dV(t) = \kappa(\theta - V(t))dt, V(0) = V; \\ d\lambda(t) = \kappa_\lambda(\theta_\lambda - \lambda(t))dt, \lambda(0) = \lambda. \end{cases} \tag{3.8}$$

This model provides a good fit to the data (Maheu and McCurdy, 2004).

3.2.5 Jump diffusions with price and volatility jumps

A jump diffusion model with both price and volatility jumps (SVJ) is proposed by Duffie et al. (2000).

$$\begin{cases} dS(t) = (r_{\mathrm{f}} - d - \lambda m)S(t)dt + \sqrt{V(t)}S(t)dW^s(t) + (e^{J^s} - 1)S(t)dN^s(t), S(0) = S; \\ dV(t) = \kappa(\theta - V(t))dt + \varepsilon\sqrt{V(t)}dW^v(t) + J^v dN^v(t), V(0) = V. \end{cases} \tag{3.9}$$

The general SVJ model includes four types of jumps: (a) jumps in the asset price; (b) jumps in the variance with exponentially distributed jump size; (c) double jumps model with jumps in the asset price and independent jumps in the variance with exponentially distributed jump size; (d) simultaneous jumps model with simultaneous correlated jumps in price and variance. This model provides a remarkable fit to

observed volatility surfaces. It is supported by a number of studies, see e.g. Duffie et al. (2000) and Eraker et al. (2003).

3.2.6 ARCH and GARCH model

The auto-regressive conditional heteroskedastic (ARCH) models were first introduced by Engle (1982). It assumes that today's conditional variance is a weighted average of past squared unexpected returns (Alexander, 2001):

$$\begin{cases} \sigma_t^2 = \alpha_0 + \alpha_1 \varepsilon_{t-1}^2 + \cdots + \alpha_p \varepsilon_{t-p}^2 \\ \alpha_0 > 0, \alpha_1, \cdots, \alpha_p \geq 0; \varepsilon_t | I_t \sim N(0, \sigma_t^2). \end{cases} \tag{3.10}$$

If a major market movement occurred yesterday, the day before yesterday, or up to p days ago, the effect is to increase today's conditional variance because all parameters are constrained to non-negative. It makes no difference whether the market moves upwards or downwards.

The full GARCH(p, q) adds q autoregressive terms to the ARCH(p), and the conditional variance equation takes the form (Alexander, 2001; Bollerslev, 1986).

$$\begin{cases} \sigma_t^2 = \alpha_0 + \alpha_1 \varepsilon_{t-1}^2 + \cdots + \alpha_p \varepsilon_{t-p}^2 + \beta_1 \sigma_{t-1}^2 + \cdots + \beta_q \sigma_{t-q}^2 \\ \alpha_0 > 0, \alpha_1, \cdots, \alpha_p, \beta_1, \cdots, \beta_q \geq 0. \end{cases} \tag{3.11}$$

However, it is rarely necessary to use more than a GARCH(1,1) model, which has just one lagged error square and one autoregressive term. The standard notation for GARCH(1,1) contains a constant ω, the GARCH error coefficient α and the

GARCH lag coefficient β, the GARCH(1,1) model is

$$\begin{cases} \sigma_t^2 = \omega + \alpha\varepsilon_{t-1}^2 + \beta\sigma_{t-1}^2 \\ \omega > 0, \alpha, \beta \geq 0. \end{cases} \tag{3.12}$$

More details about GARCH model will be presented in Chapter 6.

3.3 Summary

Various modifications to the Black-Scholes have been summarized. The main problem with most of these models is that it is difficult to obtain analytical solutions for option prices. More precisely, they might give some analytical formula for the standard European call and put options, but any analytical solutions for interest rate derivatives and path-dependent options, such as perpetual American options, barrier, and lookback options, are unlikely (Kou and Wang, 2004).

The double exponential jump diffusion model has desirable properties for both exotic options and econometric estimation. Its leptokurtic distribution has gained its popularity. Kou (2002), and Kou and Wang (2004) have shown that the model leads to nearly analytical option pricing formula for exotic and path dependent options. This is a significant advantage as most of the methods for pricing options under jump diffusion models are restricted to plain vanilla European options. Hence, the double exponential jump-diffusion model, is used in this study.

4 Double Exponential Jump Diffusion Model

Overview of the various models that have been developed to model the asset price dynamics was given in Chapter 3. In this chapter, the double exponential jump-diffusion model will be discussed in detail.

4.1 Model specification

Under the double exponential jump diffusion model, the dynamics of the asset price $S(t)$ are given by the stochastic differential equation (Kou, 2002; Kou and Wang, 2004)

$$\frac{dS(t)}{S(t-)} = \mu dt + \sigma dW(t) + d\left(\sum_{i=1}^{N(t)} (V_i - 1)\right) \tag{4.1}$$

where $W(t)$ is a standard Brownian motion, $N(t)$ is a Poisson process with rate λ, and $\{V_i\}$ is a sequence of independent identically distributed ($i.i.d.$) nonnegative random variables such that $Y = \log(V)$ has an asymmetric double exponential

distribution with density

$$f_Y(y) = p\eta_1 e^{-\eta_1 y}\mathbf{1}_{\{y\geq 0\}} + q\eta_2 e^{\eta_2 y}\mathbf{1}_{\{y<0\}} \tag{4.2}$$

$$\eta_1 > 1, \eta_2 > 0,$$

where $p,\ q \geq 0,\ p + q = 1$, represent the probabilities of upward and downward jumps, respectively. In other words,

$$\log(V) = Y \overset{\mathrm{d}}{=} \begin{cases} \xi+ & \text{with probability } p, \\ \xi- & \text{with probability } q. \end{cases} \tag{4.3}$$

where $\xi+$ and ξ- are exponential random variables with mean $1/\eta_1$, $1/\eta_2$, respectively, and the notation $\overset{\mathrm{d}}{=}$ means equal in distribution. In the model, the stochastic elements, $N(t)$, $W(t)$, and Y_{S} are assumed to be independent. For notational simplicity and in order to get analytical solutions for various option-pricing problems, the drift μ and volatility σ are assumed to be constants, and the Brownian motion and jumps are assumed to be one dimensional. The solution of the stochastic differential equation (equation (4.1)) is

$$S(t) = S(0)\exp\left\{\left(\mu - \frac{1}{2}\sigma^2\right)t + \sigma W(t)\right\}\prod_{i=1}^{N(t)} V_i \tag{4.4}$$

Note that

$$\mathbb{E}[Y] = \frac{p}{\eta_1} - \frac{q}{\eta_2}, \quad \mathbb{V}[Y] = pq\left(\frac{1}{\eta_1} + \frac{1}{\eta_2}\right)^2 + \left(\frac{p}{\eta_1^2} + \frac{q}{\eta_2^2}\right), \tag{4.5}$$

and

$$\mathbb{E}[V] = \mathbb{E}[e^Y] = q\frac{\eta_2}{\eta_2 + 1} + p\frac{\eta_1}{\eta_1 - 1}, \quad \eta_1 > 1, \quad \eta_2 > 0. \tag{4.6}$$

Again $\eta_1 > 1$ is required to ensure that $\mathbb{E}[V] < \infty$ and $\mathbb{E}[S(t)] < \infty$; this means that the average rate of upward jump can not exceed 100%.

4.2 Leptokurtic feature

The rate of return during the time interval Δt is derived from equation (4.4) and is given as (Kou and Wang, 2004)

$$\begin{aligned}\frac{\Delta S(t)}{S(t)} &= \frac{S(t+\Delta t)}{S(t)} - 1 \\ &= \exp\left\{\left(\mu - \frac{1}{2}\sigma^2\right)\Delta t + \sigma(W(t+\Delta t) - W(t)) + \sum_{i=N(t)+1}^{N(t+\Delta t)} Y_i\right\} - 1\end{aligned}$$

If the time interval Δt is sufficiently small, the higher order items can be omitted using the expansion

$$e^x = 1 + \frac{x}{1!} + \frac{x^2}{2!} + \cdots \approx 1 + x + \frac{x^2}{2}$$

and the return can be approximated by

$$\frac{\Delta S(t)}{S(t)} \approx \mu\Delta t + \sigma Z\sqrt{\Delta t} + B \cdot Y \tag{4.7}$$

where Z is a standard normal random variable and B is a Bernoulli random variable, with $\mathbb{P}(B = 1) = \lambda\Delta t$, $\mathbb{P}(B = 0) = 1 - \lambda\Delta t$ and Y is given by equation (4.3).

4.3 Option pricing

The double exponential jump diffusion model yields a closed form solution for the European call and put options, which can be obtained in terms of the Hh function. In this section, the Hh function will be introduced, and then the option-pricing formula will be derived.

4.3.1 Hh functions

For every $n \geq 0$, the Hh function is a nonincreasing function defined by, (see Kou (2002))

$$\begin{aligned} &\mathrm{Hh}_n(x) = \int_x^\infty \mathrm{Hh}_{n-1}(y)dy = \frac{1}{n!}\int_x^\infty (t-x)^n e^{-t^2/2}dt \geq 0, \quad n = 0, 1, 2, ... \\ &\mathrm{Hh}_{-1}(x) = e^{-x^2/2} = \sqrt{2\pi}\varphi(x), \\ &\mathrm{Hh}_0(x) = \sqrt{2\pi}\Phi(-x), \end{aligned} \tag{4.8}$$

The Hh function can be viewed as a generalization of the cumulative normal distribution function.

A three-term recursion is also available for the Hh function, (see Kou (2002)).

$$n\mathrm{Hh}_n(x) = \mathrm{Hh}_{n-2}(x) - x\mathrm{Hh}_{n-1}(x), \quad n \geq 1. \tag{4.9}$$

Therefore, all $\mathrm{Hh}_n(x)$, for $n \geq 1$, can be computed by using the normal density function and normal distribution.

4.3.2 European call and put options

First the following notation is introduced. For any given probability $\mathbb{P}$, lets define

$$\Upsilon(\mu, \sigma, \lambda, p, \eta_1, \eta_2; a, T) = \mathbb{P}\{\mathrm{Z}(T) \geq a\},$$

where $\mathrm{Z}(t) = \mu t + \sigma W(t) + \sum_{i=1}^{N(t)} Y_i$, Y has a double exponential distribution with density $f_{\mathrm{Y}}(y) = p \centerdot \eta_1 e^{-\eta_1 y} \mathbf{1}_{\{y \geq 0\}} + q \centerdot \eta_2 e^{\eta_2 y} \mathbf{1}_{\{y<0\}}$, and $N(t)$ is a Poisson process with rate λ. The pricing formula of call option will be expressed in terms of Υ, which can be derived as a sum of Hh functions (Kou, 2002).

Theorem 4.3.1 *The European call price is given by (Kou, 2002)*

$$\begin{aligned} \psi_c(0) = S(0)\Upsilon\left(r + \frac{1}{2}\sigma^2 - \lambda\xi, \sigma, \tilde{\lambda}, \tilde{p}, \tilde{\eta_1}, \tilde{\eta_2}; \log(K/S(0)), T\right) \\ - Ke^{-rT}\Upsilon\left(r - \frac{1}{2}\sigma^2 - \lambda\xi, \sigma, \lambda, p, \eta_1, \eta_2; \log(K/S(0)), T\right) \end{aligned} \tag{4.10}$$

where

$$\tilde{p} = \frac{p}{1+\xi} \cdot \frac{\eta_1}{\eta_1 - 1}, \quad \tilde{\eta_1} = \eta_1 - 1, \quad \tilde{\eta_2} = \eta_2 + 1,$$
$$\tilde{\lambda} = \lambda(\xi + 1), \quad \xi = \frac{p\eta_1}{\eta_1 - 1} + \frac{q\eta_2}{\eta_2 + 1} - 1.$$

The price of European put option, $\psi_p(0)$, can be obtained by the put-call parity (Bodie et al., 2008):

$$\begin{aligned} \psi_p(0) - \psi_c(0) &= e^{-rT}\mathrm{E}^*((K - S(T))^+ - (S(T) - K)^+) \\ &= e^{-rT}\mathrm{E}^*(K - S(T)) = Ke^{-rT} - S(0). \end{aligned}$$

Therefore, the following Theorem is obtained.

Theorem 4.3.2 *The price of European put option is*

$$\begin{aligned}\psi_p(0) &= Ke^{-rT} - S(0) + \psi_c(0) \\ &= Ke^{-rT} - S(0) + S(0)\Upsilon\left(r + \frac{1}{2}\sigma^2 - \lambda\xi, \sigma, \tilde{\lambda}, \tilde{p}, \tilde{\eta_1}, \tilde{\eta_2}; \log(K/S(0)), T\right) \\ &- Ke^{-rT}\Upsilon\left(r - \frac{1}{2}\sigma^2 - \lambda\xi, \sigma, \lambda, p, \eta_1, \eta_2; \log(K/S(0)), T\right)\end{aligned} \tag{4.11}$$

The surfaces of call prices estimated by the Black-Scholes model, and the Kou model are shown in Figures 4.1 (a) and (b), respectively. For comparison the surface of the market call price is shown in Figure 4.2. The surface of the call price estimated by Kou model shows a closer appearance to that of the market call price. The difference between the call prices estimated by the Kou model and the call prices estimated by the Black-Scholes model is shown in Figure 4.3.

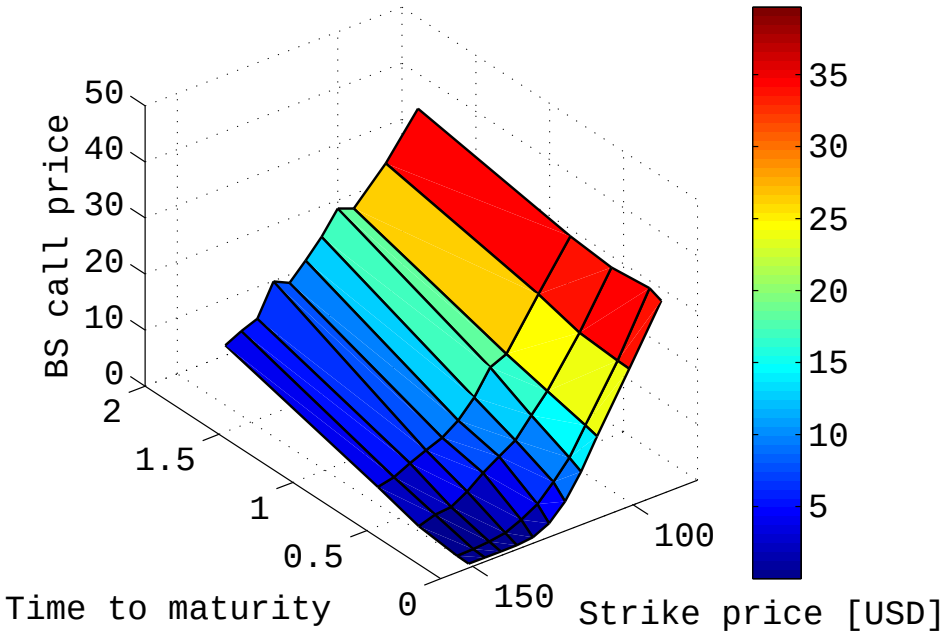

(a)

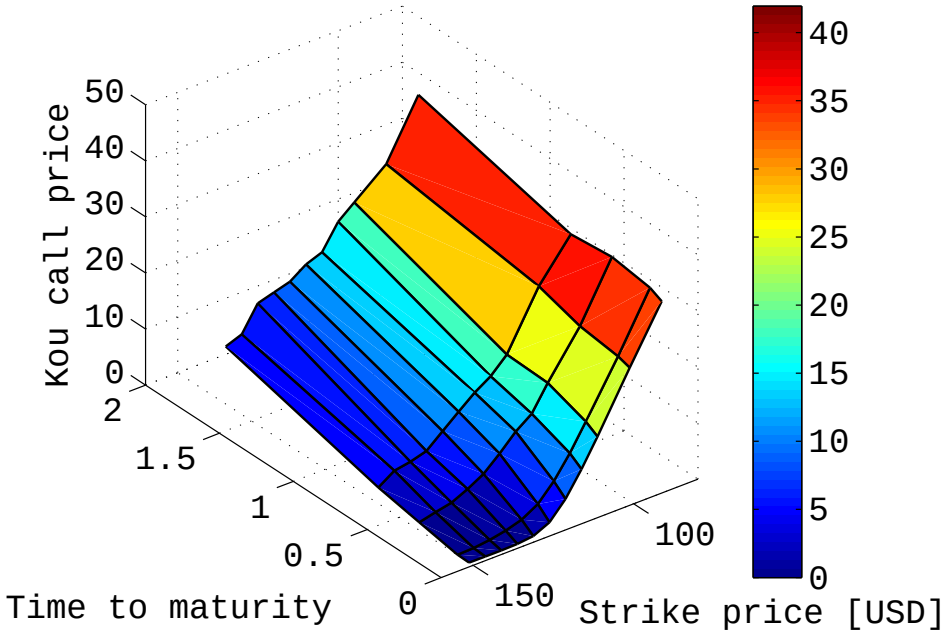

(b)

Figure 4.1: The surface of the IBM call prices, (a) estimated by the Black-Scholes model (b) estimated by the Kou model. The time to maturity T is $0 \sim 2$ years; the strike price K is USD $80 \sim 160$; the call price is USD $0 \sim 50$.

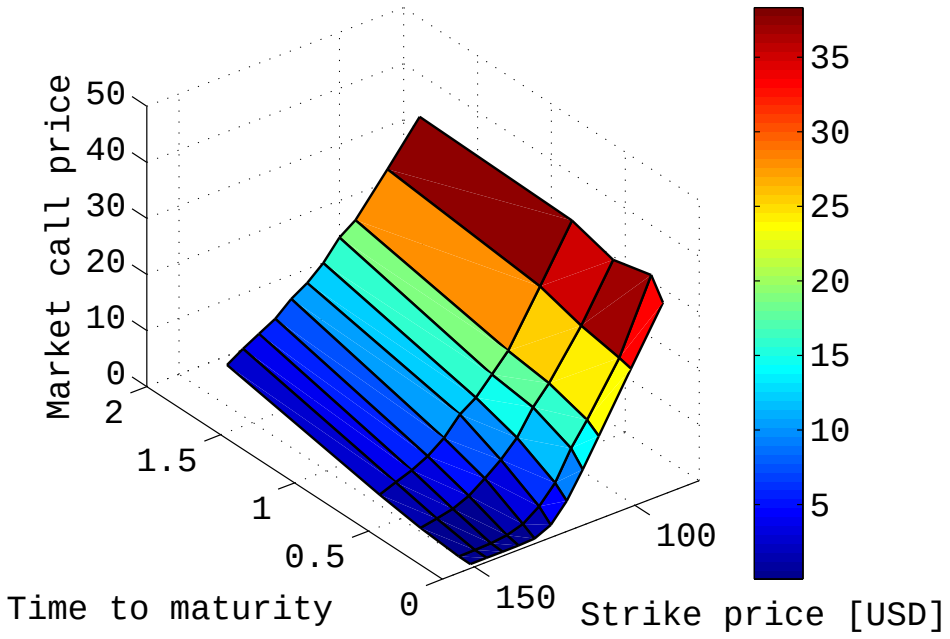

Figure 4.2: The surface of the IBM market call prices. The time to maturity T is $0 \sim 2$ years; the strike price K is USD $80 \sim 160$; the call price is USD $0 \sim 50$.

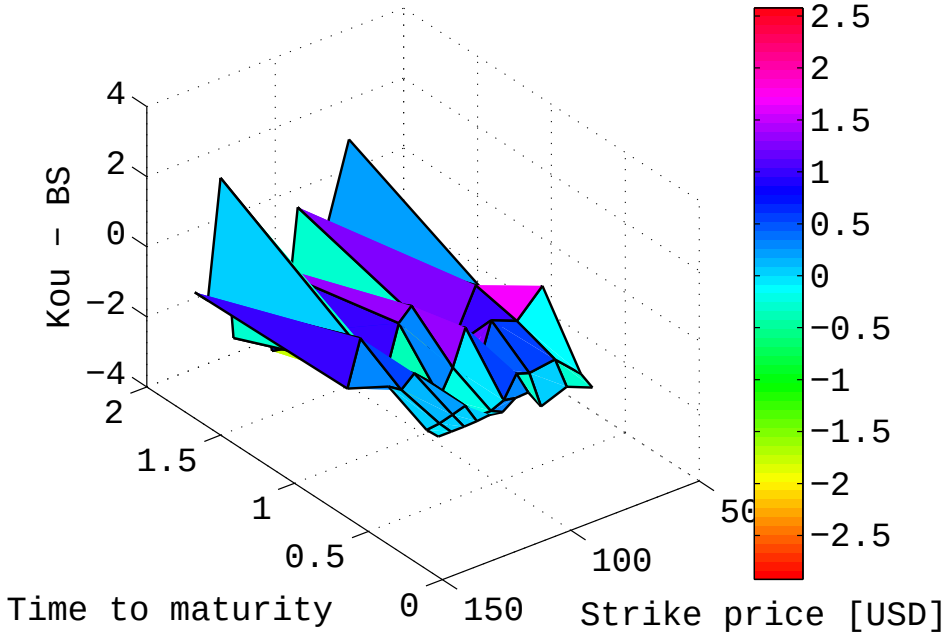

Figure 4.3: The difference of the call prices calculated by applying the Kou model and the Black-Scholes model. The time to maturity T is $0 \sim 2$ years; the strike price K is USD $80 \sim 160$; the call price is USD $0 \sim 50$.

4.4 The advantages of the double exponential jump diffusion model

The double exponential jump diffusion model has the following advantages (Kou, 2002):

- The model is simple enough to be amenable to computation. Like the Black-Scholes model, the double exponential jump diffusion model not only yields a closed-form solutions for standard European call and put options, but also leads to a variety of closed-form solutions for path-dependent options, such as, barrier options, lookback options, and perpetual American options, as well as interest rate derivatives (swaptions, caps, floors, and bond options).
- The model captures the important empirical phenomena - the asymmetric leptokurtic feature, and the volatility smile. The double exponential jump diffusion model is able to reproduce the leptokurtic feature of the return distribution and the "volatility smile" observed in option prices. In addition, some empirical tests suggest that the double exponential jump diffusion model fits stock data better than the normal jump diffusion model (Kou, 2008).
- The model can be embedded into a rational expectations equilibrium framework (Kou and Wang, 2004).
- The model has some economical, physical, and psychological interpretations. One motivation for the double exponential jump diffusion model comes from behavioral finance. It has been suggested from extensive empirical studies that markets tend to have both overreaction and underreaction to various good and bad news. One may interpret the jump part of the model as the market response to outside news. More precisely, in the absence of outside news the

asset price simply follows a geometric Brownian motion. Good and bad news arrives according to a Poisson process, and the asset price changes in response according to the jump size distribution. Because the double exponential distribution has both a high peak and heavy tails, it can be used to model both the overreaction (attributed to the heavy tails) and the underreaction (attributed to the high peak) to outside news. Therefore, the double exponential jump diffusion model can be interpreted as an attempt to build a simple model, within the traditional random walk and efficient market framework, to incorporate investors' sentiment (Kou, 2002, 2008).

5 Monte Carlo Simulation

Monte Carlo simulation is based on statistical sampling, and it may be visualized as a black box in which a stream of pseudorandom numbers enters and an estimation is obtained by analyzing the output. Typically, it is used to estimate an expected value with respect to an underlying probability distribution; for instance, an option price may be evaluated by computing the expected value of the payoff with respect to a risk-neutral probability measure (Brandimarte, 2002). Monte Carlo simulation is well suited to valuing path-dependent options and options where there are many stochastic variables (Hull, 2005).

Compared to other numerical methods, Monte Carlo simulation has several advantages. First, it is easy to implement and use. In most situations, if the sample paths from stochastic process model can be simulated, then the value can be estimated. Second, its rate of convergence typically does not depend on the dimensionality of the problem. Therefore, it is often attractive to apply Monte Carlo simulation to problems with high dimensions (Chen and Hong, 2007).

In order to estimate a financial value by Monte Carol simulation, there are typically three steps: generating sample paths, evaluating the payoff along each path, and calculating an average to obtain estimation (Chen and Hong, 2007; Glasserman,

2003; McLeish, 2005).

In this chapter, the Monte Carol simulation will be applied to the Black-Scholes model and the double exponential jump diffusion model. First, the implementation and the algorithm to simulate both models will be discussed. Then their fitness and pricing errors will be compared.

5.1 Monte Carlo simulation of the Black-Scholes model

5.1.1 Implementation of the Black-Scholes model using Monte Carlo simulation

The payoff of a derivative usually depends on the future prices of the underlying asset. Consider an European call option, whose payoff is max{S_T - K, 0 }, where S_T is the price of a stock at time T, and K is a prespecified amount called the strike price. The option gives its owner the right to buy the stock at time T for the strike price K: if $S_T > K$, the owner will exercise this right, and if not, the option expires worthless (Staum, 2002; Ugur, 2008).

If the future payoff of a derivative derives from the underlying asset, is there a way to derive the present price of the derivative from the current value of the underlying asset? A basic theorem of mathematical finance states that this price is the expectation of the derivative's discounted payoff under a risk–neutral measure (Boyle et al., 1997; Staum, 2002).

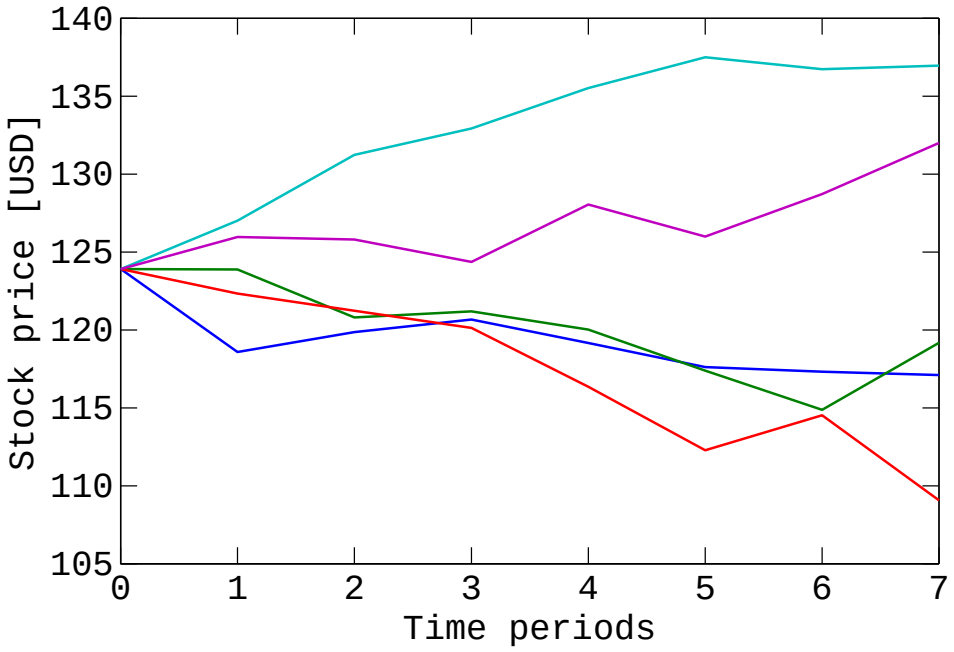

Figure 5.1: Monte Carlo simulation of the IBM stock price paths by applying the Black-Scholes model. The date of analysis is June 10, 2010; the expiration date is June 18, 2010; the time to maturity, $T = 7$; the initial stock price, $S_0 =$ USD 123.9; the historical volatility is 0.018; the simulation takes 5 random paths.

The standard Monte Carlo approach to evaluate such expectations is to simulate a state vector which depends on the underlying variables under risk–neutral measure, then to evaluate the sample average of the derivative's payoff over all trials. This is an unbiased estimation of the derivative's price, and when the number of trials n is large, the Central Limit Theorem provides a confidence interval for the estimation, based on the sample variance of the discounted payoff. The standard error is then proportional to $1/\sqrt{n}$ (Brandimarte, 2006).

In a risk-neutral world, μ in equation (1.1) can be replaced by the riskfree interest rate r_f in order to make more economic sense (Baz and Chacko, 2004). The Black-Scholes option pricing model then becomes (Forsyth, 2008; Luenberger, 1998; Staum, 2002),

$$\frac{dS_t}{S_t} = r_\mathrm{f} dt + \sigma dW_t, \tag{5.1}$$

where W_t is a Wiener process under the risk-neutral probability measure $\mathbb{Q}$.
By applying Ito's formula, the following equation is derived,

$$d \log S_t = (r_\mathrm{f} - \sigma^2/2)dt + \sigma dW_t \tag{5.2}$$

or,

$$\log S_t - \log S_{t-1} = (r_\mathrm{f} - \sigma^2/2)dt + \sigma dW_t \tag{5.3}$$

and then,

$$S_t = S_{t-1} \exp((r_\mathrm{f} - \sigma^2/2)\Delta t + \sigma \Delta W_t) \tag{5.4}$$

where W_t is normally distributed with mean 0 and variance t. Therefore, pricing the European call/put option under the Black-Scholes model requires the generation of one standard normal random variable for each path at each time period. The generated process is shown in Figure 5.1.

The simulated value of S_T on path i is

$$S_T^{(i)} = S_0 \exp\left((r_\mathrm{f} - \sigma^2/2)T + \sigma\sqrt{T}Z^{(i)}\right) \tag{5.5}$$

where $Z^{(i)}$ is a standard normal random variable.

The estimated European call option price is

$$c = \mathrm{e}^{-r_\mathrm{f}T} \cdot \frac{1}{n}\sum_{i=1}^{n} \max\{S_\mathrm{T}^{(i)} - K, 0\}^+ \tag{5.6}$$

and the estimated European put option price is

$$p = \mathrm{e}^{-r_\mathrm{f}T} \cdot \frac{1}{n}\sum_{i=1}^{n} \max\{K - S_\mathrm{T}^{(i)}, 0\}^+ \tag{5.7}$$

5.1.2 Algorithm to simulate the Black-Scholes model

1. Set the number of paths, (e.g. $paths = 1000$);
2. Set the length of time interval, $\Delta t = 1$;
3. Set the time to maturity, T, (e.g. $T = 7$);
4. Using Moving Average algorithm, calculate historical volatility, σ
5. Calculate the drift, $\mu = r_\mathrm{f} - 0.5 \times \sigma^2$, where r_f is the riskfree interest rate, usually, it is the annual interest rate of the three months Treasury Bill;
6. Create $paths \times m$ normal random variables, where $m = T/\Delta t$ time periods, here $m = T$;
7. Calculate each path daily log return, the daily log return on the path i and at time period t is
$$r_t^{(i)} = \mu\Delta t + \sigma\sqrt{\Delta t} \cdot Z_t^{(i)};$$

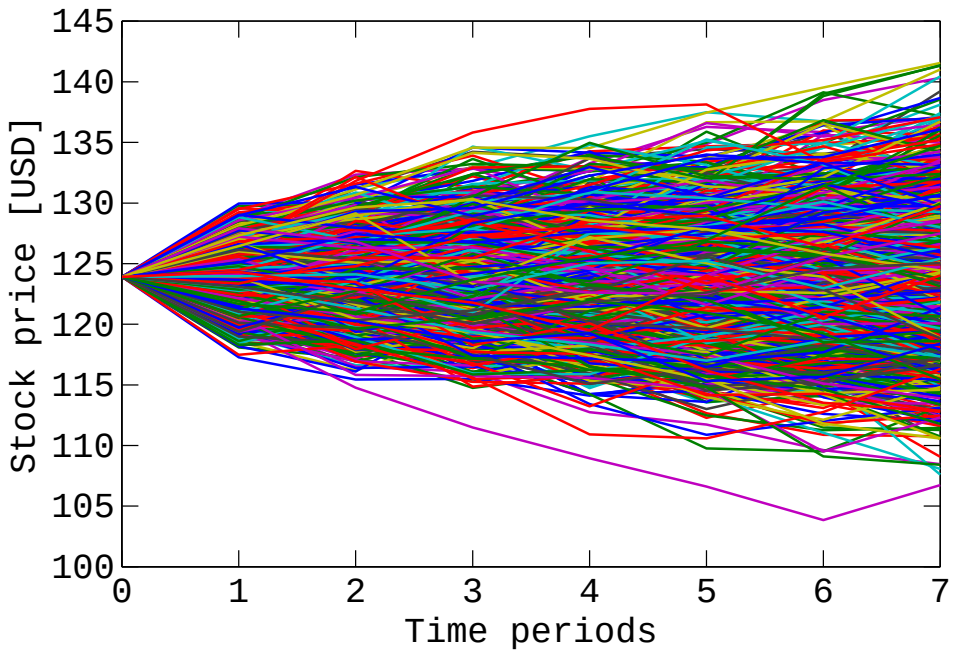

Figure 5.2: Monte Carlo simulation of the IBM stock price paths by applying Black-Scholes model. The date of analysis is June 10, 2010; the expiration date is June 18, 2010; the time to maturity, $T = 7$; the initial stock price, $S_0 =$ USD 123.9; the historical volatility is 0.018; the simulation takes 1000 random paths.

8. Calculate each path stock prices, for example, the stock prices on path i are S_1^i, S_2^i, $\cdots$, S_T^i.

   The daily return factor on path i at time period t is

$$\mathrm{DRF}_t^{(i)} = \exp\left(r_t^{(i)}\right)$$

   The stock price on path i at time period t is

$$S_t^{(i)} = S_{t-1}^{(i)} \times \mathrm{DRF}_t^{(i)}$$

9. Calculate the payoff of each path, see Figure 5.2,

   the call option payoff of path i is $\max\{S_T^i - K, 0\}$,

   the put option payoff of path i is $\max\{K - S_T^i, 0\}$.

10. The call price is the expectation of the payoff of these random paths,

$$c = \frac{1}{n}\sum_{i=1}^{n} \mathrm{e}^{-r_f T}\max\{S_{\mathrm{T}}^{(i)} - K, 0\}$$

    The put price is the expectation of the payoff of these random paths,

$$p = \frac{1}{n}\sum_{i=1}^{n} \mathrm{e}^{-r_f T}\max\{K - S_{\mathrm{T}}^{(i)}, 0\}$$

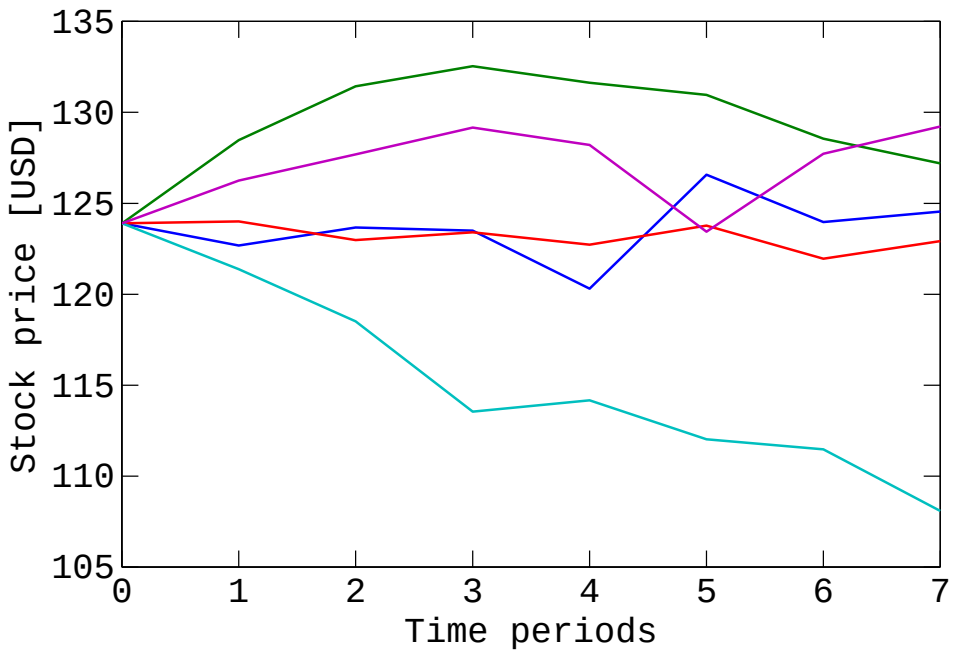

Figure 5.3: Monte Carlo simulation of the IBM stock price paths by applying the double exponential jump model. The date of analysis is June 10, 2010; the expiration date is June 18, 2010; the time to maturity, $T = 7$; the initial stock price, $S_0 =$ USD 123.9; the historical volatility is 0.018; the simulation takes 5 random paths.

5.2 Monte Carol simulation of the double exponential jump diffusion model

5.2.1 Implementation of the double exponential jump diffusion model using Monte Carlo simulation

Recall the double exponential jump model from equation (4.7), and rewrite the equation as

$$\frac{dS_t}{S_t} = \mu dt + \sigma dW_t + B \cdot Y \tag{5.8}$$

where W_t is normally distributed with mean 0 and variance t, B is a Bernoulli random variable, with $\mathbb{P}(B = 1) = \lambda\Delta t$, $\mathbb{P}(B = 0) = 1 - \lambda\Delta t$, and Y is given by equation (4.3). From Equation (5.8), the following equation can be derived,

$$\log S_t - \log S_{t-1} = (r_{\mathrm{f}} - \sigma^2/2)dt + \sigma dW_t + B \cdot Y \tag{5.9}$$

or,

$$S_t = S_{t-1} \exp\left((r_{\mathrm{f}} - \sigma^2/2)\Delta t + \sigma Z\sqrt{\Delta t} + B \cdot Y\right) \tag{5.10}$$

where Z is a standard normal random variable. Therefore, pricing the European call option under the double exponential jump model requires the generation of one standard normal random variable for each path at each time period. The generated process is shown in Figure 5.3. The simulated value of S_T on the ith path is given as

$$S_T^{(i)} = S_0 \exp\left((r_{\mathrm{f}} - \sigma^2/2)T + \sigma\sqrt{T}Z_t^{(i)} + B \cdot Y\right) \tag{5.11}$$

the estimated call option price is

$$c = \frac{1}{n}\sum_{i=1}^{n} \mathrm{e}^{-r_f T} \max\{S_{\mathrm{T}}^{(i)} - K, 0\}^+ \tag{5.12}$$

and the estimated put option price is

$$p = \frac{1}{n}\sum_{i=1}^{n} \mathrm{e}^{-r_f T} \max\{K - S_{\mathrm{T}}^{(i)}, 0\}^+ \tag{5.13}$$

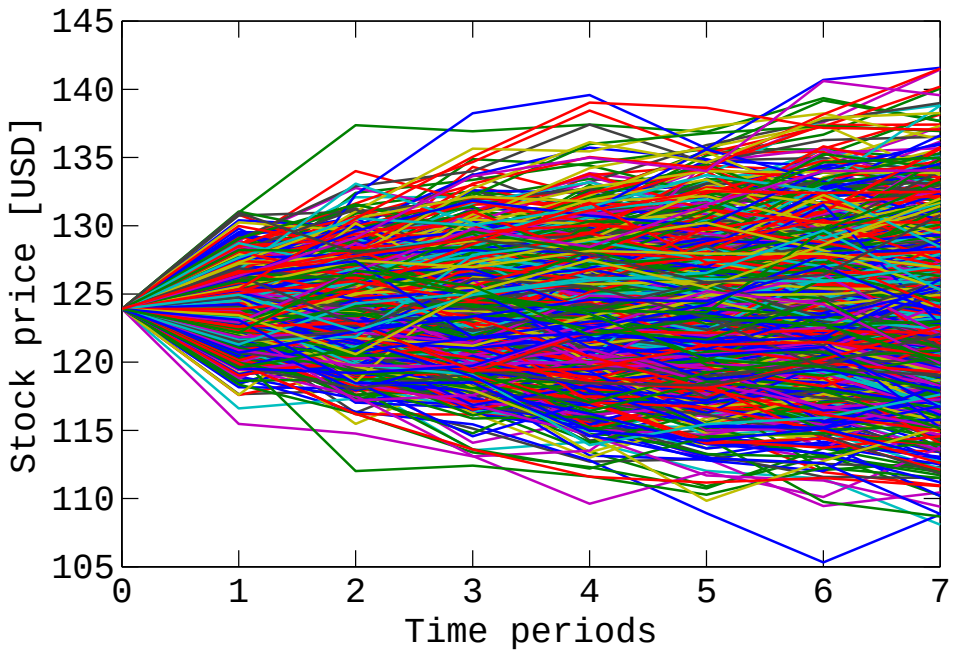

Figure 5.4: Monte Carlo simulation of the IBM stock price paths by applying the double exponential jump model. The date of analysis is June 10, 2010; the expiration date is June 18, 2010; the time to maturity, $T = 7$; the initial stock price, $S_0 =$ USD 123.9; the historical volatility is 0.018; the simulation takes 1000 random paths.

5.2.2 Algorithm to simulate the double exponential jump diffusion model

In the jump diffusion model, a jump part is added into the daily return factor, the algorithm for the jump model is shown as follows:
Steps $1 \sim 6$ are the same as for the Black-Scholes model described in Section 5.1.2;

7. Create the Jump part, $B \cdot Y$, where B is a Bernoulli random variable, and Y is an asymmetric double exponential random variable with probability p upwards and with probability $1-p$ downwards, see equation (4.3);
   (a) create a function with probability p upwards, and with probability $1-p$ downwards
   (b) create the double exponential function
   (c) create the function for a jump event, '$y = 1$' means 'a jump', '$y = 0$' means 'no jump'
8. Calculate each path daily log return, the daily return on path i at time period t is,
$$r_t^{(i)} = \mu\Delta t + \sigma\sqrt{\Delta t} \cdot Z_t^{(i)} + (B \cdot Y)_t^{(i)};$$
9. Calculate each path stock prices, for example, the stock prices on path i are S_1^i, S_2^i, $\cdots$, S_T^i.
   The daily return factor on path i at time period t is
$$\mathrm{DRF}_t^{(i)} = \exp\left(r_t^{(i)}\right)$$

The stock price on path i at time period t is

$$S_t^{(i)} = S_{t-1}^{(i)} \times \mathrm{DRF}_t^{(i)}$$

10. Calculate the payoff of each path, see Figure 5.4,
    the call option payoff of path i is $\max\{S_T^i - K, 0\}$,
    the put option payoff of path i is $\max\{K - S_T^i, 0\}$.

11. The call price is the expectation of the payoff of these random paths,

$$c = \frac{1}{n}\sum_{i=1}^{n} \mathrm{e}^{-r_f T}\max\{S_{\mathrm{T}}^{(i)} - K, 0\}$$

The put price is the expectation of the payoff of these random paths,

$$p = \frac{1}{n}\sum_{i=1}^{n} \mathrm{e}^{-r_f T}\max\{K - S_{\mathrm{T}}^{(i)}, 0\}$$

5.3 The fitness of the option prices: the Black-Scholes model versus the Kou model

In this simulation, the date of analysis is June 10, 2010; the expiration date is October 15, 2010; the time to maturity is 92 trading days. The initial IBM stock price S_0 was USD 123.9. The strike prices versus the market call prices is shown in Figure 2.5(a). The daily riskfree interest rate r_{f} is 7.3016e-005; the daily historical volatility σ is 0.018. 1000 random paths are used; the simulation processes of the stock prices applying the Black-Scholes model and applying the Kou model are shown in Figures 5.2 and 5.4, respectively.

When the time to maturity is 92 days, the comparison of the call prices estimated by the Black-Scholes model and the Kou model is shown in Figure 5.5. It can be observed that the call price estimated by Kou model is closer to the market call price. The comparison of the pricing errors between the call prices estimated by Black-Scholes model and the market prices and the pricing errors between the call prices estimated by Kou model and the market call prices is shown in Figures 5.6 (a) and (b). From these figures, it can be noted that the call price estimated by the Kou model is slightly closer to the market price than the call price estimated by the Black-Scholes model to the market price. In other words, the difference between the call price estimated by the Kou model and the market price is less than the difference between the call price estimated by the Black-Scholes model and the market call price. In a more precise way, this will be confirmed by calculating the residual sum of squares (RSS). For a 92-days maturity time, the RSS for the Black-Scholes model is 10.07 and the RSS for the Kou model is 6.42.

For multiple time to maturity ($T = 7, 27, 92, 162, 422$ days) and multiple strike prices ($K =$ USD $90, 100, 110, 115, 120, 125, 130, 135, 140, 145, 150$). the call prices estimated by the Black-Scholes model and the call prices estimated by the Kou model are shown in Figures 4.1(a) and 4.1(b), respectively. When comparing both figures with the market prices, shown in Figure 4.2, the call option price estimated by the Kou model is closer to the market price than the call option price estimated by the Black-Scholes model to the market price.

Furthermore, the difference between the call price estimated by Black-Scholes model and the market call price, and the difference between the call price estimated by Kou model and the market call price with multiple strike price (K) and multiple time to maturity (T) are shown in Figures 5.7 (a) and (b), respectively.

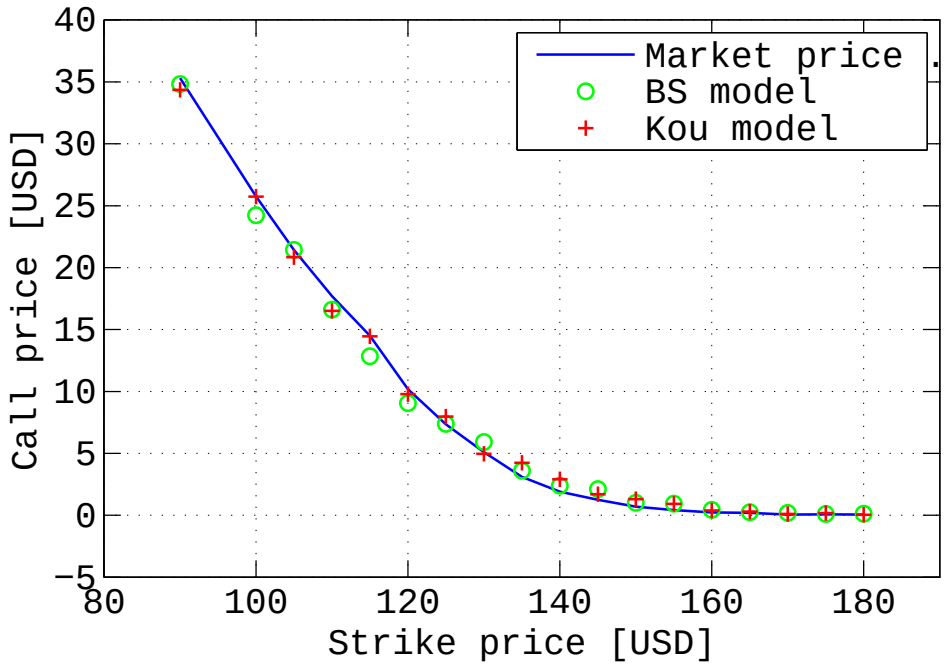

Figure 5.5: Comparison of the call option price estimated by the Black-Scholes model (o) and the Kou model (+). The solid line shows the market call price. It can be observed that the call option price estimated by Kou model is closer to the market call price.

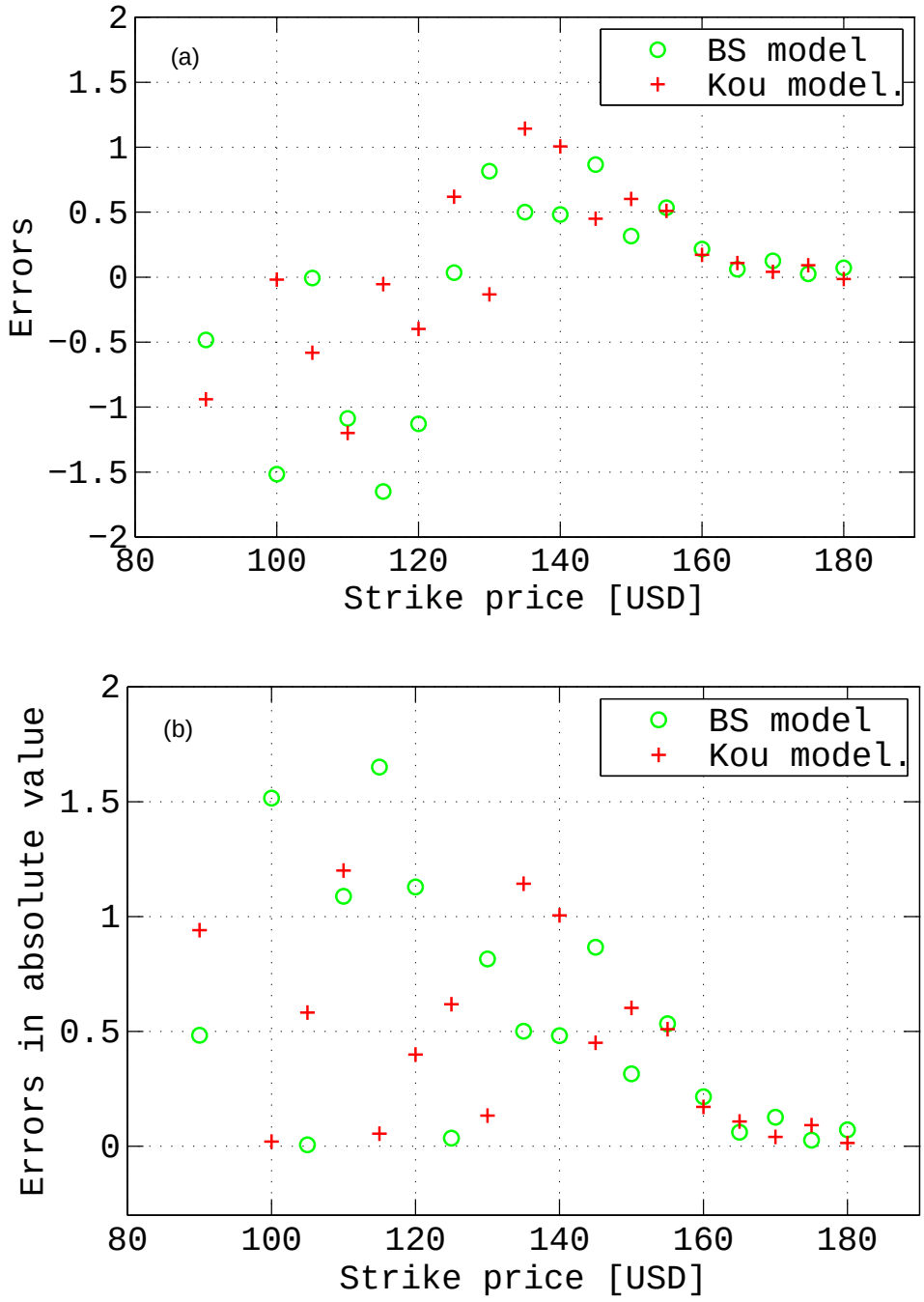

Figure 5.6: Comparison of the pricing errors. The pricing errors between the call price estimated by the Black-Scholes model and the market call price (o), the pricing errors between the call price estimated by the Kou model and the market call price (+). (a). The real values. (b). The absolute values.

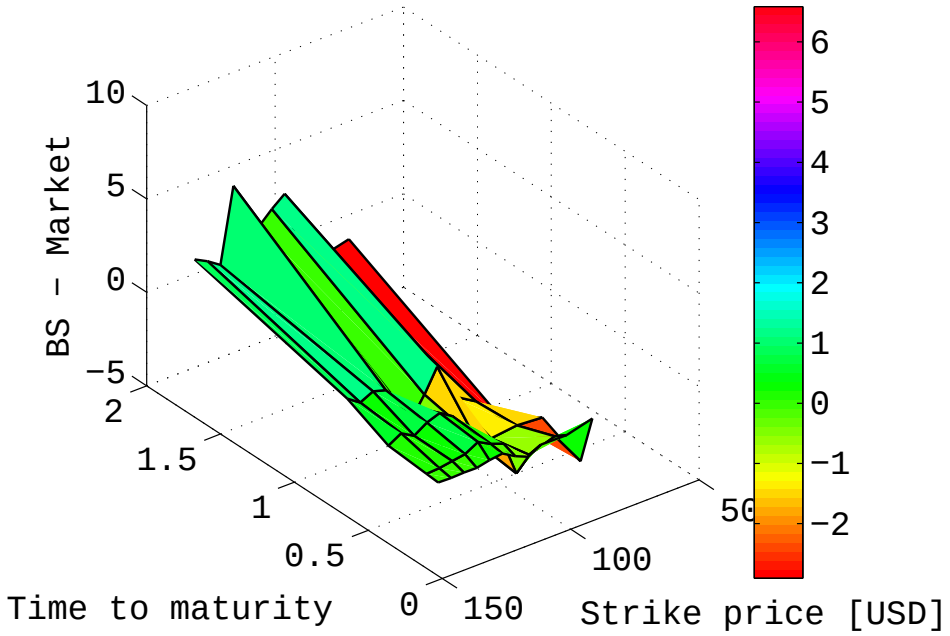

(a)

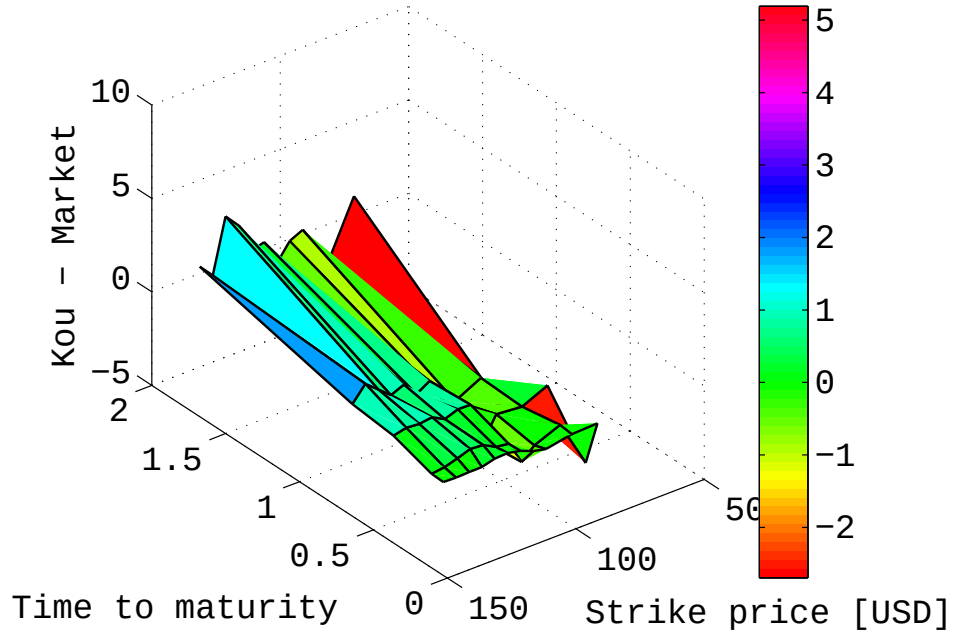

(b)

Figure 5.7: (a) Differences between call prices estimated by the Black-Scholes model and the market call prices. (b) Differences between call prices estimated by the Kou model and the market call prices. The time to maturity T is $0 \sim 2$ years; the strike price K is USD $80 \sim 160$; the call prices is USD $0 \sim 50$.

5.4 Comparing the errors from Black-Scholes model and from Kou model

With multiple time to maturity T and multiple strike price K, the comparison of the pricing errors from the estimation by the Black-Scholes model and the pricing errors from the estimation by the Kou model is shown in Figure 5.8.

The residual sum of squares (RSS) is calculated by

$$\text{RSS} = \sum_{i=1}^{n} \hat{\varepsilon}_i^2 = \sum_{i=1}^{n} (y_i - \hat{y}_i)^2, \tag{5.14}$$

When comparing the residual sum of squares (RSS) from the difference between the call price estimated by the Black-Scholes and the market call price, and from the difference between the call price estimated by the Kou model and the market call price, the Kou model shows better performance than the Black-Scholes model when comparing the RSS. This is substantiated by the results shown in Table 5.1. The data shows that the RSS for the Kou model is significantly lower than the RSS for the Black-Scholes model for all times to maturity. Therefore, the conclusion is that the call price estimated by the Kou model is closer to the market call price than the call price estimated by the Black-Scholes model. More comparison of the two models will be presented in Section 7.4.

Table 5.1: RSS comparison for the Black-Scholes model and the Kou model

RSS	T=7	T=27	T=92	T=162	T=422
Black-Scholes	1.07	17.76	10.07	111.08	169.02
Kou model	0.49	15.32	6.42	72.57	130.35

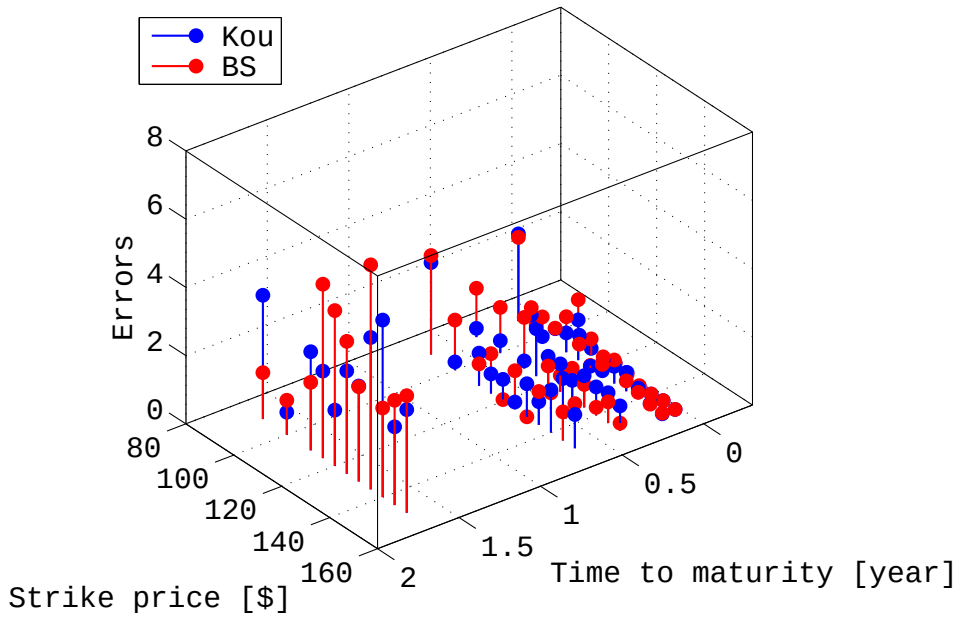

Figure 5.8: The comparison of the absolute value of the pricing errors estimated by the Kou model and the Black-Scholes model with multiple time to maturity and multiple strike prices. The time to maturity T is $0 \sim 2$ years; the strike price K is USD $80 \sim 160$; the call prices is USD $0 \sim 50$.

6 GARCH

The ARCH and GARCH models have been briefly discussed in Section 3.2.6. In this chapter, the GARCH model will be used to develop a stochastic volatility model.

6.1 What is GARCH ?

GARCH stands for Generalized Autoregressive Conditional Heteroscedasticity. Loosely speaking, "heteroscedasticity" can be taken as a time-varying variance (or, volatility); "conditional" implies a dependence on the observations of the immediate past; "autoregressive" describes a feedback mechanism that incorporates past observations into the present. Thus, GARCH is a mechanism that includes past variances in the explanation of future variance (Bollerslev, 1986; Bollerslev et al., 1992; McMillan, 2002; Zhuang and Chan, 2004).

More specifically, GARCH is a time-series technique that allows users to model the serial dependence of volatility. Whenever a time series is said to have GARCH effects, the series is heteroscedastic, i.e. its variances vary with time.

6.2 Why use GARCH ?

GARCH models are designed to capture certain characteristics that are commonly associated with financial time series (Bollerslev, 1986; Engle, 2001; Franses and van Dijk, 2000; Zivot and Wang, 2005):

- Fat tails – the probability distribution for asset returns often exhibit fatter tails than those of standard normal distribution, which were referred to as leptokurtic feature and discussed in Section 2.1.1, and were demonstrated in Figures 2.2 (a) and (b).
- Volatility clustering – large changes tend to follow large changes, and small changes tend to follow small changes. In either case, the changes from one period to the next are typically of unpredictable sign. Large disturbances, positive or negative, become part of the information set used to construct the variance forecast of the next period's disturbance. This can be seen in Figure 6.1 (a). Volatility clustering implies a strong autocorrelation in squared returns, so this can be detected by the first-order autocorrection coefficient in squared returns (Alexander, 2001). Also see Figure 6.2 (c).
- Leverage effects – asset returns are often observed to be negatively correlated with volatility change. That is, the volatility tends to rise in response to bad news and fall in response to good news (Xekalaki and Degiannakis, 2010). This can be seen in Figure 6.1 (b). For example, as the bad news were coming around the 2008 financial crisis, the volatility rose significantly at that time.

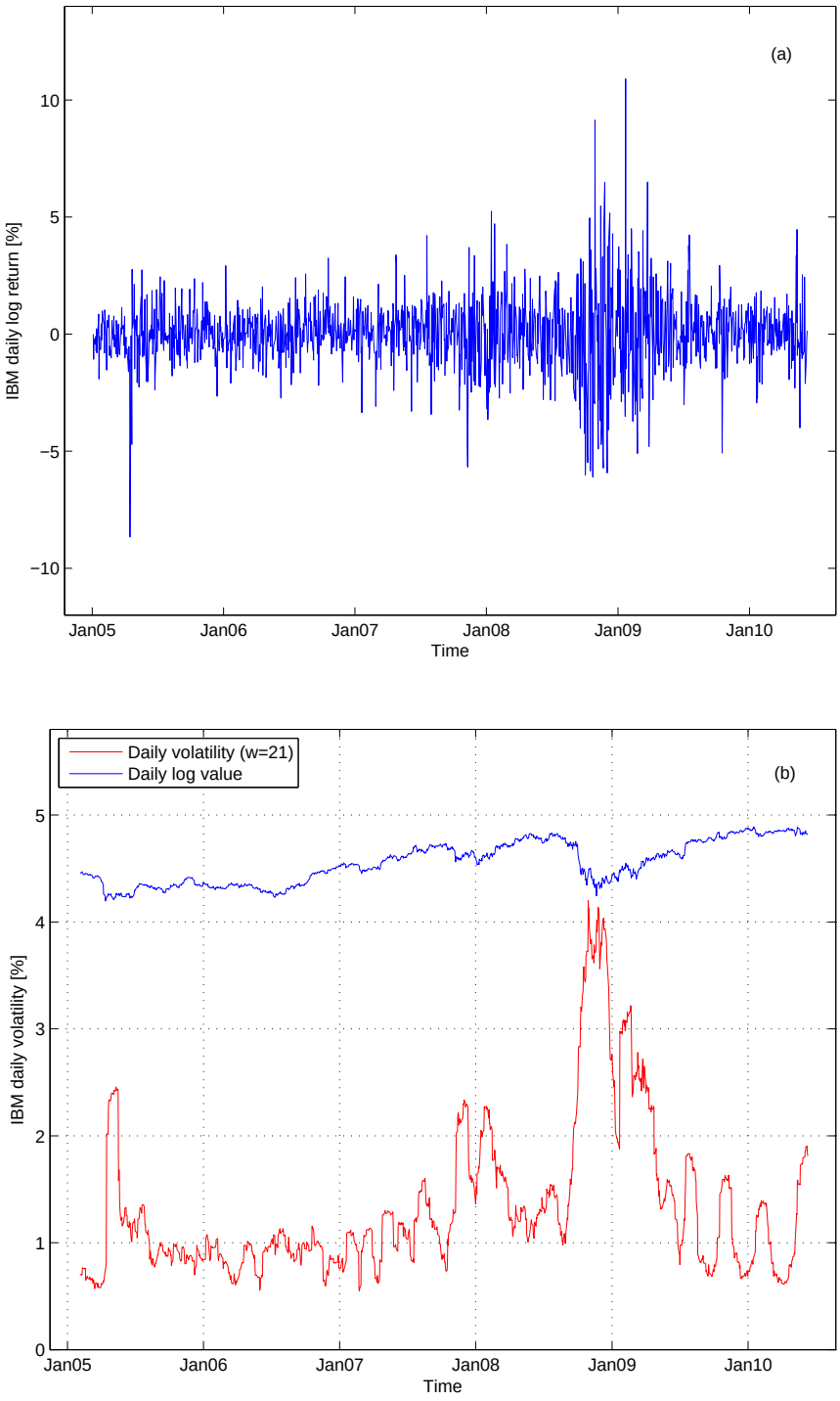

Figure 6.1: (a) IBM daily log return time series. The 'volatility clustering' can be observed. (b) IBM daily volatility time series, using moving average method with window size of 21 days. The leverage effects can be seen from (b).

6.3 The GARCH model

A GARCH model, based on the IBM stock price data for the period from January 2005 to June 2010, will be developed for predicting the stochastic volatility.

6.3.1 Preestimate Analysis

The conditional mean model is ARMAX(R, M) and the conditional variance model is GARCH(p, q). The conditional mean model ARMAX(R, M) is given by (Rachev et al., 2007)

$$y_t = C + \sum_{i=1}^{R} \phi_i y_{i-1} + \varepsilon_t + \sum_{j=1}^{M} \theta_j \varepsilon_{t-j}; \tag{6.1}$$

and the conditional variance model GARCH(p, q) is given by (Chatfield, 2003)

$$\sigma_t^2 = \omega + \sum_{i=1}^{p} \alpha_i \varepsilon_{t-i}^2 + \sum_{j=1}^{q} \beta_j \sigma_{t-j}^2. \tag{6.2}$$

First, to check for the correlation in the IBM daily log return series for the period from January 2005 to June 2010, the plots of the autocorrelation (ACF) and the partial-autocorrelation (PACF) are shown in Figures 6.2 (a) and (b), respectively. Figures 6.2 (a) and (b) indicate that the series correlations of IBM daily log return are very small, if any. That is, it is unnecessary to use any correlation structure in the conditional mean. Thus, Equation (6.1) can be simplified to become (Rachev et al., 2007),

$$y_t = C + \varepsilon_t \tag{6.3}$$

Then, to check whether a correlation in the squared IBM daily log returns for the period from January 2005 to June 2010 exists, the plot of the autocorrelation (ACF)

of the squared return is shown in Figure 6.2 (c). Figures 6.2 (c) shows that, although the returns themselves are not correlated, the variance process exhibits significant correlation. Thus, the simple GARCH$(1,1)$ model can be expressed as (Brooks, 1997; Zhuang and Chan, 2004)

$$\sigma_t^2 = \omega + \alpha\varepsilon_{t-1}^2 + \beta\sigma_{t-1}^2 \tag{6.4}$$

6.3.2 Parameter Estimation

Typically, the GARCH(1,1), GARCH(2,1), or GARCH(1,2) models are adequate for modeling volatilities over long sample periods (Bollerslev et al., 1992). In this estimation, GARCH(1,1) and GARCH(2,1) are used for comparison. Their parameters are estimated and displayed in Tables 6.1 and 6.2, respectively. In Table 6.2, it can be seen that both the value of β_2 and the T-statistic of β_2 are zero, which implies that the β_2 parameter adds nothing to the model. Furthermore, since the results for the GARCH(2,1) model are virtually identical to those obtained from the GARCH(1,1) model, the results support acceptance of the simpler restricted model, which is essentially just the GARCH(1,1) model. Thus, the GARCH(1,1) model is written as

$$\sigma_t^2 = 7.4 \times 10^{-6} + 0.83\sigma_{t-1}^2 + 0.14\varepsilon_{t-1}^2. \tag{6.5}$$

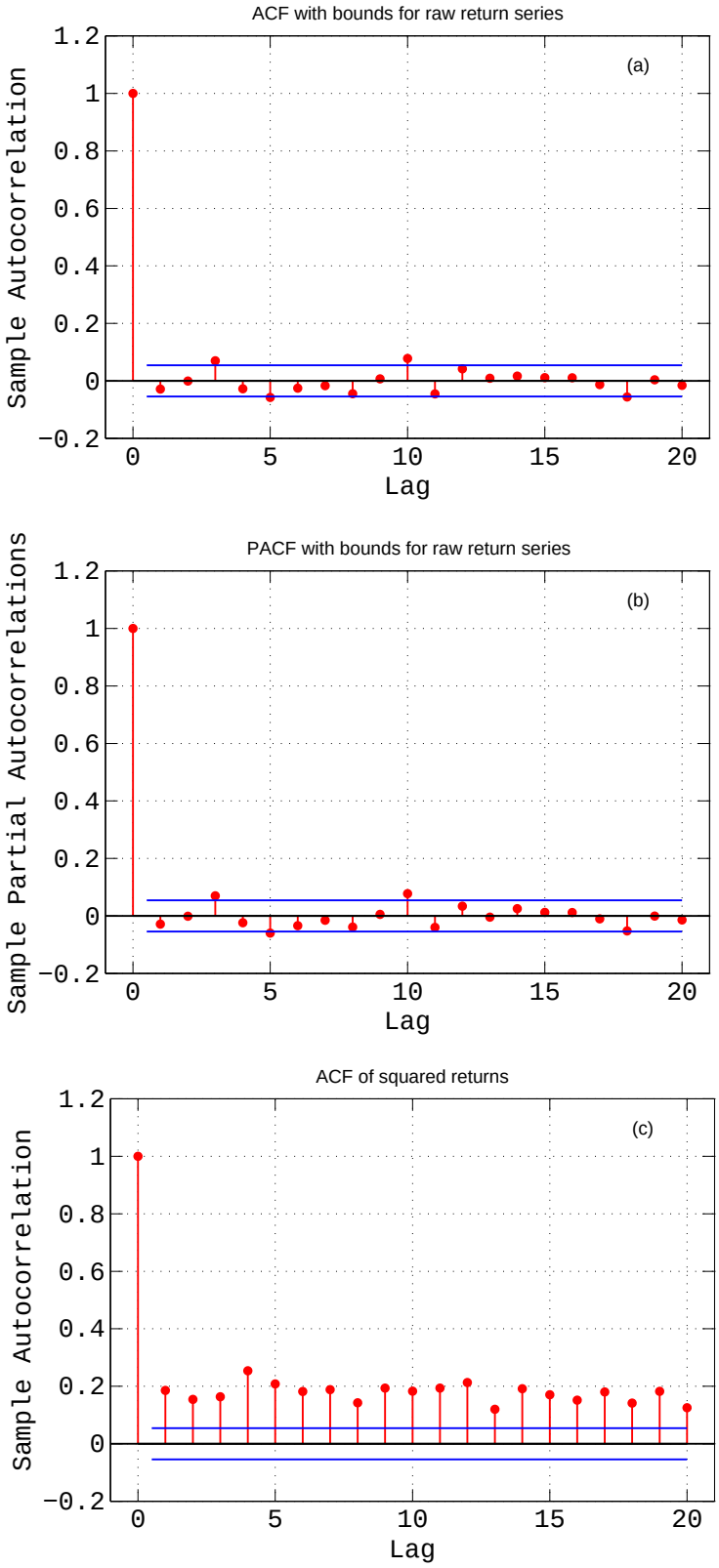

Figure 6.2: (a) Autocorrelation of IBM daily log return. (b) Partial-autocorrelation of IBM daily log return. (c) Autocorrelation of squared IBM daily log return.

Table 6.1: Parameters from the GARCH(1,1) model

Parameter	Value	Standard error	T Statistic
C	0.00064	0.00028	2.25
ω	7.4e-006	1.2e-006	6.21
α	0.14	0.014	9.50
β	0.83	0.016	51.55

Table 6.2: Parameters from the GARCH(2,1) model

Parameter	Value	Standard error	T Statistic
C	0.00064	0.00028	2.24
ω	7.4e-006	1.89e-006	3.88
α	0.14	0.02	5.74
β_1	0.83	0.19	4.22
β_2	0	0.17	0.00

6.3.3 Postestimate Analysis

The residuals (also referred to as innovation), the conditional standard deviations (also referred to as sigmas) and the returns are compared in Figure 6.3. This figure is used to inspect the relationship between the residuals derived from the fitted model, the corresponding conditional standard deviations and the observed returns. Notice that both the residuals (top plot) and the returns (bottom plot) exhibit volatility clustering. Also, notice that the sum,

$$\alpha + \beta = 0.14 + 0.83 = 0.97,$$

which is close to 1. It indicates a overstated volatility persistence in the GARCH model (Chou, 1988; Lamoureux and Lastrapes, 1990; Zhuang and Chan, 2004). This may cause poor volatility forecasting performance.

The plot of the standard innovations (the residuals divided by their conditional standard deviation) is shown in Figure 6.4 (a). It is clear that they are stable with little clustering. The ACF of the squared standardized innovations is plotted in Figure 6.4 (b). They show no correlation. Now compare the ACF of the squared standardized innovations shown in Figure 6.4 (b) to the ACF of the squared return shown in Figure 6.2 (c). The comparison shows that the model in Equation (6.5) sufficiently explains the heteroscedasticity in the return.

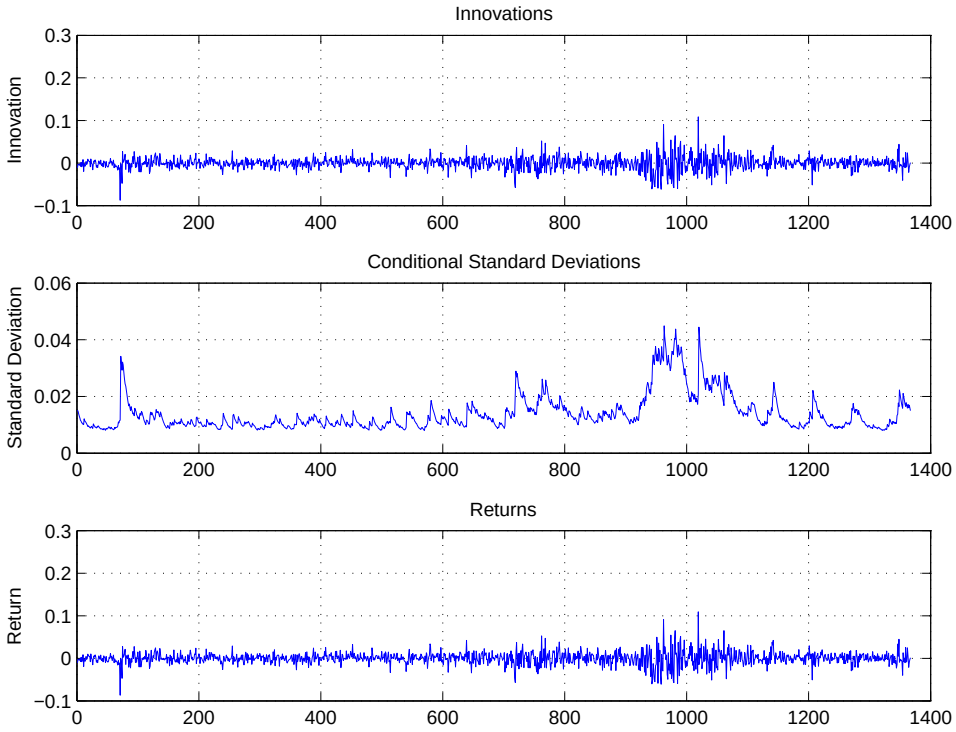

Figure 6.3: Comparison of the residuals, the conditional standard deviations, and the return. Both the residuals (top plot) and the returns (bottom plot) exhibit volatility clustering.

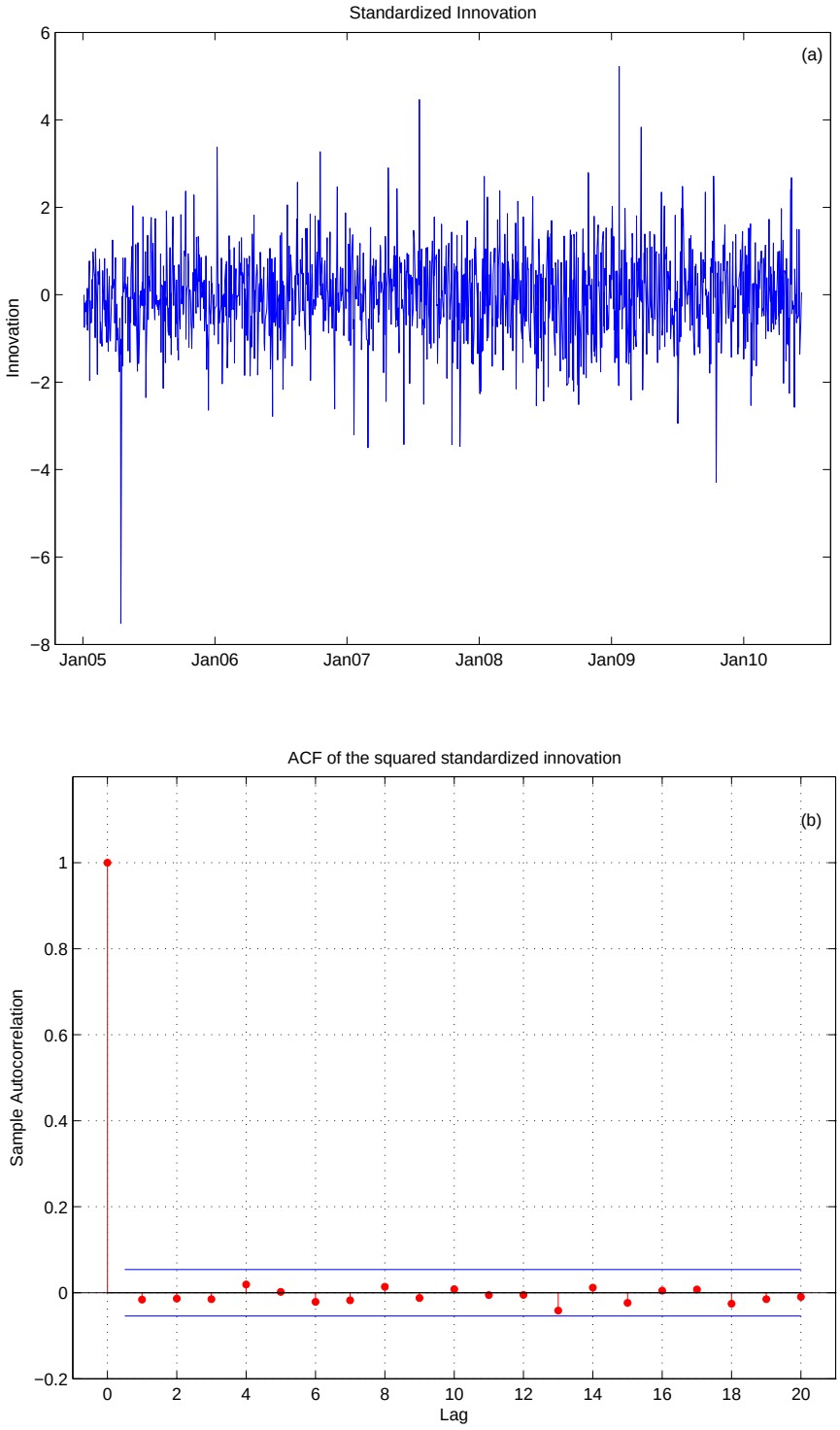

Figure 6.4: (a) The plot of the standardized innovations (the residuals divided by their conditional standard deviations). They appear stable with little clustering. (b) The ACF of the standardized innovations. They show no correlation.

6.4 GARCH limitations

GARCH models are parametric specifications that operate best under relatively stable market conditions (Gourieroux, 1997). Although GARCH is explicitly designed to model time-varying conditional variances, GARCH models often fail to capture highly irregular phenomena, including wild market fluctuations such as stock market crashes and subsequent rebounds, and other highly unanticipated events that lead to significant structural change (Duan, 1995; Gulisashvili and Stein, 2010). Furthermore, GARCH model often fail to fully capture the fat tails observed in asset return series. Heteroscedasticity explains some of the fat tail behavior, but does not capture all of its features.

7 Empirical Study

The simulations of the Black-Scholes model and the Kou model in Chapter 5 are based on a constant volatility. However, in reality the volatility is stochastic. In this chapter, two new models based on stochastic volatility will be developed. The two new models will be built based on the Black-Scholes model and the Kou model, respectively, along with the stochastic volatility model. The Monte Carlo method will be used to simulate the two new models to price the IBM call option. Finally, the results from the simulation of two new models will be compared with those of the Black-Scholes model and the Kou model discussed in Chapter 5.

7.1 Black-Scholes & GARCH model

In this section, the Black-Scholes model and the GARCH model will be combined into a new model, which is referred to as 'Black-Scholes & GARCH model'. The Black-Scholes & GARCH model will be simulated by the Monte Carlo method to estimate the IBM call option price. The results will be compared with those of the Black-Scholes model.

7.1.1 The Black-Scholes & GARCH model

The Black-Scholes & GARCH model is based on the Black-Scholes model, but the volatility is a stochastic variable instead of a constant. Hence, the model can be expressed by the following equations,

$$\begin{cases} \frac{\Delta S}{S} = \mu \Delta t + \sigma_t \Delta W_t; \\ \sigma_t^2 = \omega + \alpha \varepsilon_{t-1}^2 + \beta \sigma_{t-1}^2 \end{cases} \tag{7.1}$$

The stochastic volatility equation for predicting IBM volatility can be derived from Equation (6.5),

$$\begin{cases} \sigma_t^2 = 7.4 \times 10^{-6} + 0.83 \sigma_{t-1}^2 + 0.14 \varepsilon_{t-1}^2 \\ \sigma_0 = 0.018 \end{cases} \tag{7.2}$$

Note that the stochastic volatility equation is based on IBM historical volatility for the period from January 2005 to June 2010 and is valid only for predicting the IBM volatility.

7.1.2 Simulation of the Black-Scholes & GARCH model

The implementation of the Black-Scholes & GARCH model is similar to that of the Black-Scholes model described in Section 5.1.1, but the volatility is a stochastic variable instead of a constant.

The algorithm to simulate the Black-Scholes & GARCH model is the same as the algorithm developed for the Black-Scholes model described in Section 5.1.2, except the following modification:
step 4: use GARCH model to calculate the volatility σ_t;

step 7: the volatility is stochastic, that is, a constant σ changes into a stochastic variable σ_t.

7.1.3 Comparing the Black-Scholes model with the Black-Scholes & GARCH model

The Black-Scholes & GARCH model is used to simulate the IBM stock prices. The simulated stock prices at time T are used to determine the IBM call option price. The comparison of the call prices estimated by the Black-Scholes model and the Black-Scholes & GARCH model for a time to maturity of 92 days is shown in Figure 7.1. It is obvious that the call price estimated by the Black-Scholes model fits the market call price better than the call price estimated by the Black-Scholes & GARCH model. In fact, for a lower strike price, the Black-Scholes & GARCH model always underestimates the call price compared to the market price.

For the time to maturity, $T = 92$ days, the errors between the call option price estimated by the Black-Scholes model or the Black-Scholes & GARCH model and the market call option price are shown in Figures 7.2 (a) and (b). It is obvious that the Black-Scholes model shows better performance in pricing the call option than the Black-Scholes & GARCH model. The graphs that show the comparison of the Black-Scholes model with the Black-Scholes & GARCH model for various times to maturity from 7 to 422 days and the pricing errors between the call prices estimated by the models and the market prices are given in Appendix B.

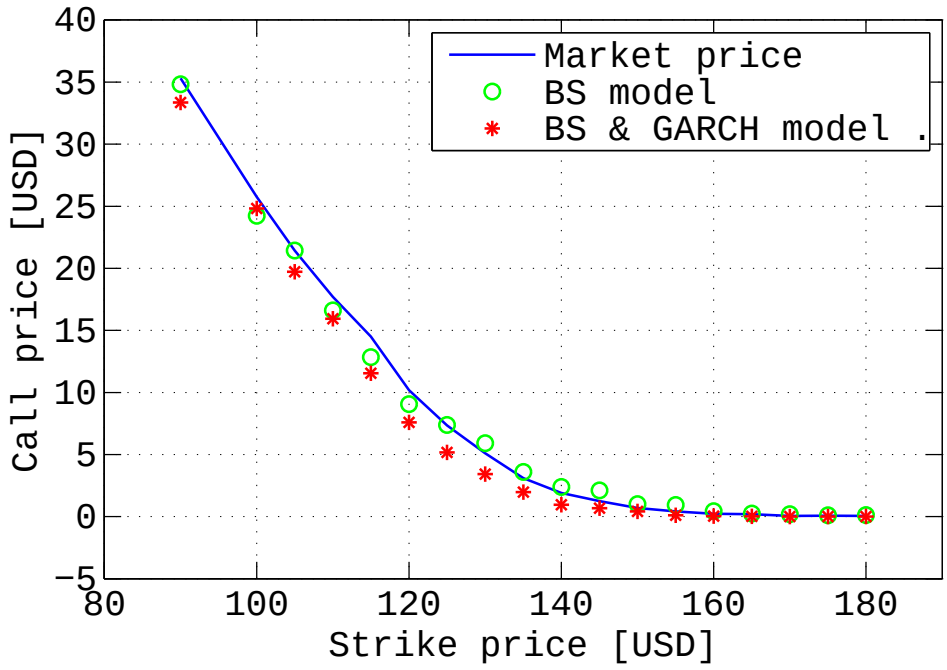

Figure 7.1: The comparison of the call option price estimated by the Black-Scholes model (o) and the Black-Scholes & GARCH model (*) for the time to maturity (T) of 92 days. The solid line shows the market call price. It can be observed the call price estimated by the Black-Scholes model is closer to the market call price than the call price estimated by the Black-Scholes & GARCH model.

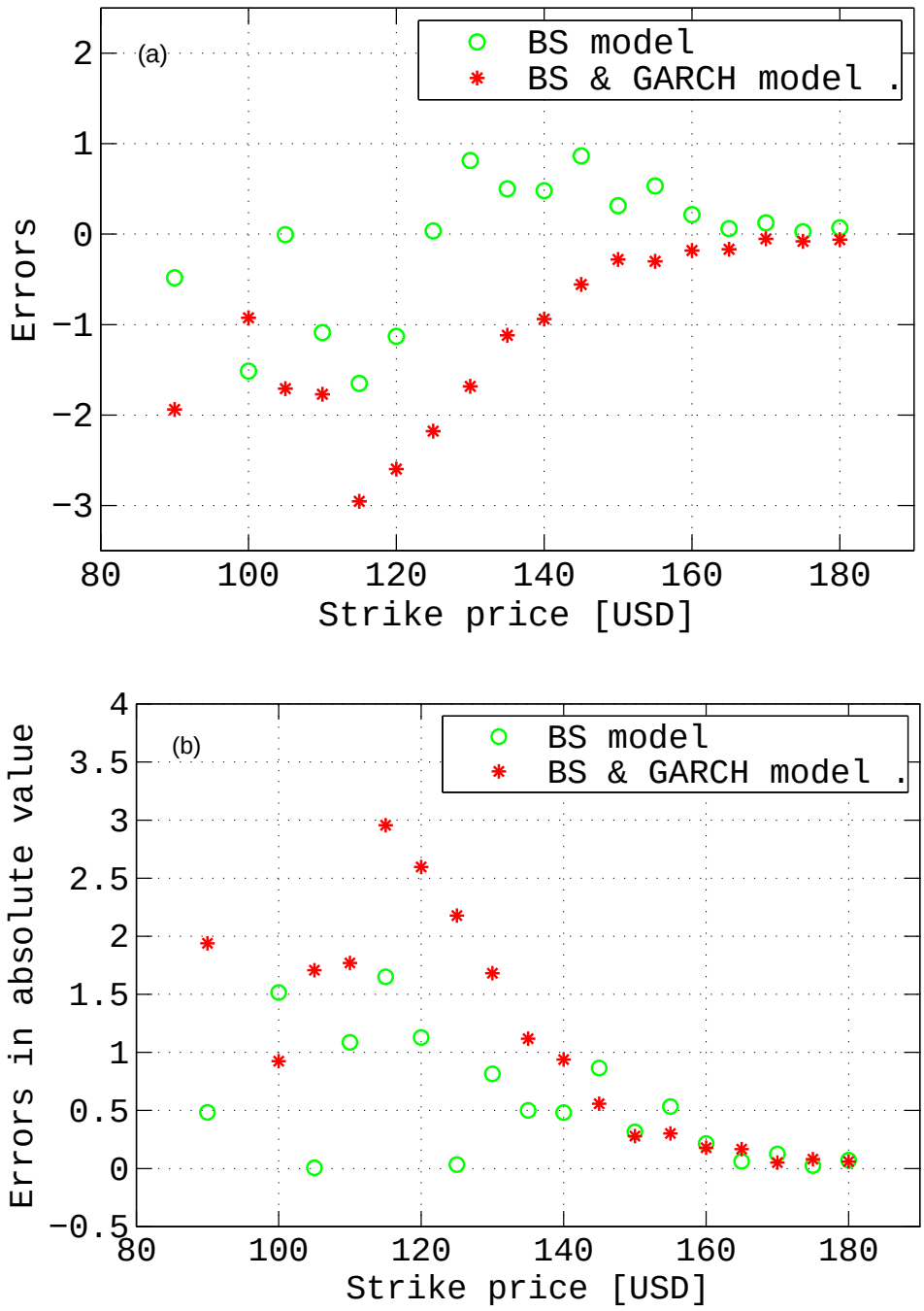

Figure 7.2: The pricing errors between the call option price estimated by the Black-Scholes model (o) or the Black-Scholes & GARCH model (*) and the market call price. It is obvious that the Black-Scholes model has less pricing errors. Figure (a) shows the real value. Figure (b) shows the absolute value. The time to maturity T is 92 days.

7.2 Kou & GARCH model

In this section, a new model which combines the Kou model with the GARCH model will be introduced. In order to simplified the name, the new model is referred to as 'Kou & GARCH model'. A Monte Carlo simulation will be applied to the Kou & GARCH model to estimate IBM call option price. The results will be compared with those of the Kou model.

7.2.1 The Kou & GARCH model

This model is based on the Kou model, but the constant volatility is replaced by a stochastic variable. Therefore, the Kou & GARCH model can be written as

$$\begin{cases} \frac{\Delta S}{S} = \mu\Delta t + \sigma_t \Delta W_t + J\Delta q; \\ \sigma_t^2 = \omega + \alpha\varepsilon_{t-1}^2 + \beta\sigma_{t-1}^2 \end{cases} \tag{7.3}$$

where J is jump size. The IBM stochastic volatility is predicted by Equation (7.2).

7.2.2 Simulation of the Kou & GARCH model

The implementation of the Kou & GARCH model is similar to that of the Kou model in Section 5.2.1, but the volatility is a stochastic variable instead of a constant.

The algorithm developed to simulate the Kou & GARCH model is the same as the algorithm developed for the double exponential jump diffusion model described in Section 5.2.2, except for the following modification:

step 4: using Equation (7.2), calculate the volatility σ_t;

step 8: the volatility is stochastic, that is, constant σ change into stochastic σ_t.

7.2.3 Comparing the Kou model with the Kou & GARCH model

The Monte Carlo method is applied to the Kou & GARCH model to estimate the IBM call option. The comparison of the call prices estimated by the Kou model and the Kou & GARCH model for time to maturity 92 days is shown in Figure 7.3. It is clear that the call prices estimated by the Kou & GARCH model fits better the market call prices than the call prices estimated by the Kou model.

For the time to maturity, $T = 92$ days, the errors between the call option price estimated by the Kou model or the Kou & GARCH model and the market call option price are shown in Figures 7.4 (a) and (b). It can be noted that the Kou & GARCH model has less pricing errors than the Kou model in most cases. That is, the Kou & GARCH model performed better than the Kou model in pricing error for most of the strike prices. The graphs that show the comparison of the Kou model with the Kou & GARCH model for various times to maturity from 7 to 422 days and the pricing errors between the call prices estimated by the models and the market prices are given in Appendix B.

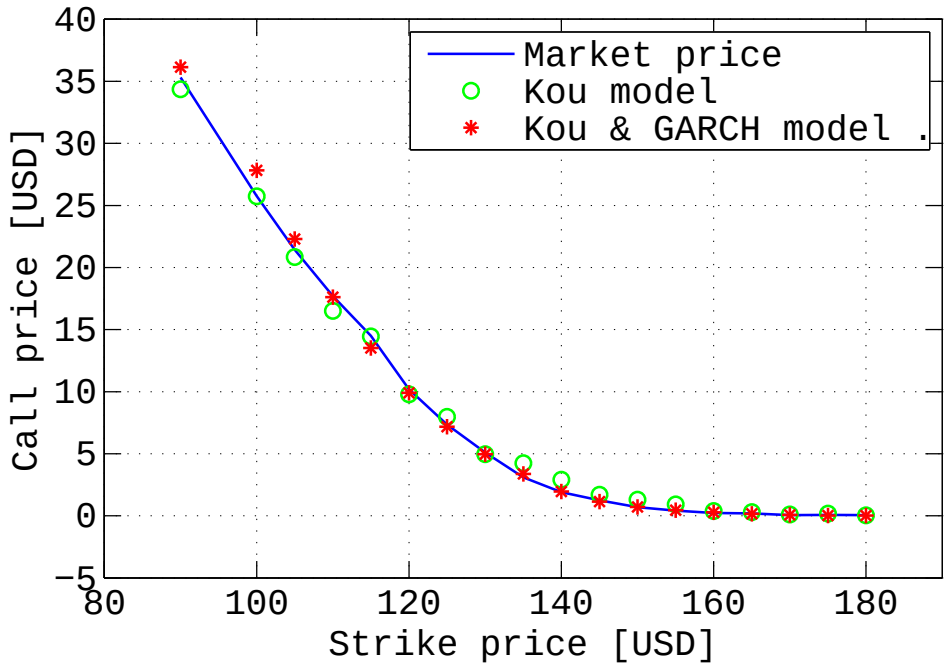

Figure 7.3: The comparison of the call option price estimated by the Kou model (o) and the Kou & GARCH model (*) for the time to maturity T of 92 days. The solid line shows the market call price. It can be observed the call price estimated by Kou & GARCH model is closer to the market call price.

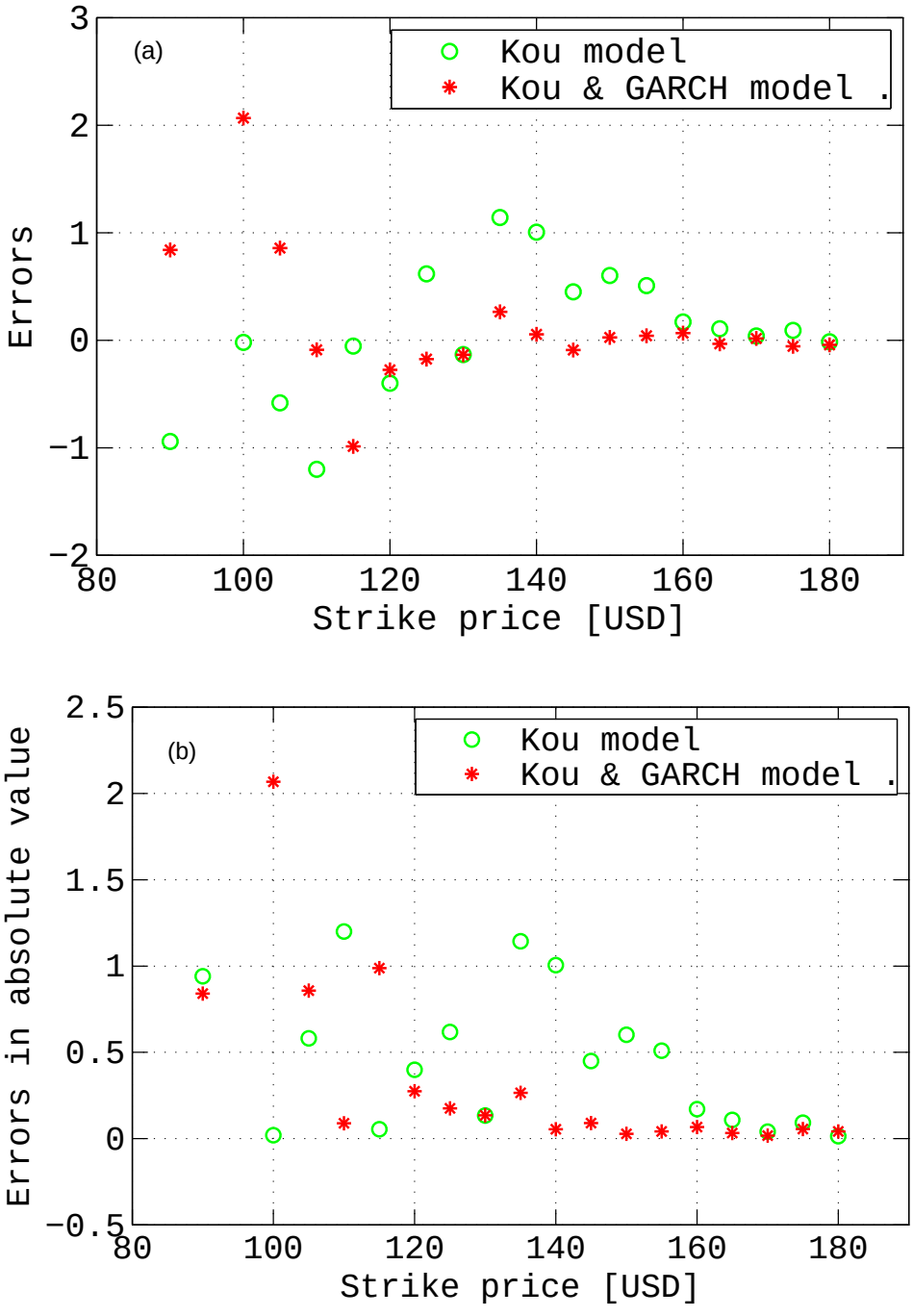

Figure 7.4: The pricing errors between the call option price estimated by the Kou model (o) or the Kou & GARCH model (*) and the market call price. It is clear that the Kou & GARCH model has less pricing errors. Figure (a) shows the real value. Figure (b) shows the absolute value. The time to maturity T is 92 days.

7.3 Comparing the four models

For the time to maturity T of 92 days, the errors between the call option price estimated by any of the four models and the market call option price are shown in Figures 7.6 (a) and (b). From Figures 7.6 (a) and (b), it can be observed that the Kou & GARCH model has the lowest pricing error for most of the strike prices. The Kou model has the second lowest pricing error. The Black-Scholes & GARCH model shows the worst performance in pricing among the four models.

When the time to maturity T is 7 days, 27 days, 162 days, 422 days, the errors between the call option price estimated by any of the four models and the market call option price are shown in Figures B.6 (a) and (b), B.12 (a) and (b), B.18 (a) and (b), B.24 (a) and (b) in Appendix B, respectively. For most of the cases, the Kou & GARCH model shows better performance than the other models.

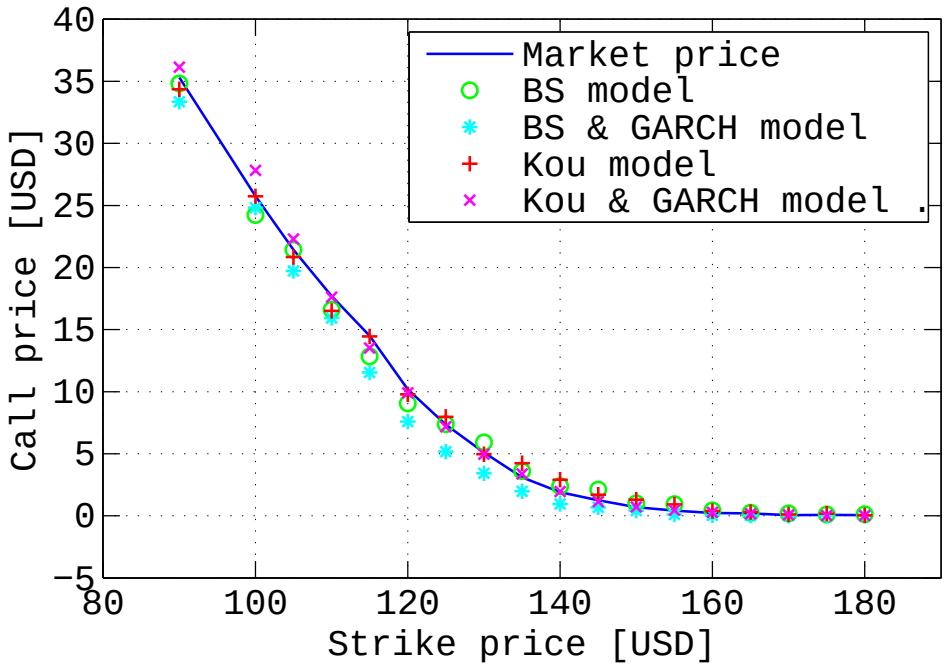

Figure 7.5: The comparison of the call option price estimated by the four models. The Black-Scholes model (o), the Black-Scholes & GARCH model (*), the Kou model (+) and the Kou & GARCH model (x) for the time to maturity T of 92 days. The solid line shows the market call price.

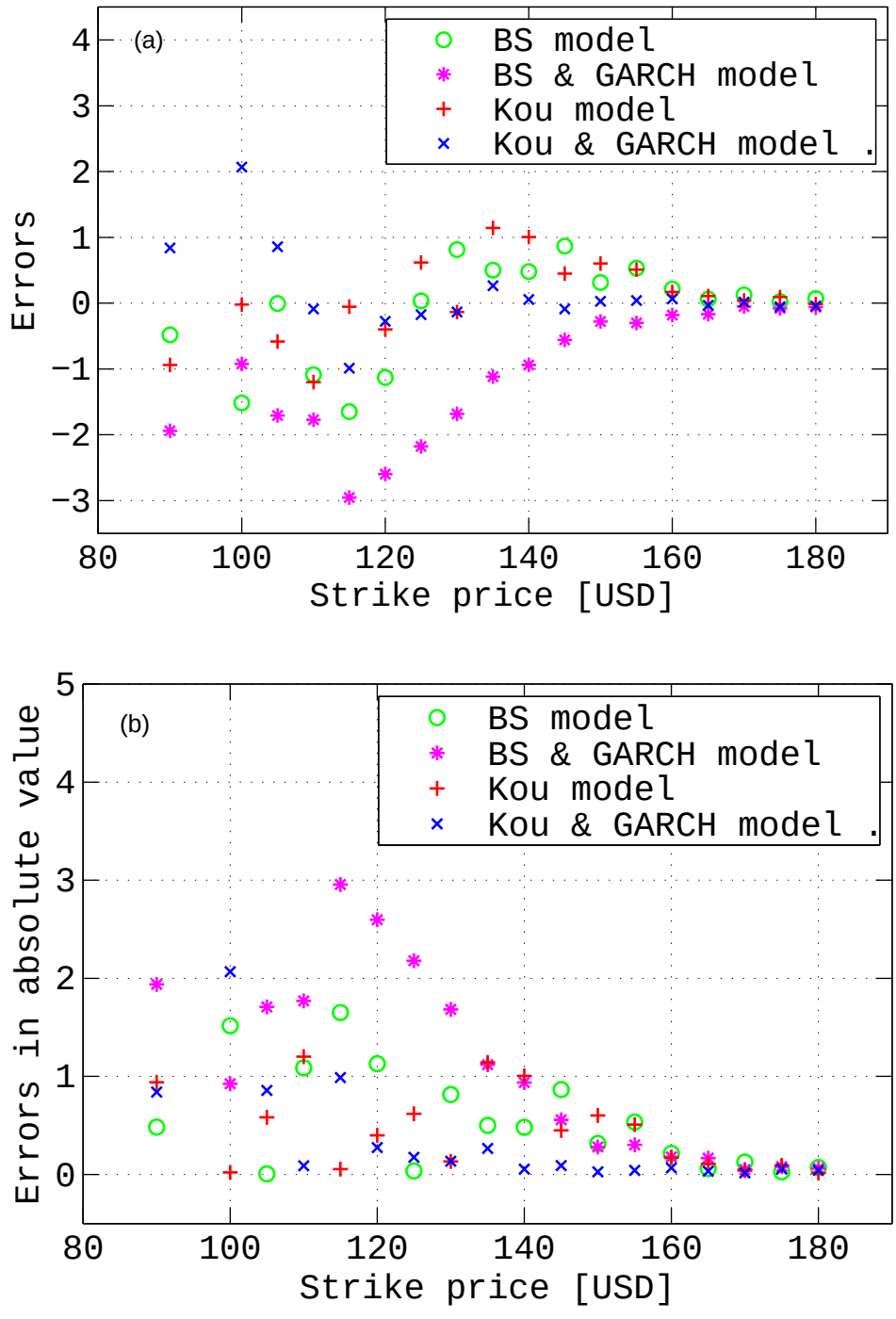

Figure 7.6: The pricing errors between the call option price estimated by any of the four models and the market call price. It can be observed that the Kou & GARCH model has the lowest pricing error for most of the strike prices. Figure (a) shows the real value. Figure (b) shows the absolute value. The time to maturity T is 92 days.

7.4 Measuring the errors

In order to compare these four models precisely, it is necessary to measure the errors based on the comparison of actual data with the values predicted by the models. In this section, the model performance will be evaluated by statistical methods. The following statistical methods will be used to measure the performance in this study (Alexander, 2001; Dittmann and Maug, 2008).

1. Mean absolute error (MAE): the mean of the absolute values of the prediction errors

$$\text{MAE} = \frac{1}{n}\sum_{i=1}^{n}|e_i| \tag{7.4}$$

The MAE measure for the four models is shown in Table 7.1. For most of the times to maturity T, the Kou model shows the best performance, but the Kou & GARCH model performs the best when the time to maturity T is 92 days.

2. Mean square error (MSE): the mean of the squares of the prediction errors

$$\text{MSE} = \frac{1}{n}\sum_{i=1}^{n}{e_i}^2 \tag{7.5}$$

The MSE measure for the four models is shown in Table 7.2. For all of the times to maturity T, the Kou model performs the best among the four models.

3. Root mean square error (RMSE): the square root of the mean of the squared prediction errors

$$\text{RMSE} = \sqrt{\frac{1}{n}\sum_{i=1}^{n}{e_i}^2} \tag{7.6}$$

The RMSE measure for the four models is shown in Table 7.3. For all of the times to maturity T, the Kou model shows the best performance. Note that the RMSE measure is different from the MAE measure in that the RMSE

measure gives more weight to the large errors.

4. Normalized root mean square error (NRMSE): the RMSE divided by the estimated standard deviation of the prediction error

$$\text{NRMSE} = \frac{\text{RMSE}}{\hat{\sigma}} = \sqrt{\frac{1}{n\hat{\sigma}^2}\sum_{i=1}^{n} {e_i}^2} \tag{7.7}$$

   The NRMSE measure for the four models is shown in Table 7.4. For most of the times to maturity T, the Kou model performs the best except for the time to maturity T of 422 days.

5. Information ratio (IR): the mean prediction error divided by the standard deviation of the prediction error

$$\text{IR} = \frac{\hat{\mu}}{\hat{\sigma}} = \frac{1}{n\hat{\sigma}}\sum_{i=1}^{n} e_i \tag{7.8}$$

   The IR measure for the four models is shown in Table 7.5. For most of the times to maturity T, the Kou model shows the best performance, except the time to maturity T of 422 days.

From Tables 7.1, 7.2, 7.3, 7.4, and 7.5, it is clear that the Kou model shows the lowest MAE, MSE, RMSE, NRMSE, and IR in most of cases among the four models. Therefore, a conclusion can be drawn from the results shown in these tables, that the Kou model is the best model explored in this study. However, it should be noted that this can only be stated for modeling the IBM stock prices.

Table 7.1: Comparing the MAE for the four models

MAE	T=7	T=27	T=92	T=162	T=422
Black-Scholes	0.18	0.52	0.55	1.24	2.19
Kou model	0.12*	0.49*	0.45	1.17*	2.16*
BS+GARCH	0.25	0.57	1.08	1.77	2.53
Kou+GARCH	0.23	0.69	0.34*	1.32	2.87

* The star indicates the lowest absolute pricing error.

Table 7.2: Comparing the MSE for the four models

MSE	T=7	T=27	T=92	T=162	T=422
Black-Scholes	0.07	0.89	0.56	3.83	7.35
Kou model	0.03*	0.77*	0.36*	2.5*	5.67*
BS+GARCH	0.27	0.93	2.02	5.61	8.8
Kou+GARCH	0.23	1.26	0.38	4.65	11.38

* The star indicates the lowest absolute pricing error.

Table 7.3: Comparing the RMSE for the four models

RMSE	T=7	T=27	T=92	T=162	T=422
Black-Scholes	0.27	0.94	0.75	1.96	2.71
Kou model	0.18*	0.88*	0.6*	1.58*	2.38*
BS+GARCH	0.52	0.96	1.42	2.37	2.97
Kou+GARCH	0.48	1.12	0.62	2.16	3.37

* The star indicates the lowest absolute pricing error.

Table 7.4: Comparing the NRMSE for the four models

NRMSE	T=7	T=27	T=92	T=162	T=422
Black-Scholes	0.96	1.07	0.98*	1	1.14*
Kou model	0.95*	1.03*	0.98*	0.99*	1.44
BS+GARCH	0.95*	1.18	1.5	1.25	1.77
Kou+GARCH	0.99	1.23	0.99	1.12	1.28

* The star indicates the lowest absolute pricing error.

Table 7.5: Comparing the absolute value of IR for the four models

|IR|	T=7	T=27	T=92	T=162	T=422
Black-Scholes	0.18	0.44	0.13*	0.17	0.58*
Kou model	0*	0.33*	0.13*	0.07*	1.06
BS+GARCH	0.17	0.66	1.14	0.77	1.47
Kou+GARCH	0.33	0.75	0.21	0.54	0.82

* The star indicates the lowest absolute pricing error.

7.5 Results and discussion

In Section 7.4, there is a conflict in the results from the statistical methods and what is observed by visual inspection. According to pricing errors, the statistical study shows that the Kou model is the best model. However, Figures 7.6 (a) and (b), B.6 (a) and (b), B.12 (a) and (b), and B.18 (a) and (b) shows that the Kou & GARCH model is the best model for most of strike prices, in particularly, for the higher part of strike prices.

Now, lets divided the dataset into two parts: one is that the strike prices are less than \$130; the other is that the strike prices are equal to or greater than \$130. Recalculate the mean absolute error (MAE) and root mean square error (RMSE) for both parts. The results are listed in Tables 7.6, 7.7, 7.8, and 7.9. From Tables 7.6 and 7.8, it can be seen that the Kou model has the lowest pricing errors for all the time to maturity. It means that the Kou model is the best pricing model among the four models for the strike prices that are less than \$130. From Tables 7.7 and 7.9, the Black-Scholes & GARCH model has the lowest pricing error for the time to maturity 7 days; the Kou & GARCH model has the lowest pricing errors for the time to maturity T of 27 days, 92 days, and 162 days; the Black-Scholes model has the lowest pricing error for the time to maturity 422 days. That is, for the time to maturity T of 27 days, 92 days, and 162 days, the Kou & GARCH model is the best model for the higher strike prices, equal to or larger than \$130.

The Kou & GARCH model is expected to be the best model among the four models since it provides the solutions for both the jump part and the stochastic volatility. Why are the above results not consistent with this statement ? One of the reasons for this is that the volatility predicted by the GARCH model is different from the

Table 7.6: Comparing the MAE for the four models (for $K < \$130$)

MAE	T=7	T=27	T=92	T=162	T=422
Black-Scholes	0.25	0.91	0.84	1.91	2.06
Kou model	0.17*	0.8*	0.54*	1.69*	1.98*
BS+GARCH	0.38	1.07	2.01	2.61	2.69
Kou+GARCH	0.34	1.37	0.76	2.37	3.38

* The star indicates the lowest absolute pricing error.

volatility used by market. The GARCH model predicts the volatility based on the historical volatility. But the market uses implied volatility based on the future. That is, the historical volatility used by the Kou & GARCH model is not the same as the implied volatility used by the market. In other words, volatility forecasts in GARCH model may lead to unsatisfactory performance (Canina and Figlewski, 1993; Figlewski, 1997; Poon and Granger, 2003).

The possible poor volatility forecasting performance was mentioned in Section 6.3.3. Zhuang and Chan (2004) pointed out that this high persistence is due to the structure changes (e.g. shift of volatility levels) in the volatility processes, which GARCH can not capture. To solve this problem, a GARCH model based on Hidden Markov Models (HMMs) may be the solution. By using the concept of hidden states, HMMs allow for periods with different volatility levels characterized by the hidden states. Within each state, local GARCH models can be applied to model conditional volatility (Yin, 2007). This will be left for future work.

Table 7.7: Comparing the MAE for the four models (for $K \geq \$130$)

MAE	T=7	T=27	T=92	T=162	T=422
Black-Scholes	0.04	0.19	0.36	0.52	2.31*
Kou model	0.04	0.23	0.39	0.61	2.34
BS+GARCH	0.02*	0.16	0.49	0.88	2.39
Kou+GARCH	0.04	0.13*	0.08*	0.21*	2.41

* The star indicates the lowest absolute pricing error.

Table 7.8: Comparing the RMSE for the four models (for $K < \$130$)

RMSE	T=7	T=27	T=92	T=162	T=422
Black-Scholes	0.34	1.35	1.05	2.64	2.93
Kou model	0.23*	1.23*	0.68*	2.08*	2.31*
BS+GARCH	0.67	1.4	2.1	3.06	3.2
Kou+GARCH	0.61	1.65	0.99	2.98	3.96

* The star indicates the lowest absolute pricing error.

Table 7.9: Comparing the RMSE for the four models (for $K \geq \$130$)

RMSE	T=7	T=27	T=92	T=162	T=422
Black-Scholes	0.06	0.34	0.46	0.67	2.49
Kou model	0.07	0.4	0.54	0.74	2.45*
BS+GARCH	0.03*	0.29	0.71	1.26	2.73
Kou+GARCH	0.06	0.27*	0.1*	0.29*	2.72

* The star indicates the lowest absolute pricing error.

7.6 Summary

The Monte Carlo simulation is applied to these four models – the Black-Scholes model, the Kou model, the Black-Scholes & GARCH model, the Kou & GARCH model – to estimate the IBM call option price. When the time to maturity is 7 days, or 27 days, or 92 days, or 162 days, the Kou & GARCH model shows the best performance in pricing errors, for most of the strike prices, visually. However, if their errors are measured by statistical methods such as mean absolute error (MAE), mean square error (MSE), root mean square error (RMSE), normalized root mean square error (NRMSE), information ratio (IR), the Kou model shows the lowest errors. The reason is that there exist some large pricing errors when the strike prices are low and the large errors add a big value to MAE, MSE and RMSE to make the comparison less descriptive. A solution is to divide the dataset into two parts. One is for the strike prices that are lower than \$130; the other is for the strike prices is equal to or larger than \$130. The Kou model shows the best performance in the pricing error for the lower part of strike prices, and the Kou & GARCH model shows better performance in the pricing error for the higher part of the strike prices when the time to maturity is 27 days, 92 days, 162 days.

It should be noted that the conclusion is based on a special dataset, the IBM historical stock and call option price. In other words, it does not mean that this conclusion is valid for any other dataset. Sepp (2003) points out that there is no accepted model for every market and every market has its own favorite.

8 Conclusion & future work

Due to the two puzzles that the Black-Scholes model is unable to explain, the double exponential jump diffusion model is introduced to model the jump that occurs in stockprices caused by the overaction or underaction to outside news. The two models were used to price the IBM call option by Monte Carlo simulation. The results show that the double exponential jump diffusion model creates less pricing errors than the Black-Scholes model does.

Furthermore, a stochastic volatility model based on GARCH(1,1) is developed to forecast the non-constant volatility. Two new models, the Black-Scholes & GARCH model and the Kou & GARCH model, based on the Black-Scholes model and the double exponential jump diffusion model, respectively, but with stochastic volatility, are developed. The two new models were also applied to price the IBM call option by Monte Carlo simulation. The four models are compared by the pricing errors both visually and statistically. For the higher part of strike prices, both visual observation and statistical study show that the Kou & GARCH model has the best performance on the pricing error. However, the lower part of the strike prices, the double exponential jump diffusion model performs the best. Theoretically, the Kou & GARCH model is expected to be the best model among the four models. The inconsistency may be caused by poor volatility forecasting performance from the

GARCH model.

Therefore, a future work could be to build a GARCH model based on Hidden Markov Models (HMMs). By using the concept of hidden states, HMMs allows for periods with different volatility levels characterized by the hidden states. Within each state, local GARCH models can be applied to model conditional volatility.

This study is based on an individual dataset, IBM historical stock and option price. Thus, the conclusion may be different for other datasets. The performance of the four models needs to be checked on other data sets as well as against other models. This is left for future work.

In fact, the market is always influenced by the global economy. When the economy is stable and not much outside news, the Black-Scholes model may be the best model. However, if the economy is turbulent, such as, after the 1987 crash or the "Panic of 2008", the double exponential jump diffusion model or the Kou & GARCH model may perform better.

A Figures for volatility smile

The figures of the volatility smile for the time to maturity T of 7 days and 92 days were given in Section 2.1.2. In order to compare and contrast the volatility smile for different time to maturity, the volatility smile for the time to maturity T of 27 days, 162 days, and 422 days is given in this appendix.

A.1 Volatility smile for 27 days maturities

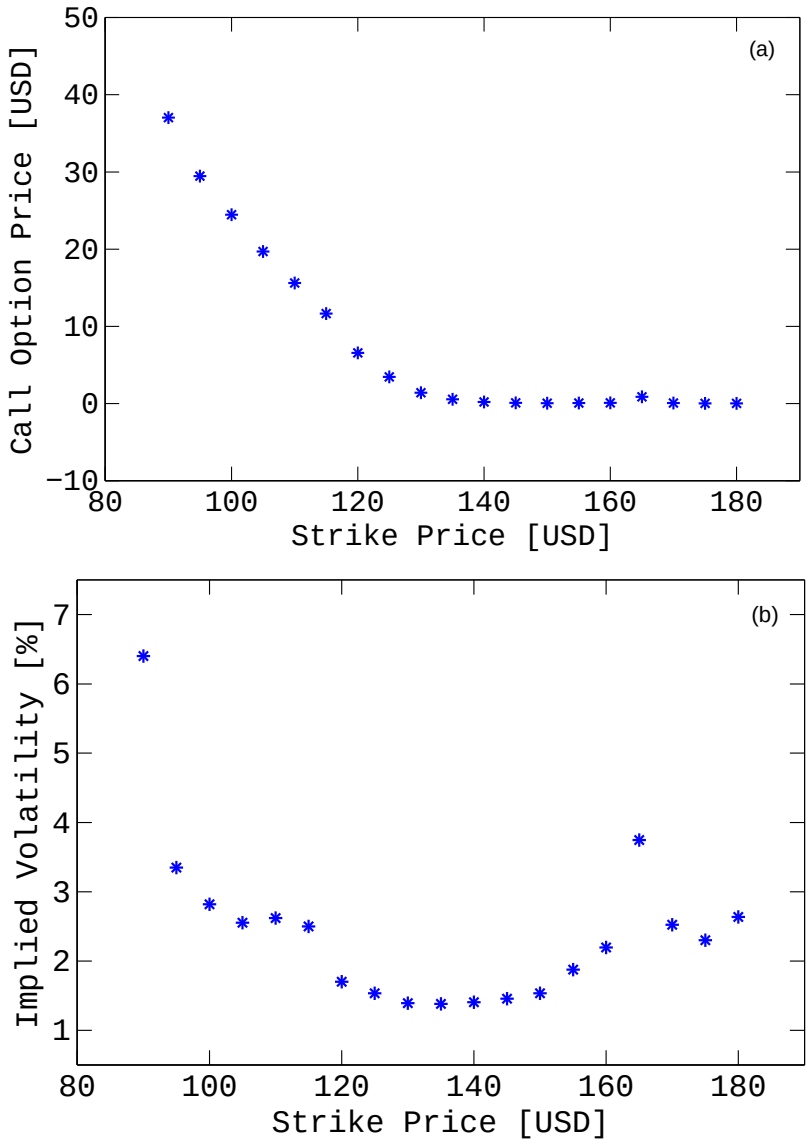

Figure A.1: (a) The call option price versus the strike price for IBM stock. (b) The observed implied volatility curve. The time to maturity T is 27 days.

A.2 Volatility smile for 162 days maturities

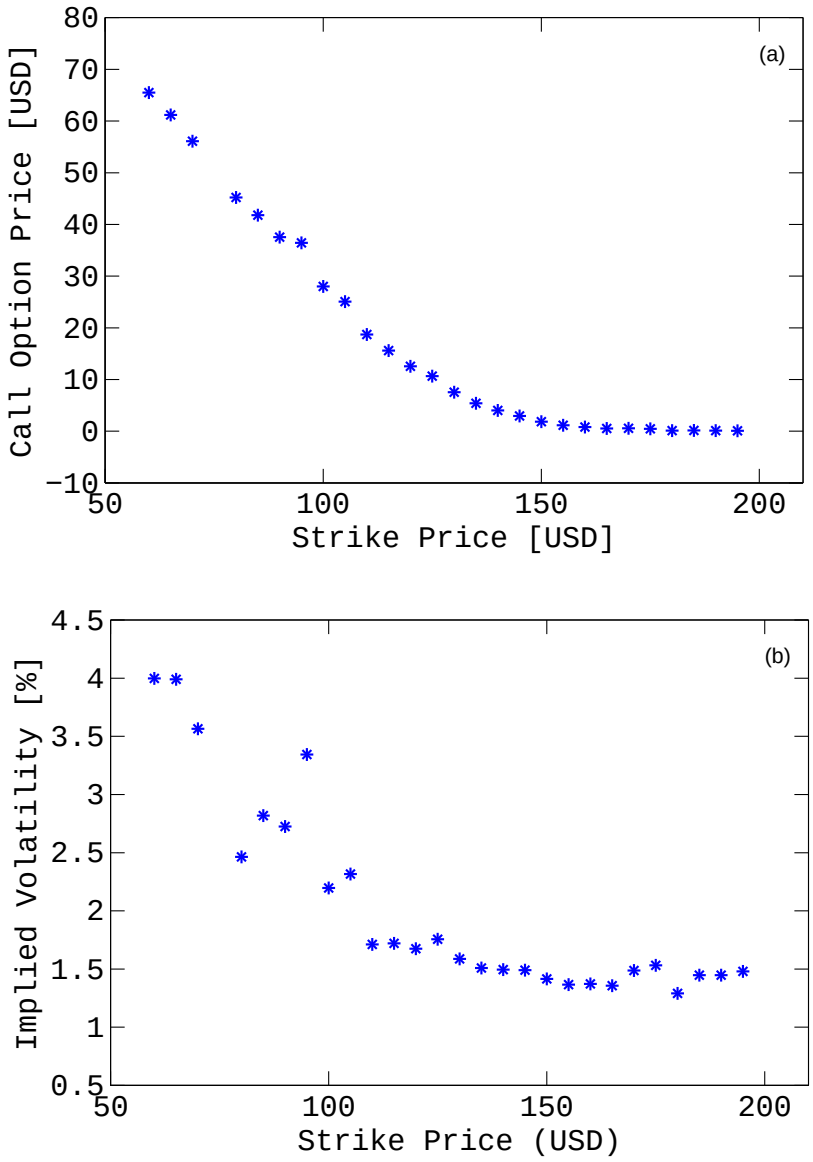

Figure A.2: (a) The call option price versus the strike price for IBM stock. (b) The observed implied volatility curve. The time to maturity T is 162 days.

A.3 Volatility smile for 422 days maturities

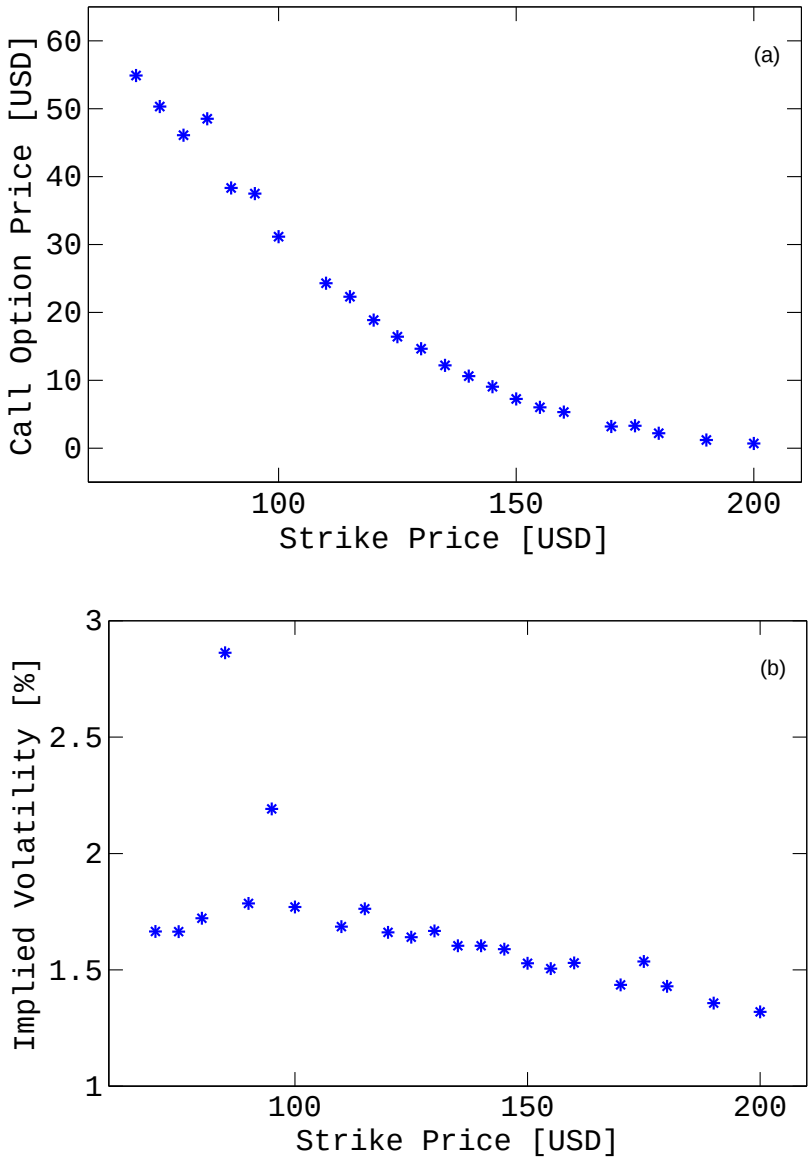

Figure A.3: (a) The call option price versus the strike price for IBM stock. (b) The observed implied volatility curve. The time to maturity T is 422 days.

B Figures for comparing the four models

The comparison of the call price estimated by the models with the market call price, and the pricing error between the call price estimated by the models and the market price for time to maturity of 92 days was discussed in Chapter 7. Here, the comparison of the call price estimated by the models with the market call price and the pricing error between the call price estimated by the models and the market price for time to maturity of 7 days, 27 days, 162 days, 422 days will be shown.

B.1 Time to maturity is 7 days

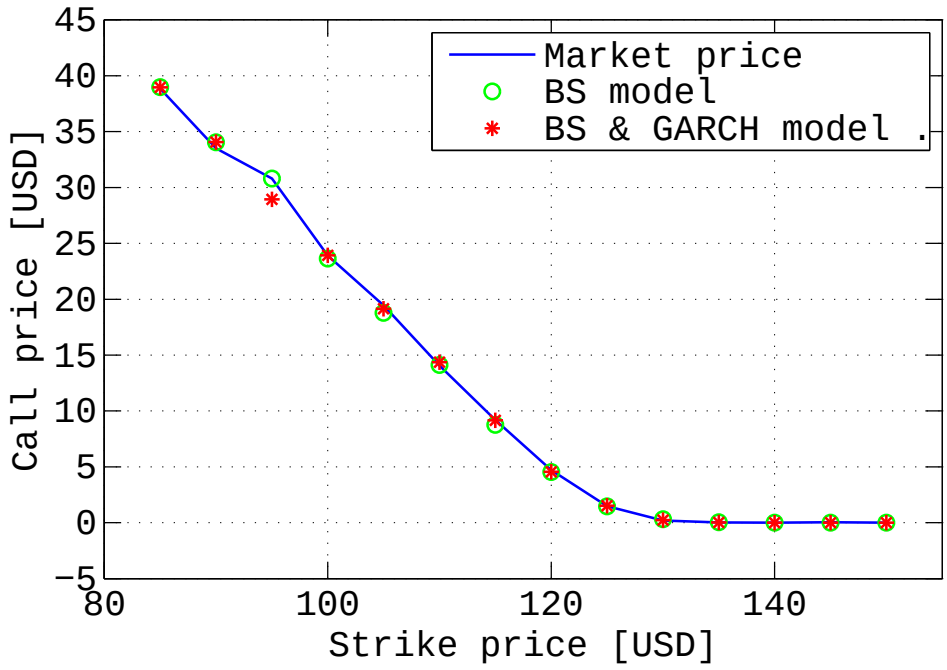

Figure B.1: The comparison of the call option price estimated by the Black-Scholes model (o) and the Black-Scholes & GARCH model (*) for the time to maturity T of 7 days. The solid line shows the market call price.

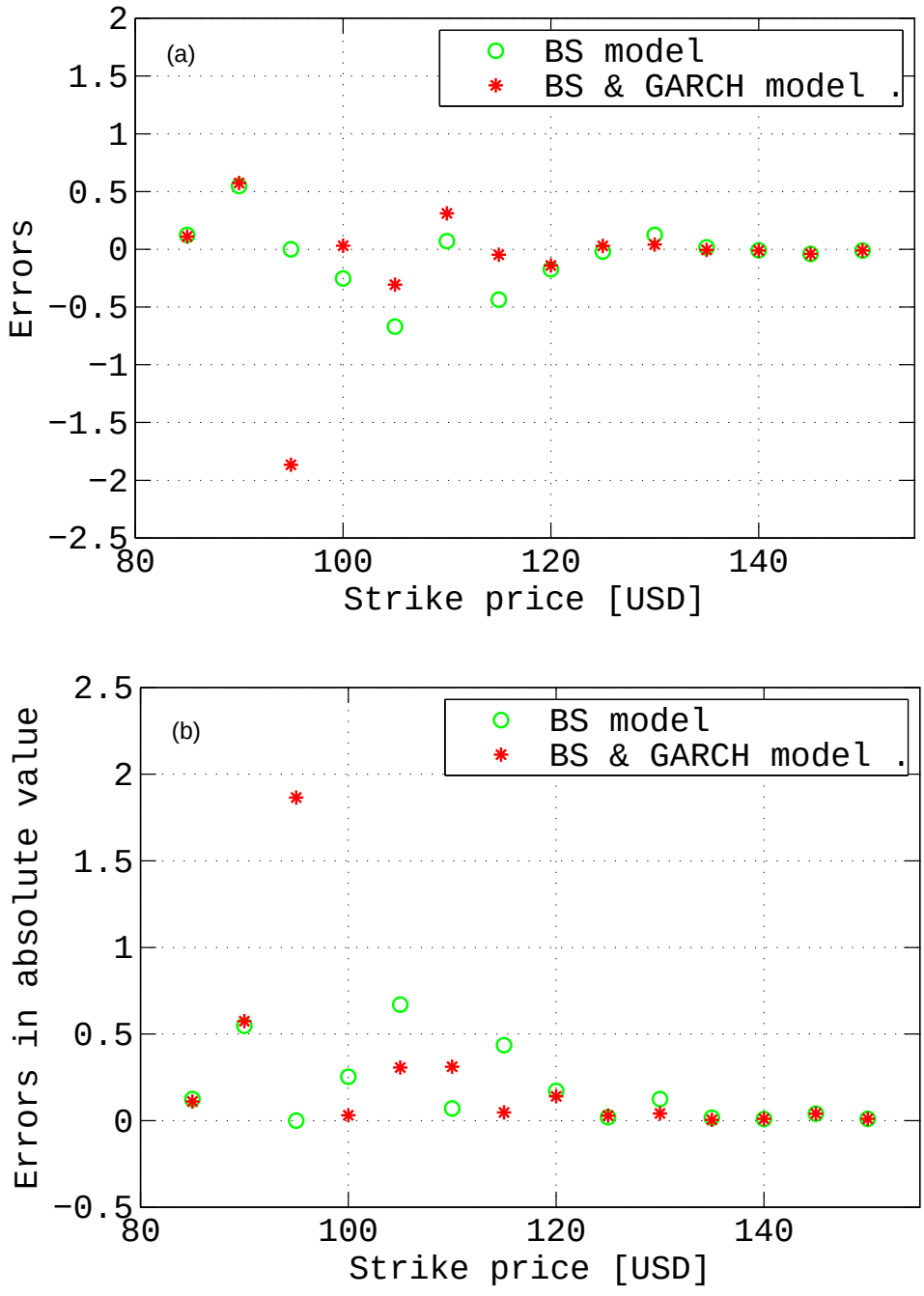

Figure B.2: The pricing errors between the call option price estimated by the Black-Scholes model (o) or the Black-Scholes & GARCH model (*) and the market call price. Figure (a) shows the real value. Figure (b) shows the absolute value. The time to maturity T is 7 days.

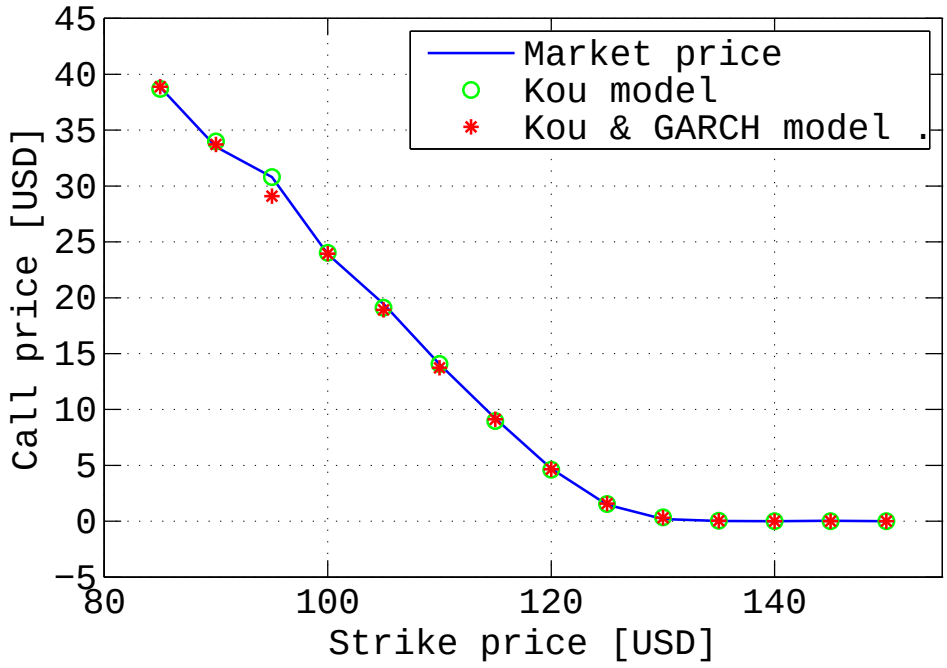

Figure B.3: The comparison of the call option price estimated by the Kou model (o) and the Kou & GARCH model (*) for the time to maturity T of 7 days. The solid line shows the market call price.

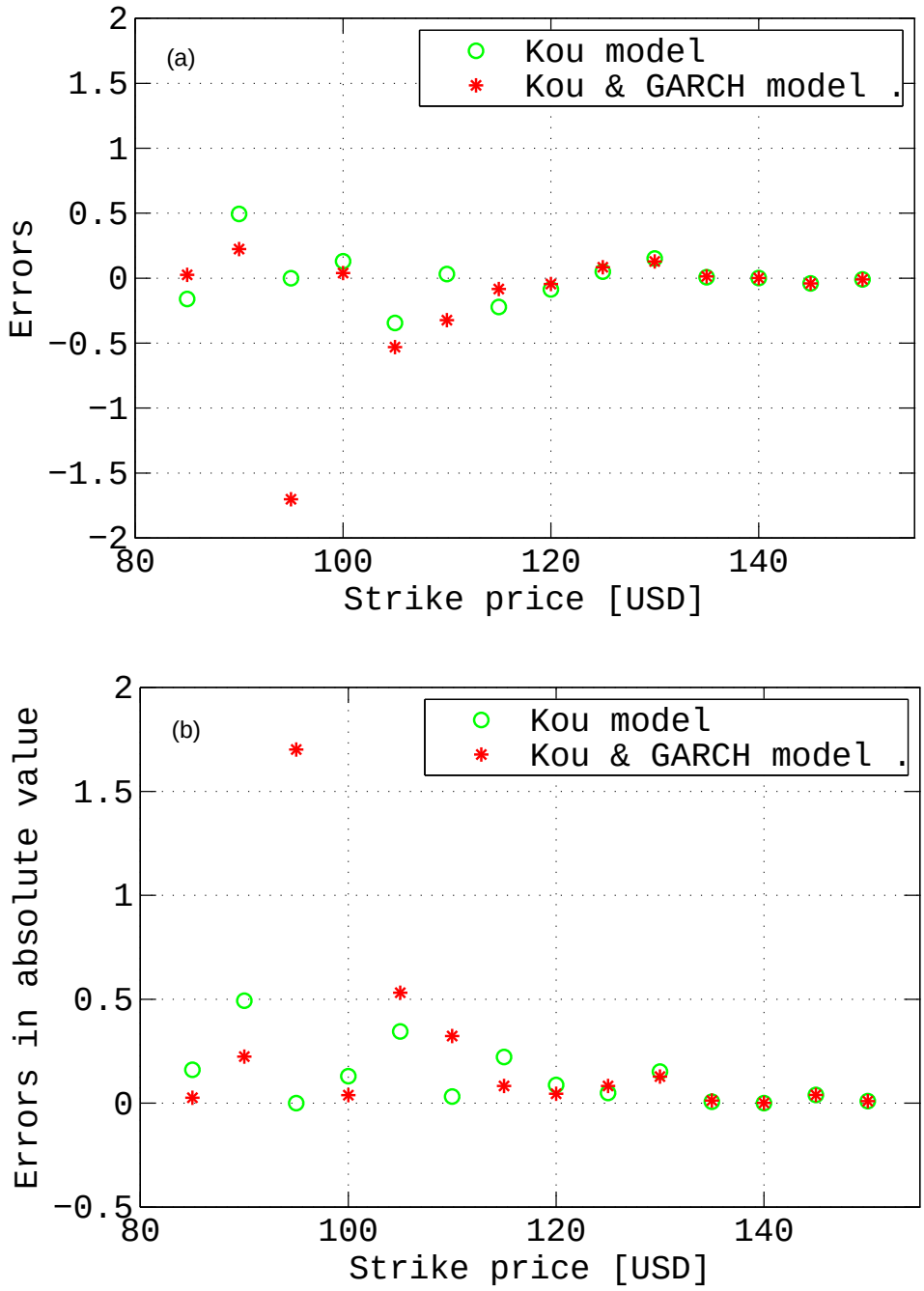

Figure B.4: The pricing errors between the call option price estimated by the Kou model (o) or the Kou & GARCH model (*) and the market call price. Figure (a) shows the real value. Figure (b) shows the absolute value. The time to maturity T is 7 days.

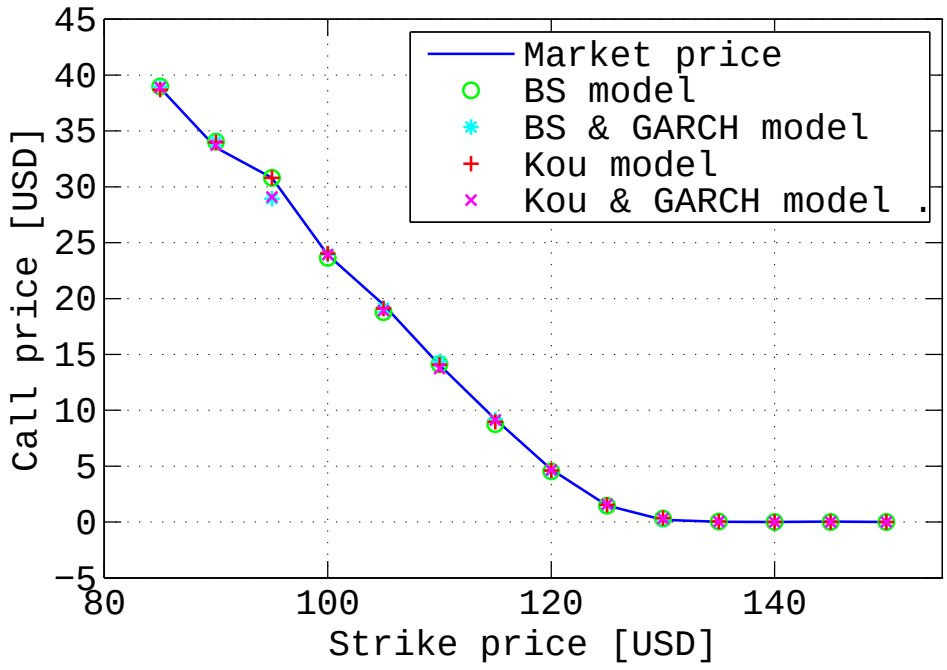

Figure B.5: The comparison of the call option price estimated by the four models. The Black-Scholes model (o), the Black-Scholes & GARCH model (*), the Kou model (+) and the Kou & GARCH model (x) for the time to maturity T of 7 days. The solid line shows the market call price.

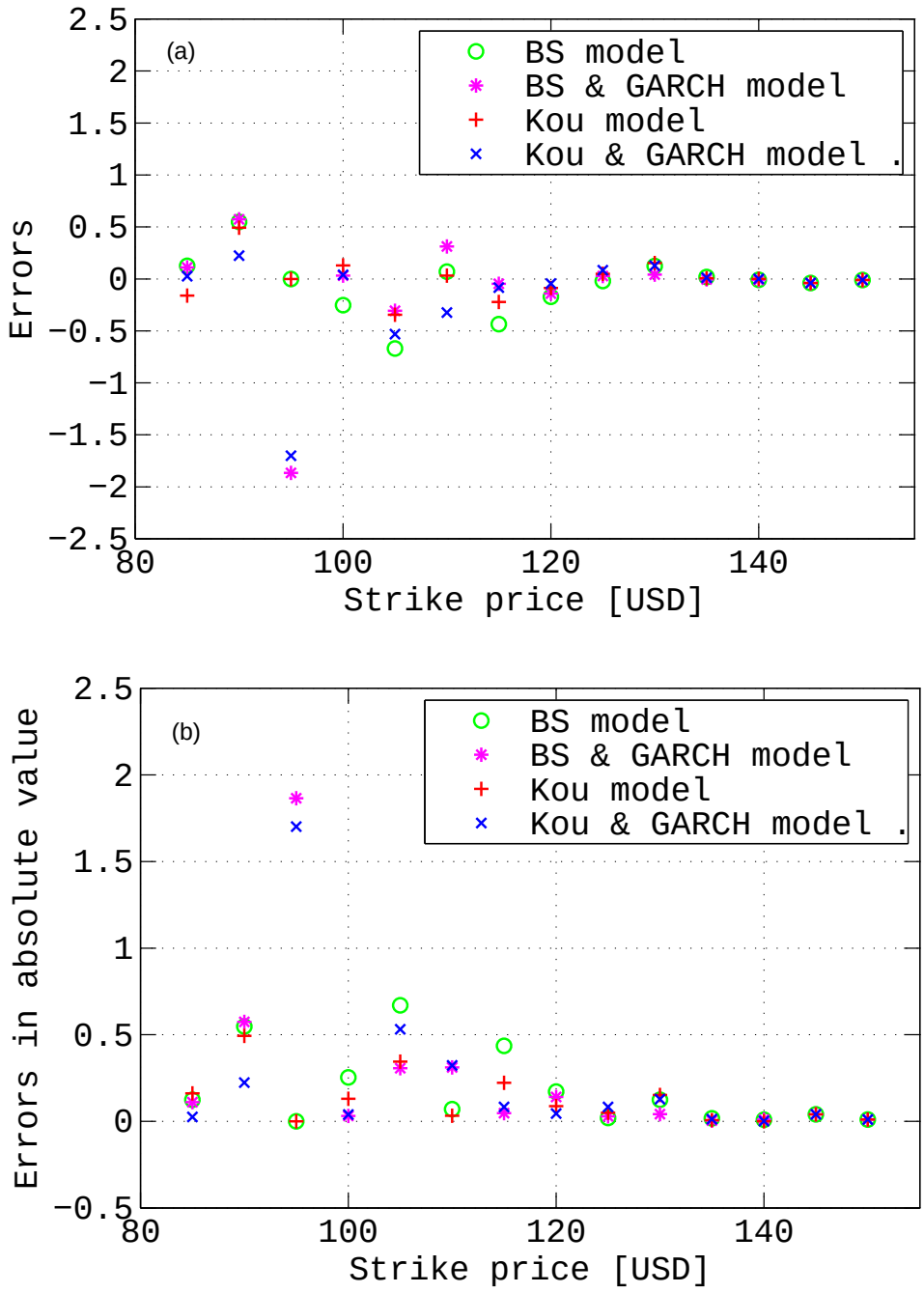

Figure B.6: The pricing errors between the call option price estimated by any of the four models and the market call price. The Black-Scholes model (o), the Black-Scholes & GARCH model (*), the Kou model (+) and the Kou & GARCH model (x) for the time to maturity T of 7 days. Figure (a) shows the real value. Figure (b) shows the absolute value.

B.2 Time to maturity is 27 days

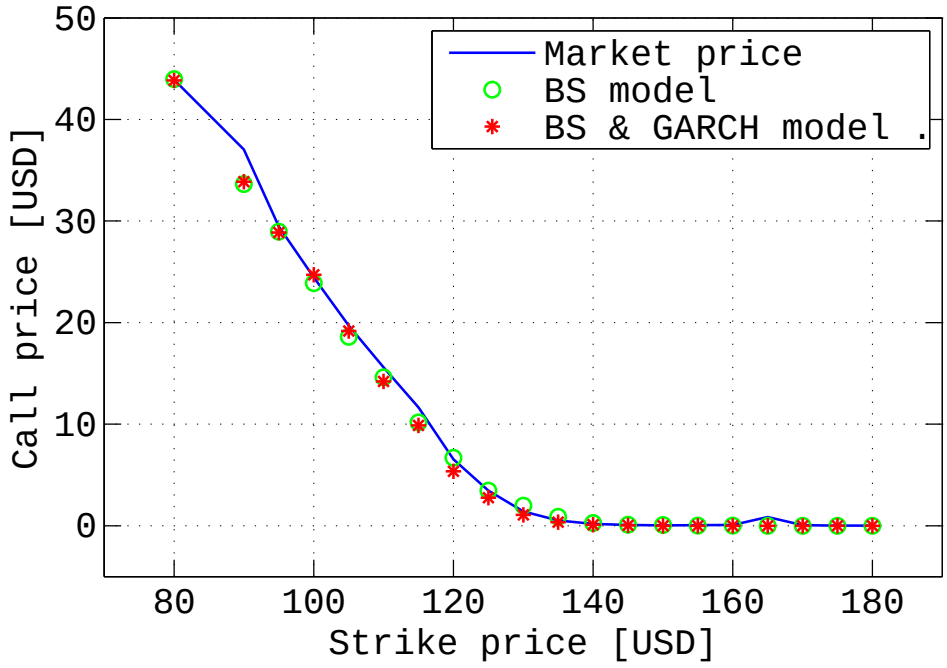

Figure B.7: The comparison of the call option price estimated by the Black-Scholes model (o) and the Black-Scholes & GARCH model (*) for the time to maturity T of 27 days. The solid line shows the market call price.

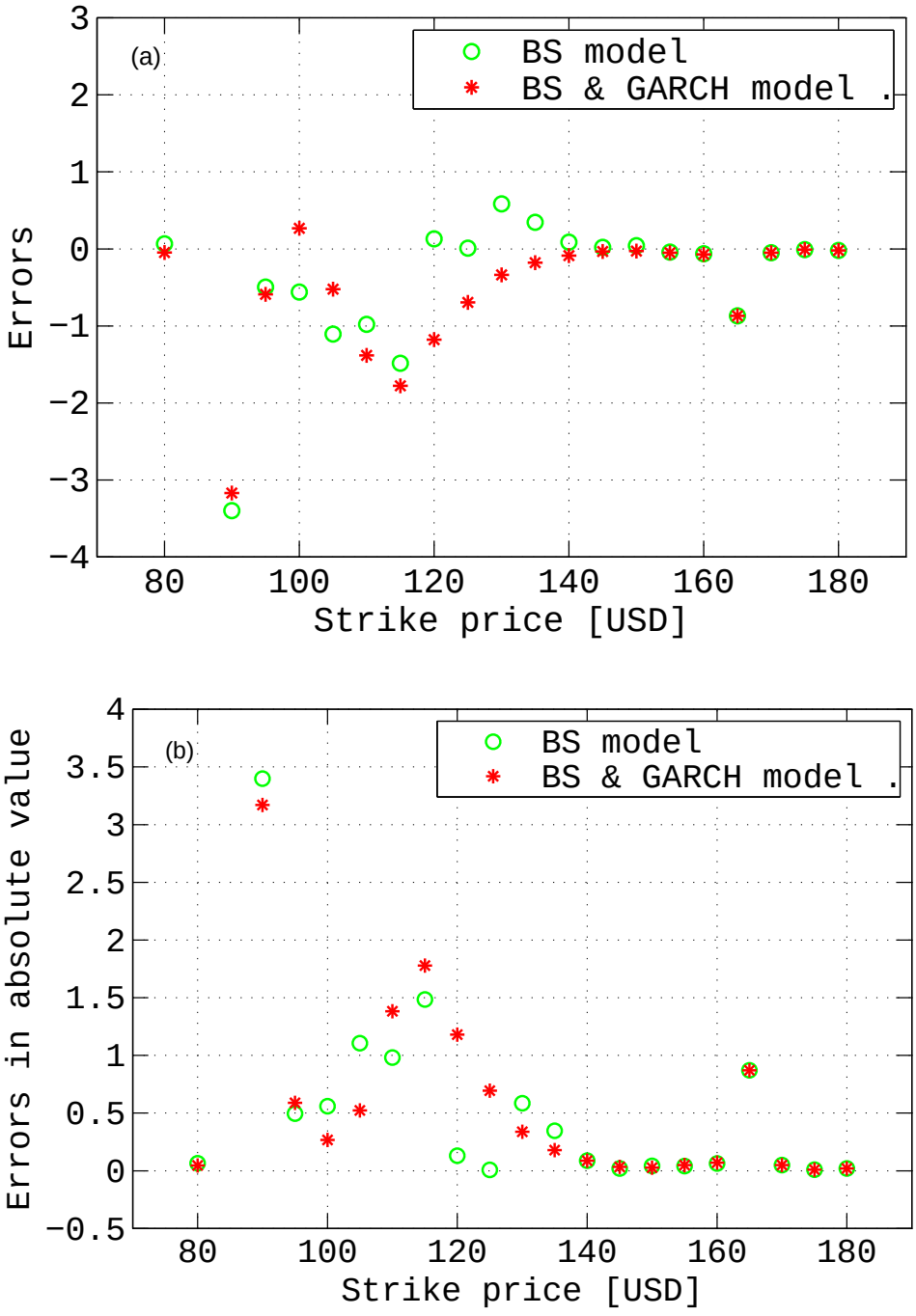

Figure B.8: The pricing errors between the call option price estimated by the Black-Scholes model (o) or the Black-Scholes & GARCH model (*) and the market call price. Figure (a) shows the real value. Figure (b) shows the absolute value. The time to maturity T is 27 days.

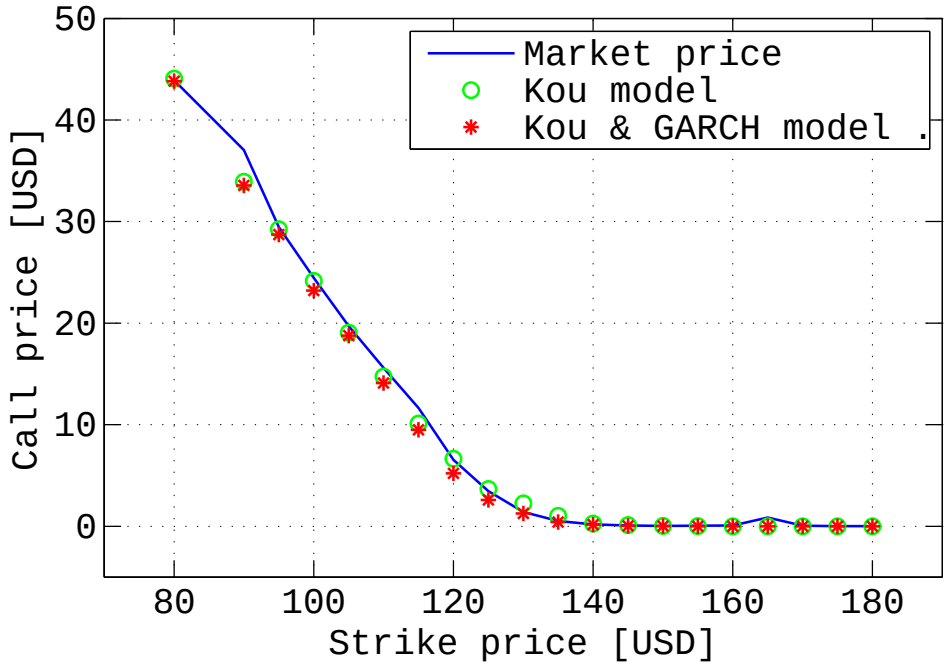

Figure B.9: The comparison of the call option price estimated by the Kou model (o) and the Kou & GARCH model (*) for the time to maturity T of 27 days. The solid line shows the market call price.

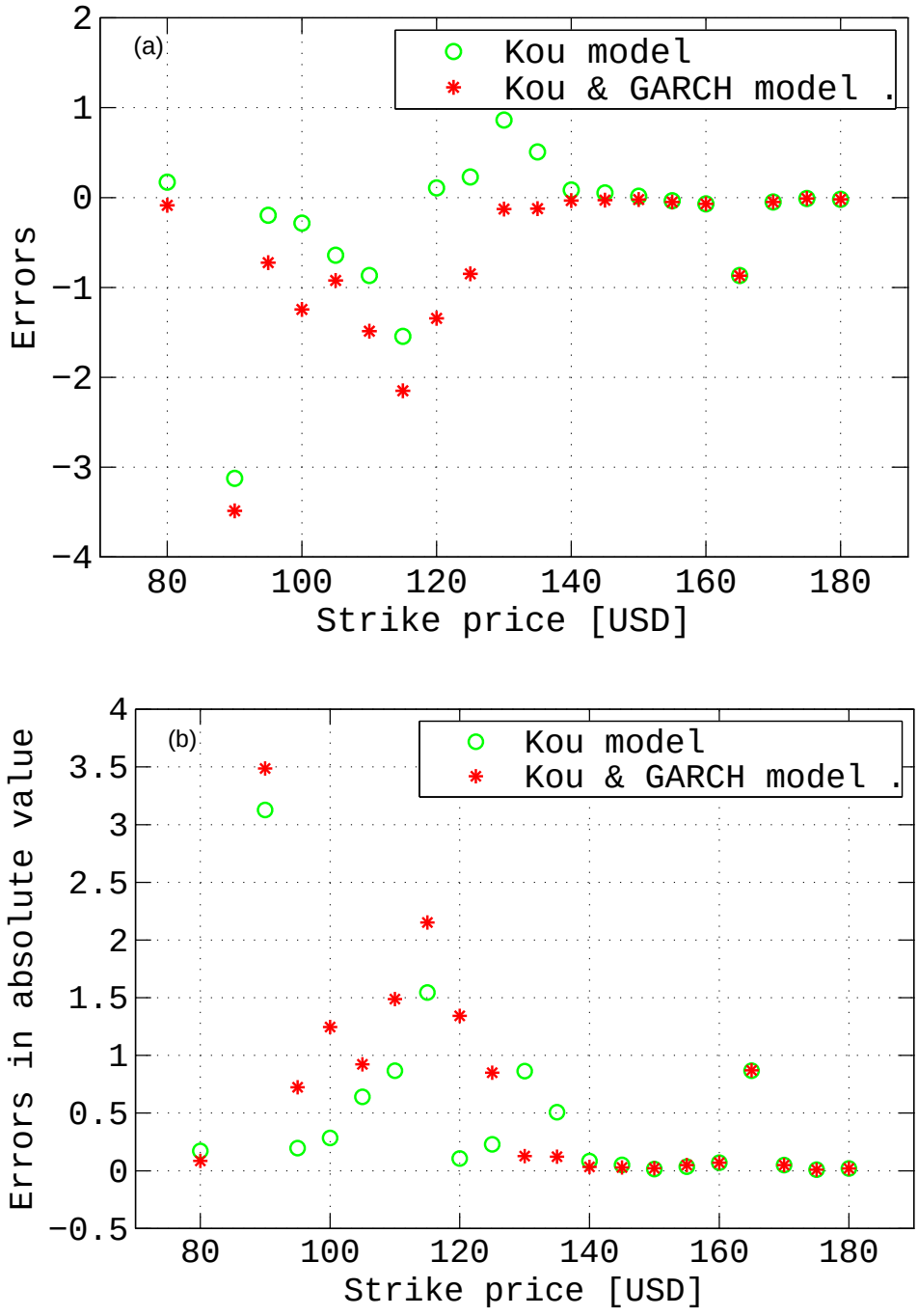

Figure B.10: The pricing errors between the call option price estimated by the Kou model (o) or the Kou & GARCH model (*) and the market call price. Figure (a) shows the real value. Figure (b) shows the absolute value. The time to maturity T is 27 days.

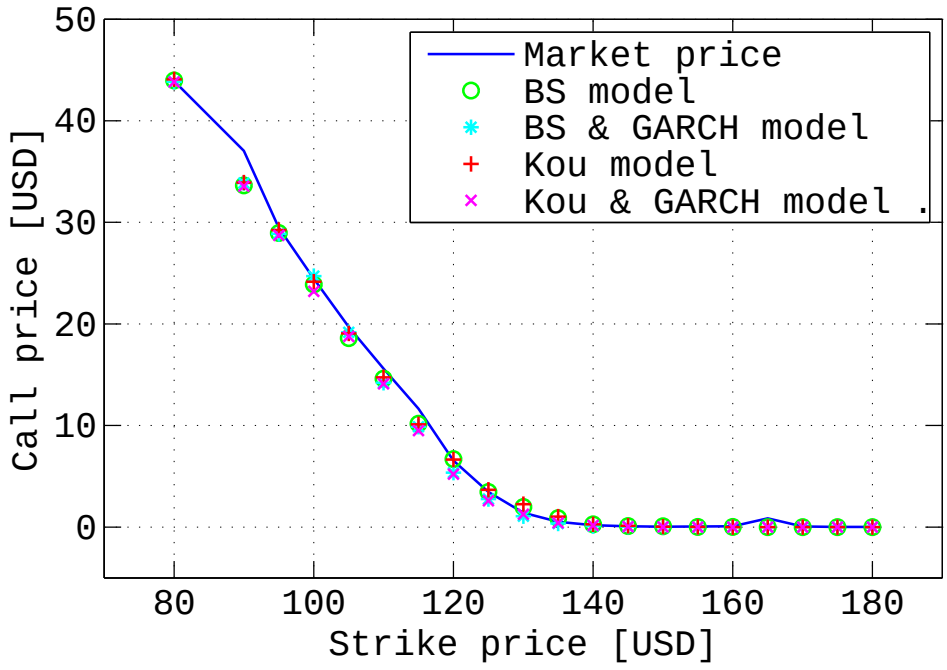

Figure B.11: The comparison of the call option price estimated by the four models. The Black-Scholes model (o), the Black-Scholes & GARCH model (*), the Kou model (+) and the Kou & GARCH model (x) for the time to maturity T of 27 days. The solid line shows the market call price.

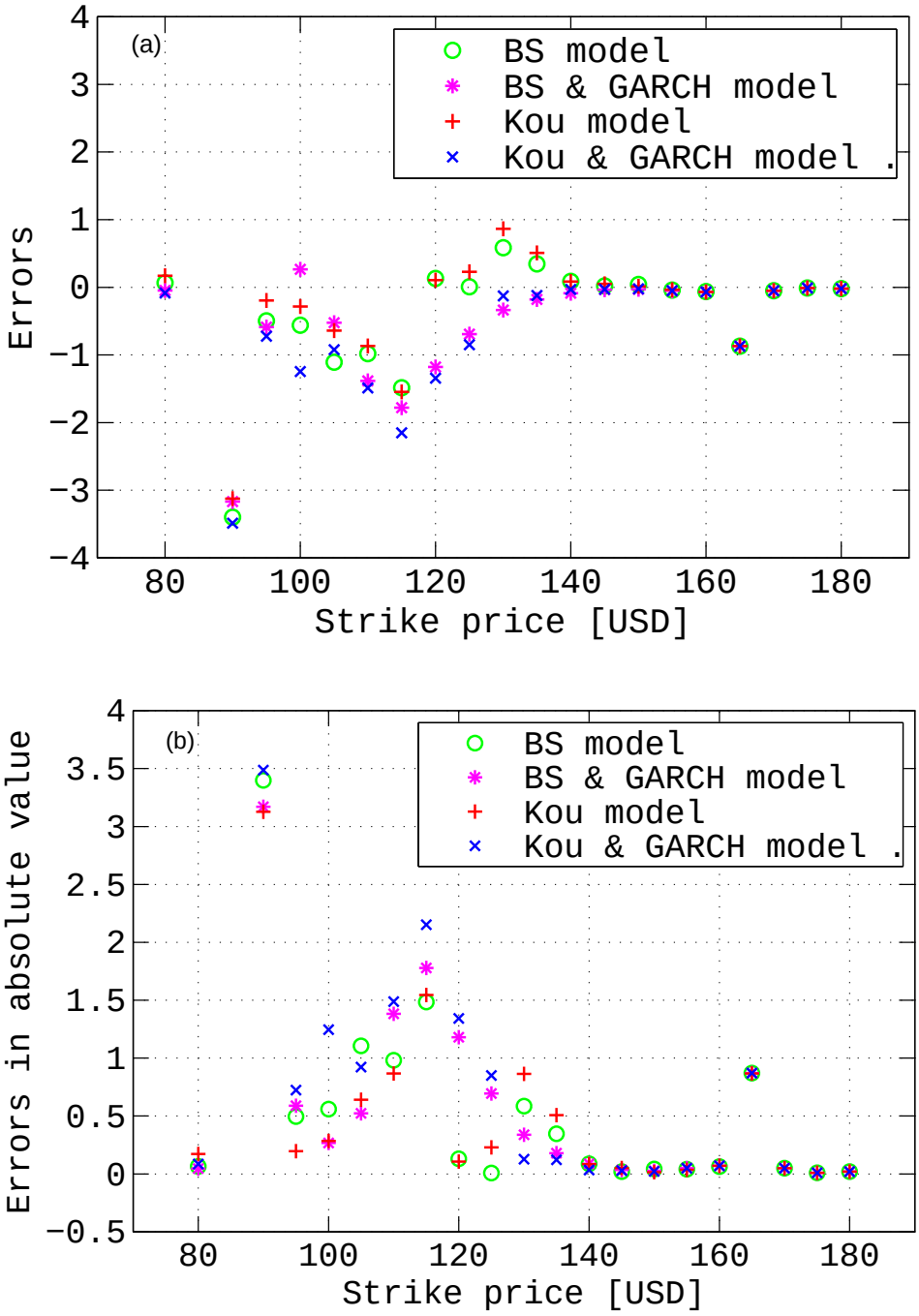

Figure B.12: The pricing errors between the call option price estimated by any of the four models and the market call price. The Black-Scholes model (o), the Black-Scholes & GARCH model (*), the Kou model (+) and the Kou & GARCH model (x) for the time to maturity T of 27 days. Figure (a) shows the real value. Figure (b) shows the absolute value.

B.3 Time to maturity is 162 days

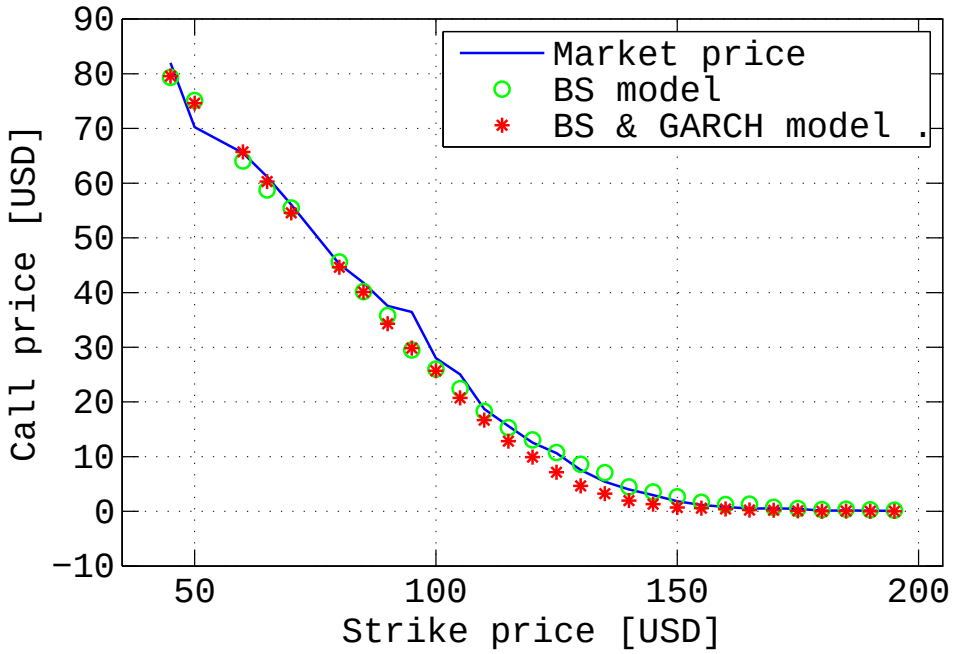

Figure B.13: The comparison of the call option price estimated by the Black-Scholes model (o) and the Black-Scholes & GARCH model (*) for the time to maturity T of 162 days. The solid line shows the market call price.

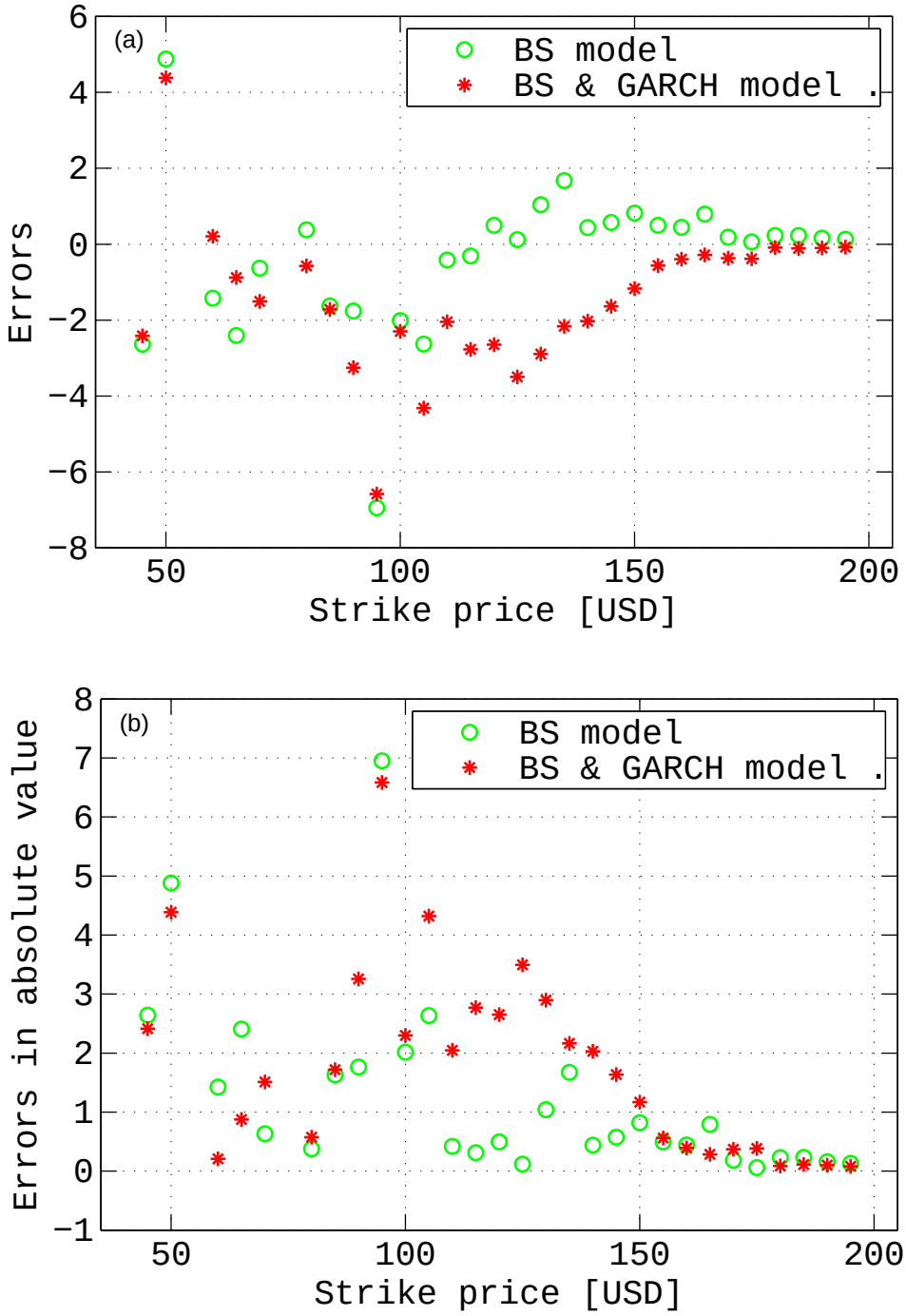

Figure B.14: The pricing errors between the call option price estimated by the Black-Scholes model (o) or the Black-Scholes & GARCH model (*) and the market call price. Figure (a) shows the real value. Figure (b) shows the absolute value. The time to maturity T is 162 days.

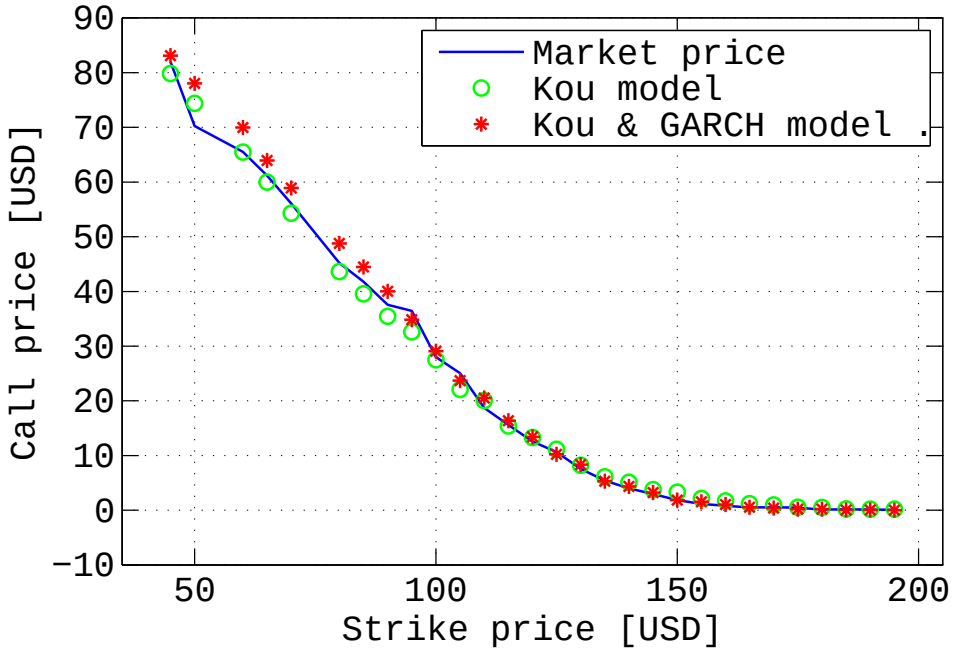

Figure B.15: The comparison of the call option price estimated by the Kou model (o) and the Kou & GARCH model (*) for the time to maturity T of 162 days. The solid line shows the market call price.

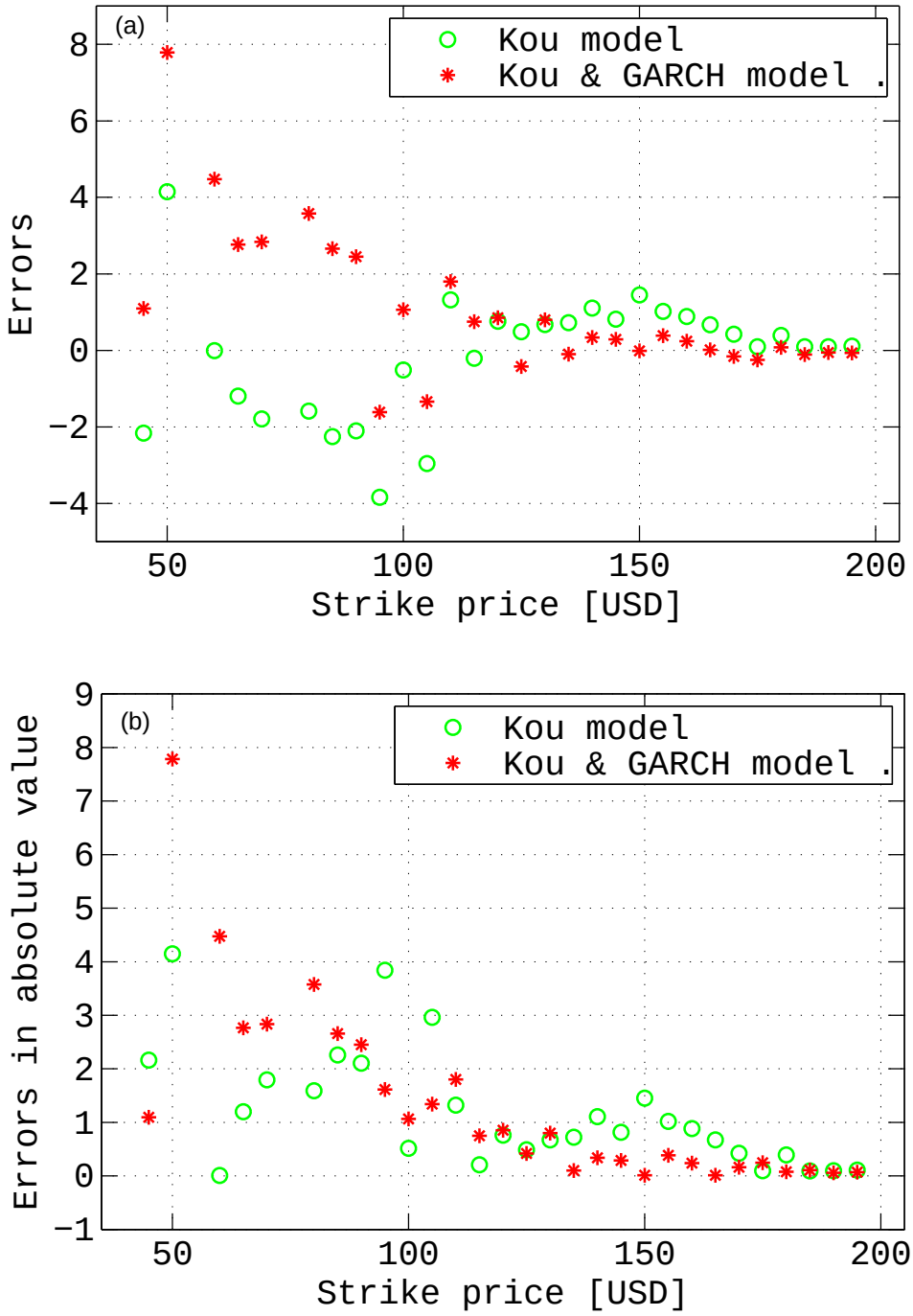

Figure B.16: The pricing errors between the call option price estimated by the Kou model (o) or the Kou & GARCH model (*) and the market call price. Figure (a) shows the real value. Figure (b) shows the absolute value. The time to maturity T is 162 days.

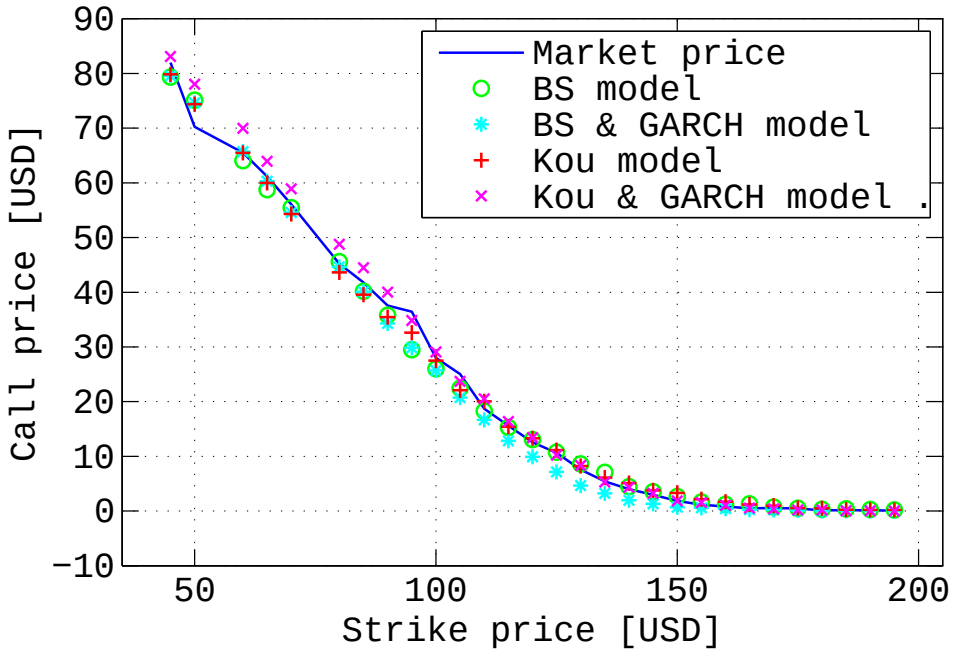

Figure B.17: The comparison of the call option price estimated by the four models. The Black-Scholes model (o), the Black-Scholes & GARCH model (*), the Kou model (+) and the Kou & GARCH model (x) for the time to maturity T of 162 days. The solid line shows the market call price.

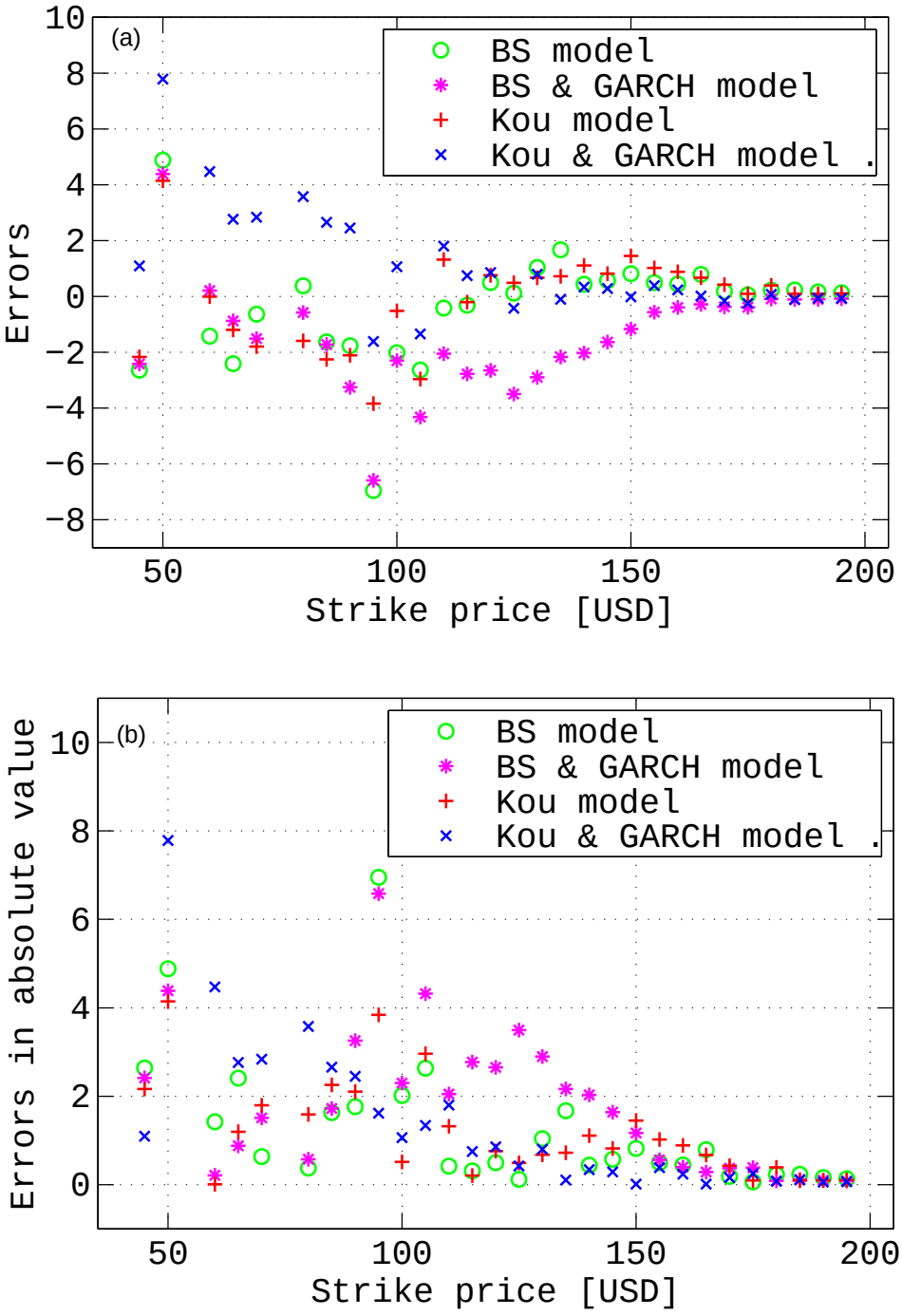

Figure B.18: The pricing errors between the call option price estimated by any of the four models and the market call price. The Black-Scholes model (o), the Black-Scholes & GARCH model (*), the Kou model (+) and the Kou & GARCH model (x) for the time to maturity T of 162 days. Figure (a) shows the real value. Figure (b) shows the absolute value.

B.4 Time to maturity is 422 days

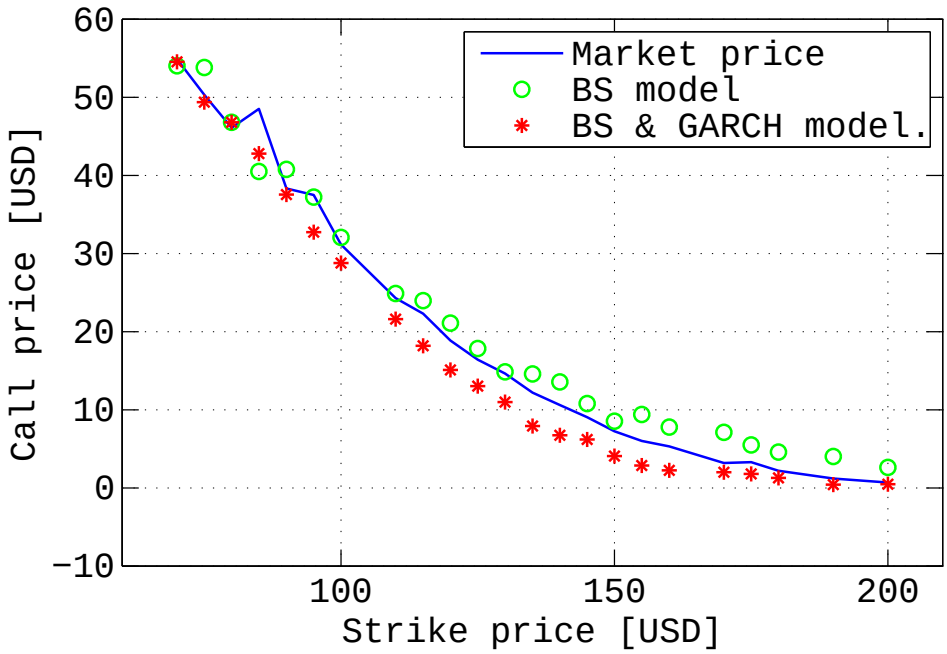

Figure B.19: The comparison of the call option price estimated by the Black-Scholes model (o) and the Black-Scholes & GARCH model (*) for the time to maturity T of 422 days. The solid line shows the market call price.

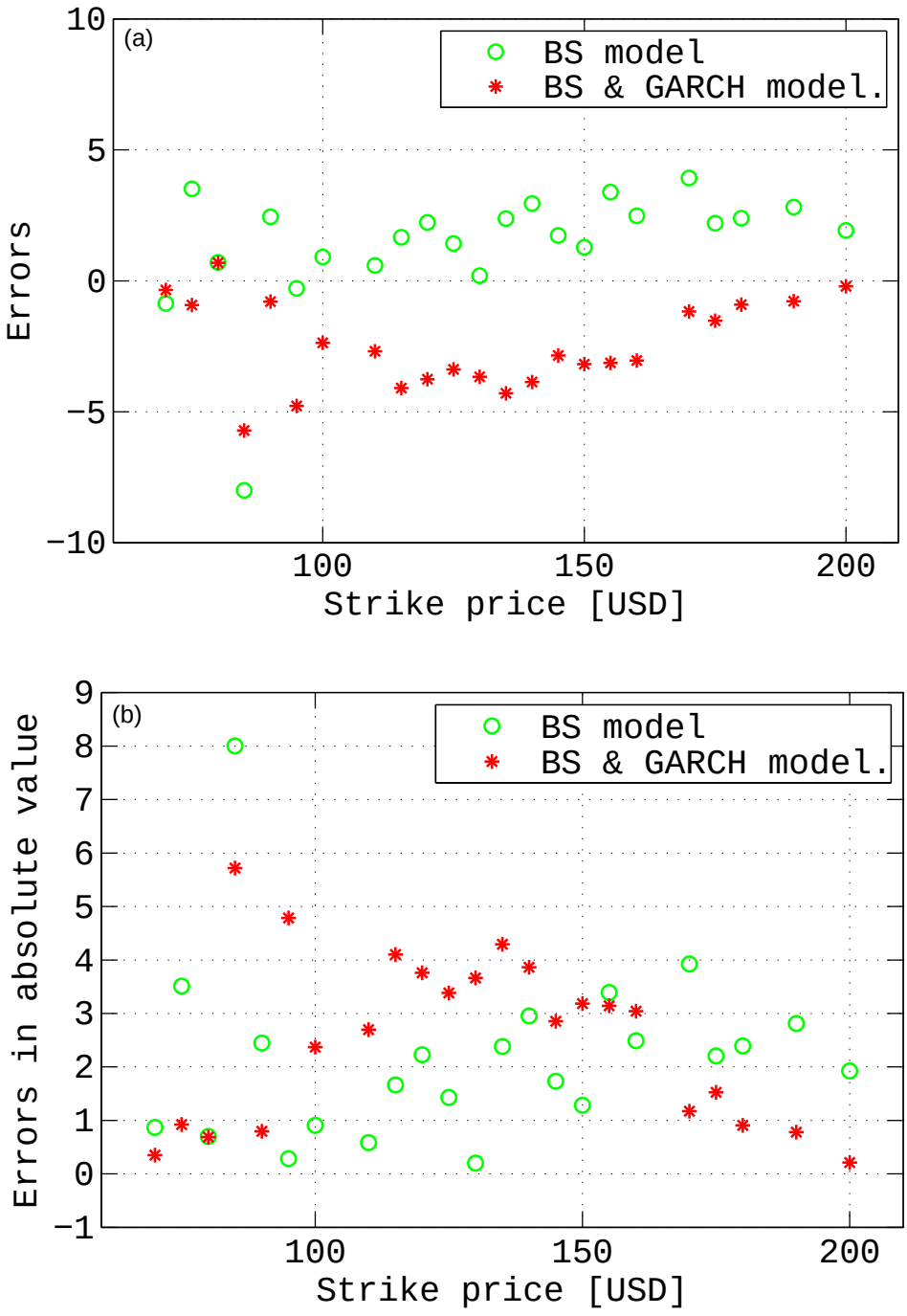

Figure B.20: The pricing errors between the call option price estimated by the Black-Scholes model (o) or the Black-Scholes & GARCH model (*) and the market call price. (a) the real value. (b) the absolute value. The time to maturity T is 422 days.

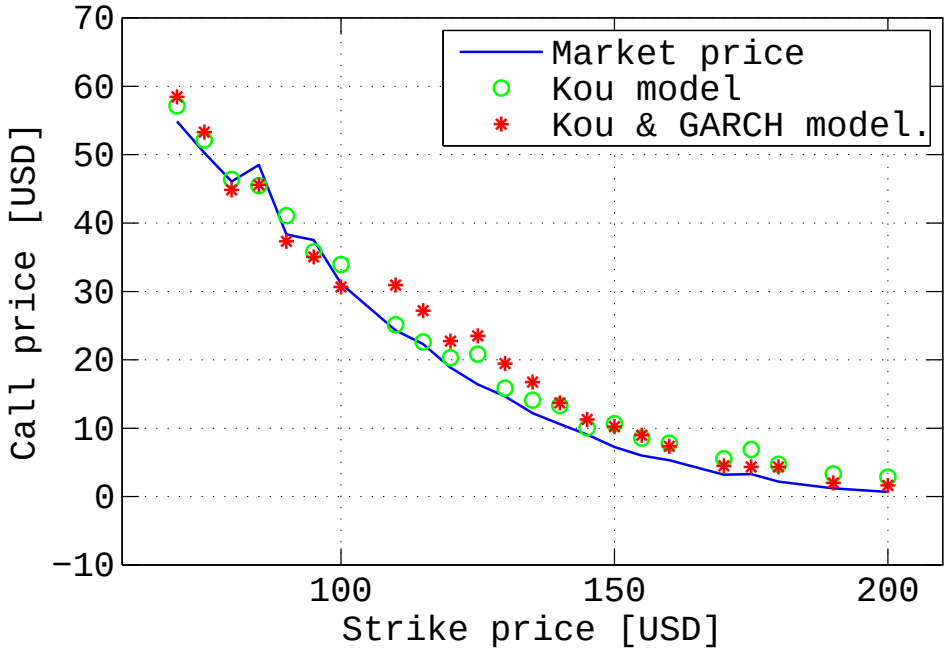

Figure B.21: The comparison of the call option price estimated by the Kou model (o) and the Kou & GARCH model (*) for the time to maturity T of 422 days. The solid line shows the market call price.

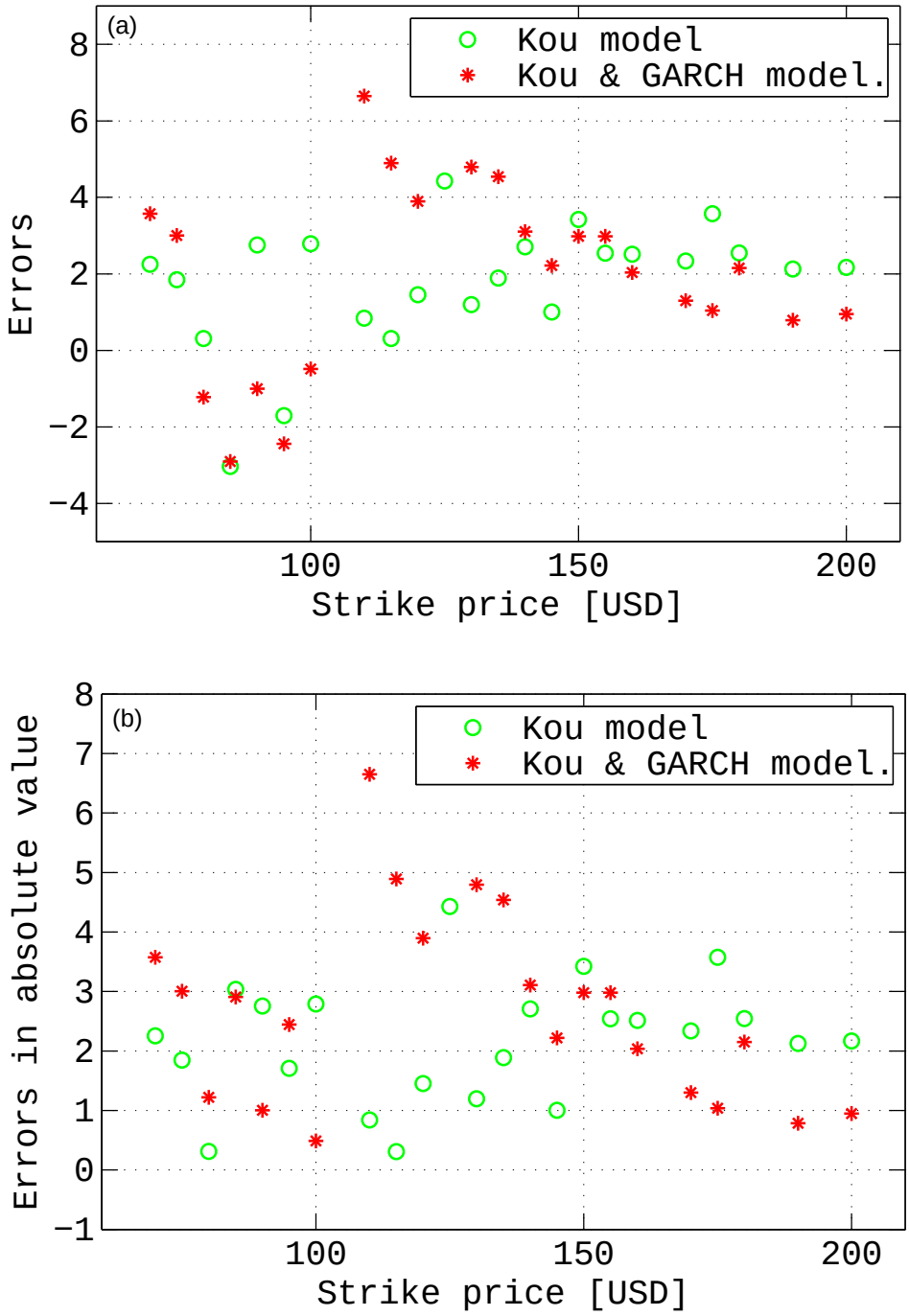

Figure B.22: The pricing errors between the call option price estimated by the Kou model (o) or the Kou & GARCH model (*) and the market call price. Figure (a) shows the real value. Figure (b) shows the absolute value. The time to maturity T is 422 days.

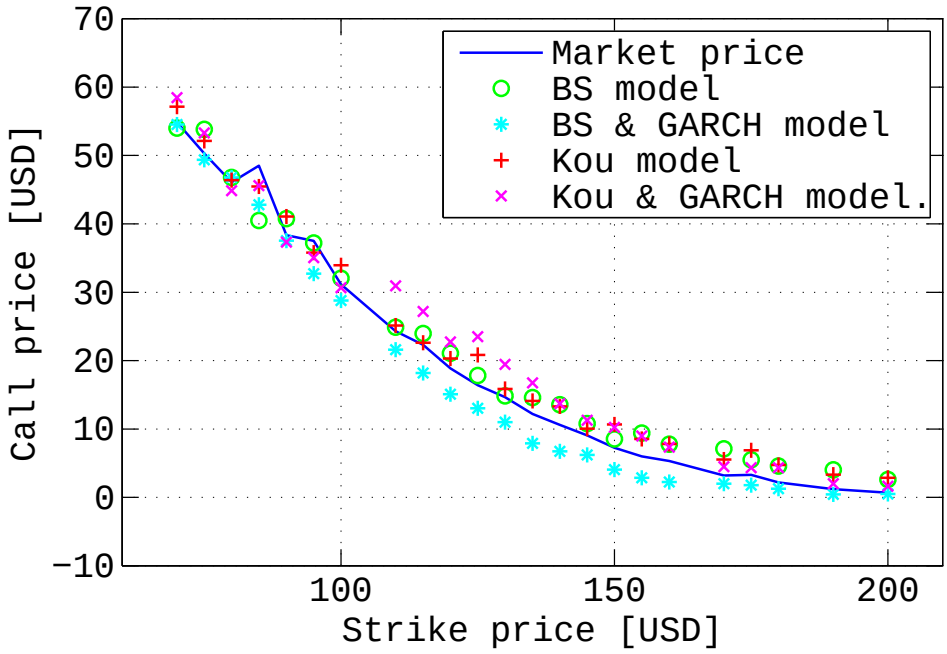

Figure B.23: The comparison of the call option price estimated by the four models. The Black-Scholes model (o), the Black-Scholes & GARCH model (*), the Kou model (+) and the Kou & GARCH model (x) for the time to maturity T of 422 days. The solid line shows the market call price.

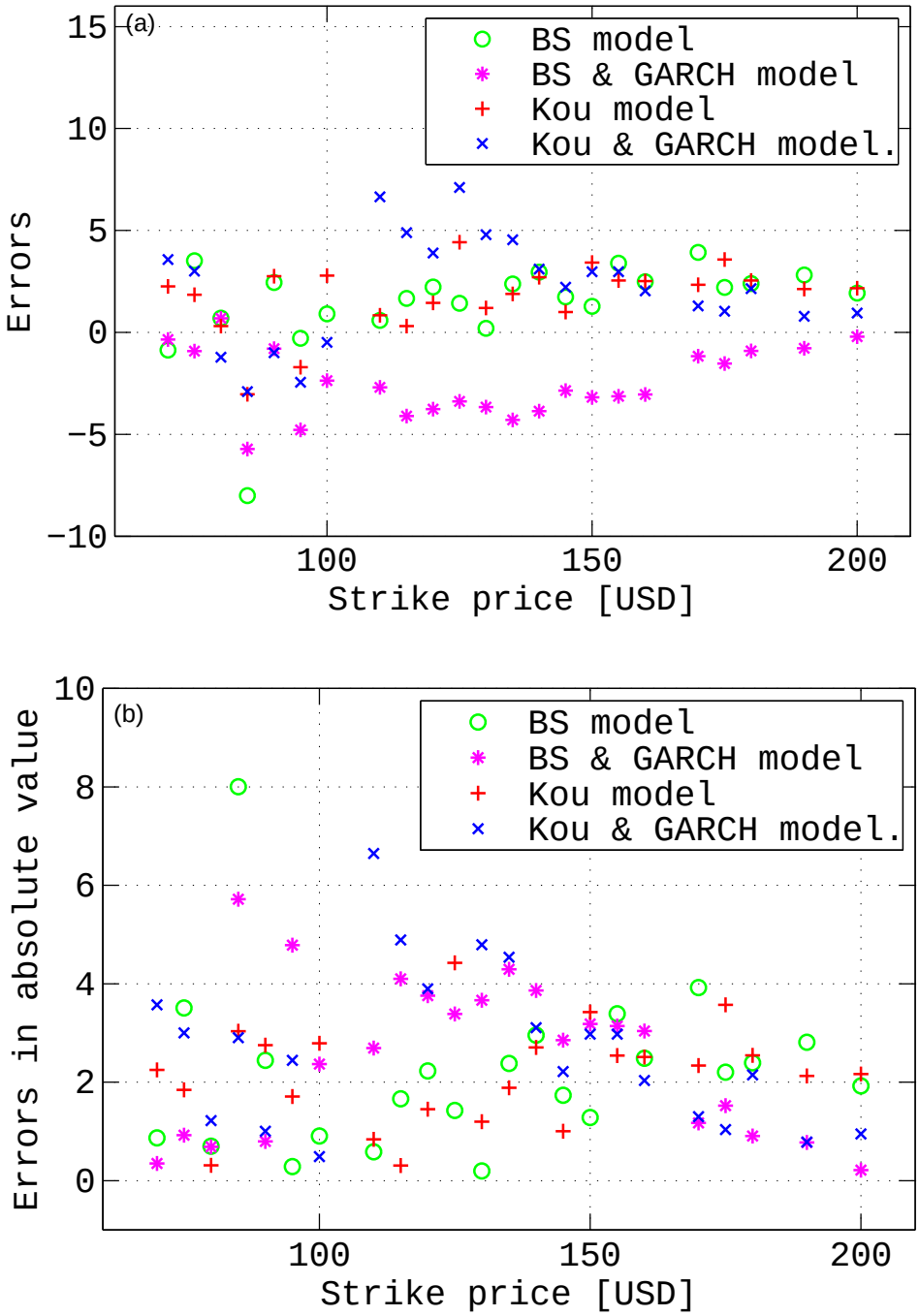

Figure B.24: The pricing errors between the call option price estimated by any of the four models and the market call price. The Black-Scholes model (o), the Black-Scholes & GARCH model (*), the Kou model (+) and the Kou & GARCH model (x) for the time to maturity T of 422 days. Figure (a) shows the real value. Figure (b) shows the absolute value.

List of Tables

List of Figures

Bibliography

Ait-Sahalia, Y. (2002). Maximum likelihood estimation of discretely sampled diffusions: A closed-form approximation approach. *Econometrica 70*(1), 223–262.

Alexander, C. (2001). *Market Models: A Guide to Financial Data Analysis*. West Sussex, UK: John Wiley & Sons.

Allen, A. O. (1978). *Probability, Statistics, and Queuing Theory: with Computer Science Applications*. New York: Academic Press.

Andersen, L. and J. Andersen (2000). Jump-diffusion processes: Volatility smile fitting and numerical methods for option pricing. *Review of Derivatives Research 4*(3), 231–262.

Andersen, L. B. G. and R. Brotherton-Ratcliffe (1998). The equity option volatility smile: An implicit finite-difference approach. *The Journal of Computational Finance 1*(2), 5–38.

Andersen, T. G., L. Benzoni, and J. Lund (2002). An empirical investigation of continuous-time equity return models. *Journal of Finance 57*(3), 1239–1284.

Bakshi, G., C. Cao, and Z. Chen (1997). Empirical performance of alternative option pricing models. *Journal of Finance 52*(5), 2003 – 2049.

Bates, D. (1996). Jumps and stochastic volatility: Exchange rate processes implicit in the PHLX Deutschemark options. *Review of Financial Studies 9*(1), 69–107.

Baz, J. and G. Chacko (2004). *Financial Derivatives*. Cambridge, UK: Cambridge University Press.

Black, F. and M. Scholes (1973). The pricing of options and corporate liabilities. *The Journal of Political Economy 81*(3), 637–654.

Bodie, Z., A. Kane, and A. J. Marcus (2008). *Investments* (7 ed.). New York: McGraw-Hill.

Bollerslev, T. (1986). Generalized autoregressive conditional heteroscedasticity. *Journal of Econometrics 31*(3), 307–327.

Bollerslev, T., R. Y. Chou, and K. F. Kroner (1992). ARCH modeling in finance: A review of the theory and empirical evidence. *Journal of Econometrics 52*(1-2), 5–59.

Boyle, P., M. Broadie, and P. Glasserman (1997). Monte Carlo methods for security pricing. *Journal of Economic Dynamics and Control 21*(8-9), 1267–1321.

Brandimarte, P. (2002). *Numerical Methods in Finance*. New York: John Wiley & Sons.

Brandimarte, P. (2006). *Numerical Methods in Finance and Economics* (2 ed.). Torino, Italy: John Wiley & Sons.

Broadie, M. and O. Kaya (2006). Exact simulation of stochastic volatility and other affine jump diffusion processes. *Operations Research 54*(2), 217–231.

Brooks, C. (1997). GARCH modeling in finance: A review of the software options. *The Economic Journal 107*(443), 1271–1276.

Canina, L. and S. Figlewski (1993). The informational content of implied volatility. *The Review of Financial Studies 6*(3), 659–681.

Chatfield, C. (2003). *The Analysis of Time Series: An Introduction* (6 ed.). Statistical Science. Chapman and Hall/CRC.

Chen, N. and L. J. Hong (2007). Monte Carlo simulation in financial engineering. In S. G. Henderson, B. Biller, M.-H. Hsieh, J. Shortle, J. D. Tew, and R. R. Barton (Eds.), *Proceedings of the 2007 Winter Simulation Conference*, December 9 - 12, Washington D.C., pp. 919–931.

Chernov, M., A. R. Gallant, E. Ghysels, and G. Tauchen (2003). Alternative models of stock prices dynamics. *Journal of Econometrics 116*(1-2), 225–257.

Chou, R. Y. (1988). Volatility persistence and stock valuations: Some empirical evidence using GARCH. *Journal of Applied Econometrics 3*(4), 279–294.

Craine, R., L. A. Lochstoer, and K. Syrtveit (2000). Estimation of a stochastic-volatility jump-diffusion model. *Revista de Análisis Económico 15*(1), 61–87.

Derman, E. (2003). Laughter in the dark - the problem of the volatility smile. Lecture Notes, Master Program in Financial Engineering, Columbia University, `http://www.ederman.com/new/docs/laughter.html`.

Derman, E. and I. Kani (1994a). Riding on a smile. *RISK magazine 7*(2), 32–39.

Derman, E. and I. Kani (1994b, January). The Volatility Smile and Its Implied Tree. Technical report, Goldman-Sachs.

Dittmann, I. and E. Maug (2008). Biases and error measures: How to compare valuation methods. Working Paper, Erasmus University Rotterdam, Rotterdam, Netherlands, `http://ssrn.com/abstract=947436`.

Doran, J. S. and E. I. Ronn (2005). The bias in Black-Scholes/Black implied volatility: An analysis of equity and energy markets. *Review of Derivatives Research 8*(3), 177–198.

Duan, J.-C. (1995). The GARCH option pricing model. *Mathematical Finance 5*(1), 13–32.

Duffie, D., J. Pan, and K. Singleton (2000). Transform analysis and asset pricing for affine jump-diffusions. *Econometrica 68*(6), 1343–1376.

Dupire, B. (1994). Pricing with a smile. *RISK magazine 7*(1), 18–20.

Engle, R. F. (1982). Autoregressive Conditional Heteroscedasticity with estimates of the variance of United Kingdom inflation. *Econometrica 50*(4), 987–1007.

Engle, R. F. (2001). GARCH 101: An introduction to the use of ARCH/GARCH models in applied econometrics. *Journal of Economic Perspectives 15*(4), 157–168.

Eraker, B., M. S. Johannes, and N. Polson (2003). The impact of jumps in volatility and returns. *Journal of Finance 58*(3), 1269–1300.

Fang, H. (2000). Option pricing implications of a stochastic jump rate. Working Paper, Department of Economics. University of Virginia. Charlottesville, VA.

Feng, L. and V. Linetsky (2008). Pricing options in jump-diffusion models: An extrapolation approach. *Operations Research 56*(2), 304–325.

Figlewski, S. (1997). Forecasting volatility. *Financial Markets, Institutions and Instruments 6*(2), 1–88.

Forsyth, P. (2008). Introduction to Computational Finance Without Agonizing Pain. School of Computer Science, University of Waterloo, Ontario, Canada.

Franses, P. H. and D. van Dijk (2000). *Non-Linear Time Series Models in Empirical Finance*. Cambridge, UK: Cambridge University Press.

Garcia, R., E. Ghysels, and E. Renault (2004). The econometrics of option pricing. Working Paper, Université de Montréal-CIREQ/Départment de Science Économiques.

Glasserman, P. (2003). *Monte Carlo Methods in Financial Engineering*. New York: Springer.

Gourieroux, C. (1997). *ARCH Models and Financial Applications*. New York: Springer.

Gulisashvili, A. and E. M. Stein (2010). Asymptotic behavior of distribution densities in models with stochastic volatility. *Mathematical Finance 20*(3), 447–477.

Heston, S. (1993). A closed-form solution for options with stochastic volatility with applications to bond and currency options. *The Review of Financial Studies 6*(2), 327–343.

Hull, J. C. (2005). *Options, Futures and Other Derivatives* (6 ed.). Upper Saddle River, New Jersey: Prentice Hall.

Hull, J. C. and A. White (1987). The pricing of options with stochastic volatilities. *Journal of Finance 42*(2), 281–300.

Kou, S. G. (2002). A jump-diffusion model for option pricing. *Management Science 48*(8), 1086–1101.

Kou, S. G. (2008). Jump-diffusion models for asset pricing in financial engineering. In J. R. Birge and V. Linetsky (Eds.), *Handbooks in Operations Research and Management Science, Vol. 15*, Chapter 2, pp. 73–116. Amsterdam: North-Holland.

Kou, S. G. and H. Wang (2003). First passage times of a jump diffusion process. *Advances in Applied Probability 35*(2), 504–531.

Kou, S. G. and H. Wang (2004). Option pricing under a double exponential jump diffusion model. *Management Science 50*(9), 1178–1192.

Lamoureux, C. G. and W. D. Lastrapes (1990). Persistence in variance, structural change, and the GARCH model. *Journal of Business & Economic Statistics 8*(2), 225–234.

Luenberger, D. G. (1998). *Investment Science*. New York: Oxford University Press.

Maekawa, K., S. Lee, T. Morimoto, and K. Kawai (2008). Jump diffusion model with application to the Japanese stock market. *Mathematics and Computers in Simulation 78*(10), 223–236.

Maekawa, K., S. Lee, T. Morimoto, and K. Kawai (December 2005). Jump diffusion model: An application to the japanese stock market. In A. Zerger and R. M. Argent (Eds.), *MODSIM 2005 International Congress on Modeling and Simulation: Advances and Applications for Management and Decision Making*, pp. 893–899. Modeling and Simulation Society of Australia and New Zealand.

Maheu, J. M. and T. H. McCurdy (2004). News arrival, jump dynamics, and volatility components for individual stock returns. *The Journal of Finance 59*(2), 755–793.

Massey, F. J. (1951). The Kolmogorov-Smirnov test for goodness of fit. *Journal of the American Statistical Association 46*(253), 68–78.

McLeish, D. L. (2005). *Monte Carol Simulation and Finance*. Hoboken, New Jersey: John Wiley & Sons.

McMillan, L. G. (2002). *Options as a Strategic Investment* (4 ed.). New York Institute of Finance.

Merton, R. C. (1971). Optimum consumption and portfolio rules in a continuous-time model. *Journal of Economic Theory 3*(4), 373–413.

Merton, R. C. (1976). Option pricing when underlying stock returns are discontinuous. *Journal of Financial Economics 3*(1-2), 125–144.

Miller, L. H. (1956). Table of percentage points of Kolmogorov statistics. *Journal of the American Statistical Association 51*(273), 111–121.

Poon, S.-H. and C. W. J. Granger (2003). Forecasting volatility in financial markets: A review. *Journal of Economic Literature 41*(3), 478–539.

Rachev, S. T., S. Mittnik, F. J. Fabozzi, S. M. Focardi, and T. Jai (2007). *Financial Econometrics: from Basics to Advanced Modeling Techniques*. Frank J. Fabozzi. New Jersey: John Wiley & Sons.

Rameszani, C. A. and Y. Zeng (1998). Maximum likelihood estimation of asymmetric jump-diffusion processes: application to security prices. Working Paper, Finance Department, California Polytechnic, San Luis Obispo, California.

Rameszani, C. A. and Y. Zeng (2006). An empirical assessment of the double exponential jump-diffusion process. Working Paper, Finance Department, California Polytechnic, San Luis Obispo, California.

Rameszani, C. A. and Y. Zeng (2007). Maximum likelihood estimation of the double exponential jump-diffusion process. *Annals of Finance 3*(4), 487–507.

Sepp, A. (2003). Fourier transform for option pricing under affine jump-diffusions: An overview. Working Paper, Institute of Mathematical Statistics, University of Tartu, Tartu, Estonia, `http://ssrn.com/abstract=1412333`.

Staum, J. (2002). Simulation in financial engineering. In E. Yucesan, C.-H. Chen, J. L. Snowdon, and J. M. Charnes (Eds.), *Proceedings of the 2002 Winter Simulation Conference*, December 8 - 11, San Diego, California, pp. 1481–1492.

Stein, E. M. and J. C. Stein (1991). Stock price distributions with stochastic volatility: An analytic approach. *The Review of Financial Studies 4*(4), 727–752.

Tankov, P. and E. Voltchkova (2009). Jump-diffusion models: A practitioner's guide. Banque et Marchés, March - April.

Thomas, R. L. (2005). *Using Statistics in Economics*. Berkshire, UK: McGraw-Hill.

Tsay, R. S. (2005). *Analysis of Financial Time Series* (2 ed.). New Jersey: John Wiley & Sons.

Ugur, O. (2008). *An Introduction to Computational Finance*, Volume 1. London: Imperial College Press.

Xekalaki, E. and S. Degiannakis (2010). *ARCH Models for Financial Applications*. Chichester, West Sussex, UK: John Wiley & Sons.

Yin, P. (2007, August). *Volatility Estimation and Price Prediction using a Hidden Markov Model with Empirical Study*. Ph. D. thesis, University of Missouri-Columbia.

Zhuang, X.-F. and L.-W. Chan (2004). Volatility forecasts in financial time series with HMM-GARCH models. *Lecture Notes in Computer Science 3177*, 807–812.

Zivot, E. and J. Wang (2005). *Modeling Financial Time Series with S-PLUS* (2 ed.). Seattle, WA, US: Springer.